

April 2012

Surface and Materials Analysis of Roll Forming Dies

Jessica A. Booth
Worcester Polytechnic Institute

Mackenzie N. Massey
Worcester Polytechnic Institute

Follow this and additional works at: <https://digitalcommons.wpi.edu/mqp-all>

Repository Citation

Booth, J. A., & Massey, M. N. (2012). *Surface and Materials Analysis of Roll Forming Dies*. Retrieved from <https://digitalcommons.wpi.edu/mqp-all/1783>

This Unrestricted is brought to you for free and open access by the Major Qualifying Projects at Digital WPI. It has been accepted for inclusion in Major Qualifying Projects (All Years) by an authorized administrator of Digital WPI. For more information, please contact digitalwpi@wpi.edu.

Project Number: CAB 0901

Surface and Materials Analysis of Thread Rolling Dies

A Major Qualifying Project Report

Submitted to the faculty of

WORCESTER POLYTECHNIC INSTITUTE

in partial fulfillment of the requirements for the

Degree of Bachelor of Science

in Mechanical Engineering

by

Jessica Booth

Mackenzie Massey

Date: April 26 2012

Approved By:

Professor Christopher A. Brown, Major Advisor

Keywords: multi-scale, relative area, tools, wear, discriminate, thread rolling

Table of Contents

<i>Table of Figures</i>	3
<i>Table of Tables</i>	4
Abstract.....	4
1.0 Introduction.....	5
1.1 Objectives.....	5
1.2 Rationale.....	5
1.3 State-Of-The-Art.....	5
1.3.1 Surface Characteristics.....	6
1.3.2 Materials Characteristics	6
1.4 Approach.....	7
2.0 Methods	7
2.1 Sectioning.....	7
2.2 Materials Analysis	8
2.2.1 Alloy Analysis	8
2.2.2 Microstructure.....	8
2.2.3 Hardness profiles	10
2.2.4 Failure Mode.....	11
2.3 Surface Measurement.....	12
2.4 Surface Analysis Methods.....	13
3.0 Results.....	14
3.1 Materials Properties	14
3.1.1 Alloy.....	14
3.1.2 Microstructure.....	18
3.1.3 Failure Mechanism.....	26
3.2 Surface Analysis	29
3.2.1 New vs. Used	29
3.2.2 New vs. New.....	31
3.2.3 Used vs. Used	34
4.0 Discussion	38
4.1 Alloy Type	38
4.2 Hardness Profiles.....	39
4.3 Failure Mode	40
4.4 New vs. Used Surfaces.....	40
4.5 New Surfaces.....	41
4.6 Used Surfaces.....	41
4.7 Relative Area of New Dies & Lifetime.....	41
4.8 Study Expansion	41
5.0 Conclusions and Hypothesis	43
5.1 Conclusions	43
5.2 Hypothesis.....	43
6.0 References.....	44
7.0 Appendices.....	46
7.1 Appendix A: Microstructure Images	46

7.2 Appendix B: Depth Calculation for Hardness Tests	53
7.3 Appendix C: Rough data for Hardness Tests	56
7.4 Appendix D: New vs. Used – Graphs	67
7.5 Appendix E: New vs. New - Graphs.....	73
7.6 Appendix F: Used vs. Used - Graphs.....	88
7.7 Appendix G: Conference Materials	103

Table of Figures

Figure 1: Diagram showing cuts made by EDM on each die.....	7
Figure 2: Polished region for microstructure examination.	7
Figure 3: OES sample points	8
Figure 4: Epoxy mount of A3-3	9
Figure 5: Hardness profile diagram.....	10
Figure 6: Hardness profile mount.....	10
Figure 7: Screenshot of LEXT software.....	13
Figure 8: Depth vs. Hardness graph	13
Figure 9: New and Used thread regions	14
Figure 10: Overview of image processing	15
Figure 11: Relative area as function of scale.....	16
Figure 12: Microstructure of A-type steel.....	18
Figure 13: Microstructure of D2.....	20
Figure 14: Microstructure of M42	20
Figure 15: PM microstructure of high speed steel.....	20
Figure 16: Microstructure of M-type high speed tool steel.....	21
Figure 17: Hardness vs. Depth graph for A1	22
Figure 18: Hardness vs. Depth graph for A2.....	22
Figure 19: Hardness vs. Depth graph for A3.....	24
Figure 20: Hardness vs. Depth graph for A4.....	24
Figure 21: Hardness vs. Depth graph for A5.....	25
Figure 22: Hardness vs. Depth graph for A6.....	25
Figure 23: Box and Whisker Plot	26
Figure 24: Thread crest of die A1	26
Figure 25: Thread crest of die A2.....	27
Figure 26: Thread crest of die A3	27
Figure 27: Spalled thread crests on D2 tool steel	27
Figure 28: Thread crests of die A4.....	28
Figure 29: Thread crests of die A5	28
Figure 30: Thread crests of die A6	28
Figure 31: Height parameters for new vs. used	29
Figure 32: Relative area and F-test for new vs. used	29
Figure 33: Discrimination by relative area new vs. used	30
Figure 34: Complexity new vs. used	30
Figure 35: Discrimination by complexity new vs. used	31
Figure 36: Relative area summary new regions	31
Figure 37: Height parameters new	32
Figure 38: Relative area and F-test new region	32
Figure 39: Discrimination by relative area new region	33
Figure 40: Complexity and F-test of new regions	33
Figure 41: Discrimination by complexity new region	34

Figure 42: Height parameters used region	35
Figure 43: Relative area and F-test for used region	35
Figure 44: Discrimination by Area-scale used regions	36
Figure 45: Complexity and F-test for used regions	36
Figure 46: Discrimination by complexity for used regions	37
Figure 47: Highlighted carbide bands in A3	39

Table of Tables

Table 1: OES composition of die A1.....	15
Table 2: OES composition of die A2.....	15
Table 3: OES composition of die A3.....	16
Table 4: OES composition of die A4.....	16
Table 5: OES composition of die A5 (Crucible Industries).....	17
Table 6: OES composition of die A6.....	17
Table 7: Alloy features. (Roberts, Krauss, & Kennedy, 1998), (Crucible Industries, n.d.).....	18
Table 8: Summary of statistical values	25

Abstract

Six thread rolling die specimens were compared based on surface characteristics and material properties. These comparisons were then used to make hypotheses about improving the lifetime of similar dies. This research is important in providing insights into why some tools may perform better than others which can give manufacturers a competitive edge when improving their tools. Surface characteristics were quantified by measuring five locations on both new and used portions of each die. These measurements were compared using F-tests of conventional height parameters in addition to F-tests on relative area and complexity plots. Material characteristics were compared by examining the alloy, microstructure, and microhardness profiles on threads. Failure modes on each die were identified by comparing the appearance of failed threads at low magnification to known failure modes. It was found that the larger dies were made of A2 or D2 tool steel, while the smaller dies were made of high speed tool steel. The larger dies appeared to have failed from spalling, while the smaller dies may have failed through abrasive wear. Hardness vs. depth profiles were different for each die and may be influenced by the existence of carbide bands in the microstructure. It was also found that it is possible to discriminate between the surface regions of the dies with greatest success using area-scale analysis and with limited success using height parameters. At scales between 1 and 10 μm^2 , relative area appears to correlate well to lifetime.

1.0 Introduction

1.1 Objectives

The objective of this MQP will be to conduct a case study that:

- 1) Quantitatively compares six rolling die specimens based on surface topography and material properties
- 2) Uses these comparisons to make hypotheses correlate these properties to lifetime

This MQP begins to investigate the question of what surface or materials characteristics in a rolling die may affect lifetime. More research will be needed to fully address this issue; this MQP only seeks to compare six dies.

1.2 Rationale

Rolled threads are preferred over ground threads for their superior mechanical properties, and considering that more screw threads are produced each year than any other machine element, improving thread rolling could have a large economic impact on industry (DeGarmo, Black, & Kohser, 2003). Finding ways to improve the number of parts produced by each die will decrease the cost of each component as well as decrease waste through broken tooling and labor. Describing surface and materials characteristics that may impact the lifetime of a rolling die will help manufacturers make improvements on their designs and gain a competitive edge.

1.3 State-Of-The-Art

There are many factors involved in the performance of thread rolling dies. The surface of the die interacts directly with the parts being made, so the surface properties affect the end products. The bulk material affects how the surface reacts to different processing methods and may have mechanical properties that make it good or bad for a particular application. This section provides a brief overview of previous research that has been done to investigate how the lifetime of dies and other metal tools relate to the tools surface or material characteristics.

1.3.2 Surface Characteristics

The roughness of a surface affects its operation and performance relating to tribology, lubrication, contact mechanics, and wear properties (Persson, 2006). Many studies have used scale-sensitive fractal analysis, complexity, F-tests and other analysis methods to distinguish between surfaces and to find correlations with performance. In at least two cases, relative area has been shown to correlate well with performance properties. Berglund et al. (2010) found that the friction coefficient between milled steel dies and sheet steel correlate well with relative area and complexity at certain scales. Complexity correlated best at a scale of about $200 \mu\text{m}^2$ and relative area around $10 \mu\text{m}^2$. Relative area has also been shown to correlate well with adhesive strength (Brown & Siegmann, 2001). Adhesion and friction are both present in roll forming so connections could potentially exist between lifetime and relative area.

1.3.2 Materials Characteristics

There has been little work within the past 10 years on how to improve the materials of thread rolling dies. Many studies found in the literature search were conducted between 1980 and 2000, and few recent publications exist. Thread rolling was invented in 1836 by William Keene, and since then there has been little improvement made on the process (Clarke, 1978). Though the process has not changed, the die materials have. Thread rolling dies are conventionally made from A2, D2, M1, or M2 steel (Davis, 1995). Each type of steel has its own benefits and drawbacks, though the performance of D2 and M-type steels is often found to be similar, while A2 performance is somewhat less (Davis, 1994). The major considerations when selecting a material are good hardness, toughness, and wear resistance, properties those four alloys are known to have (Gagg, 2001). Hardness must be sufficient to withstand the high stresses encountered during rolling, and the hardness of most dies is around 60 HRC (Davis, 1995). Wear resistance is critical because thread rolling depends on the sliding interaction between surfaces, and dies most often fail from spalling or abrasive wear, especially with insufficient lubrication. Toughness is important for the longevity of the die through the repeated impact of a blank being formed.

1.4 Approach

This MQP will compare and contrast six thread rolling dies, labeled A1 through A6. A1, A2, and A3 are larger dies with coarser threads, and A4, A5, and A6 are smaller dies with finer threads. For each die, a surface analysis and a materials analysis will be conducted. The surfaces of new and used threads on each die were measured. Relative area, complexity, and conventional height parameters were calculated and compared between the dies. The materials analysis consisted of composition analysis for alloy identification, near-surface hardness profile creation, microstructure analysis, and determination of possible failure mode on each die. These characteristics will be compared between each die to determine if there are obvious connections with the lifetime.

2.0 Methods

2.1 Sectioning

Upon receiving the dies, they were cut into smaller pieces that would fit under the microscope. Each die had three pieces cut out of it, as seen in Figure 1. Ax-1 was used for surface measurements of the threads, Ax-2 was used for thread hardness profiles and optical emissive spectroscopy for alloy identification, and Ax-3 was used

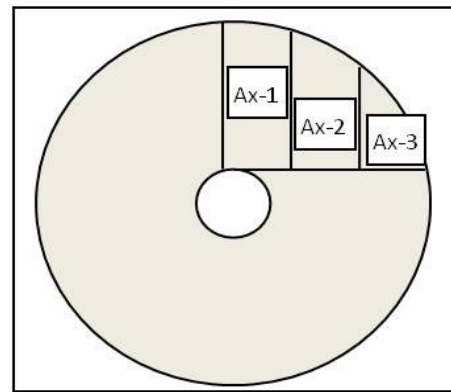


Figure 1: Diagram showing cuts made by EDM on each die. Dimensions not shown because they varied between dies.

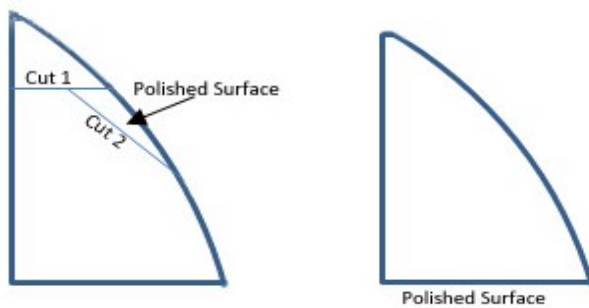


Figure 2: Diagram of Ax-3 showing what region was polished for microstructure examination. (Left) cuts made for parts A1-3, A2-3, A3-3. (Right) No additional cuts were made for parts A4-3, A5-3, A6-3.

for microstructure examination. The dies were cut using electrical discharge machining (EDM) and the dimensions of the sections varied between each die. Pieces were marked with a permanent marker on the EDM surface to ensure that the number would not wash or wipe off.

Sections A1-3, A2-3, and A3-3 were originally intended to be used for the creation of hardness profiles, so additional cuts (Figure 2) were made with a diamond grit

abrasive cutting wheel on a cross sectioning saw. It was later decided that the cuts did not achieve the intended result, so the angled surface was re-polished and etched for microstructure examination.

Sections A4-3, A5-3, and A6-3 did not undergo any additional cutting operations and were ground, mounted, and polished in the configuration seen in Figure 2.

2.2 *Materials Analysis*

2.2.3 Alloy Analysis

The chemical composition of each die was measured using optical emissive spectroscopy (OES). OES measures the composition of a solid by vaporizing it into a gas with an electrical discharge and analyzing the emitted spectrum. Each specimen was prepared by using a belt grinder with alumina sandpaper to remove any surface contamination remaining from the EDM process, an example of which can be seen in Figure 3. Alumina paper was used to minimize carbon contamination that would have resulted from silicon carbide (SiC) paper. Four readings were taken on each specimen, and the chemical composition by percent was recorded in a spreadsheet. The alloy was determined by comparing the composition data to standard composition limits and finding the alloy that matched the composition patterns the closest. In many cases, the alloy limits did not exactly match the composition data but was similar enough such that an alloy could be identified.



Figure 3: OES sample points (round discolorations) on a specimen that has been partially mounted in epoxy.

Once the alloy was identified, evidence from the literature provided a basis for comparing the dies based on hardness, toughness, hardness, and wear resistance which are some of the most important factors to consider in alloys for die lifetime (Davis, 1995).

2.2.4 Microstructure

Metallographic mounts were created from the Ax-3 piece from each die. The dies are made of hardened steel so cutting the parts required a diamond abrasive wheel and lots of time. Due to the time requirements, the smallest number of cuts were made as possible, which resulted in pieces that were too large to fit in a conventional mount mold. Alternative molds were made

for the pieces and Buehler Epo-Kwick epoxy was used as a mounting medium for its dimensional flexibility, ease of removal, and good edge retention. Silicone mold release was sprayed on the inside of the mold to ease removal of the cured mount. A photo of the mount for A3-3 can be seen in Figure 4.

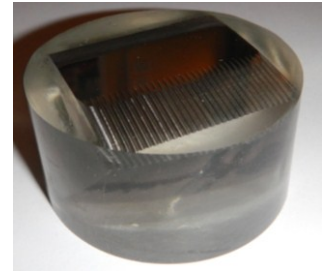


Figure 4: Epoxy mount of A3-A3-3. About 2 inches in diameter.

Once cured, the mount was removed and manually ground flat using a water-cooled rotary grinding/polishing machine. Grits used in series were 60, 120, 180, 320, 400, and 600.

After rough grinding and polishing, specimens were polished using a using 1 μ m diamond suspension and lapping oil on a Vibromet machine with nylon cloth. The parts were left on the machine between 12 and 18 hours to ensure thorough polishing. The abrasive medium was cleaned from the mounts using acetone on a cotton ball and rinsed off until visually clean.

To reveal the microstructure of the metal, a 2-4% nital solution was applied to the polished surface using a cotton swab for 2-4 minutes until the polished surface became slightly hazy. Nital was used because it is the most common etchant for iron and steel and is good for the martensitic structure of tool steels (Voort & Manilova, 2009).

The microstructure was examined and photographed using a confocal laser scanning microscope. The snapshot feature was used when the surface was very flat and little depth of field was required. If the surface was not flat, a 3D profile was taken and the image layer of the measurement was used as a micrograph. Objective lenses used were 5x, 10x, 20x, 50x, and 100x.

2.2.5 Hardness profiles

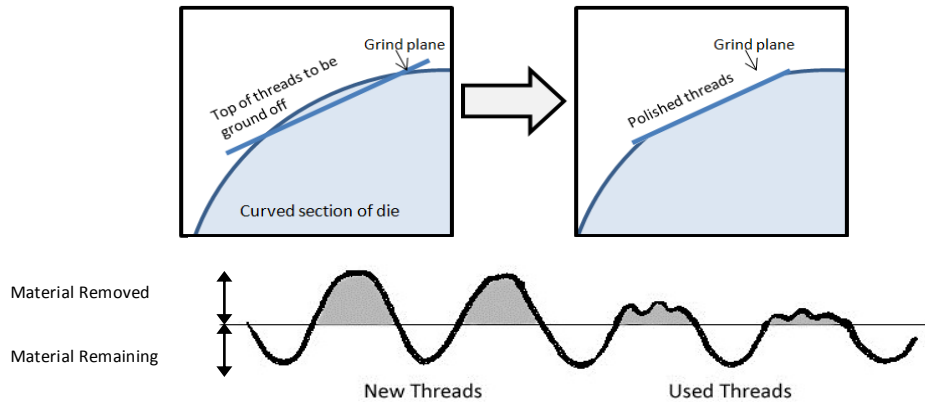


Figure 5: (Top) diagram showing the large-scale view of how threads were ground off. Line indicates plane that was ground flat when part was mounted. (Bottom) diagram showing what part of a new and used thread were ground off. The area in grey is the ‘wear region’ and was removed.

Microhardness profiles were created from Knoop hardness tests taken on material near the surface of the used and new threads. The material close to the surface was revealed by mounting a piece from each die in epoxy, threads down, such that a small amount of the threads were removed when the mount was ground and polished flat. Figures 5 and 6 show what region of the threads was removed and how the pieces were mounted. Hardness tests were taken at regular intervals along the length of a polished thread of both the new and used sections on each specimen. The indents were measured using a stitched image from the confocal laser scanning microscope. The LEXT software was used to measure the length of each indent as well as the distance between indents, and, indirectly, the length of the entire polished surface. A visual example of how these measurements were taken can be seen in Figure 7.

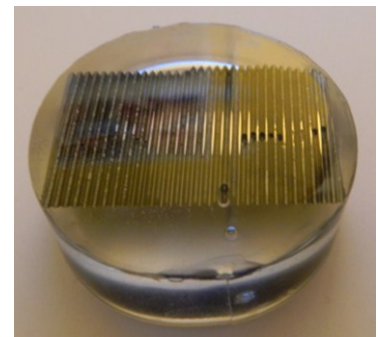


Figure 6: Mount showing small parts of threads removed.

The indent lengths in micrometers were converted to Knoop hardness with a Knoop value table and Equation 1.

$$\text{Knoop Hardness} = \text{load} * \text{knoop reading at } 1gf$$

Equation 1: Equation for knoop hardness (Chandler, 1999)

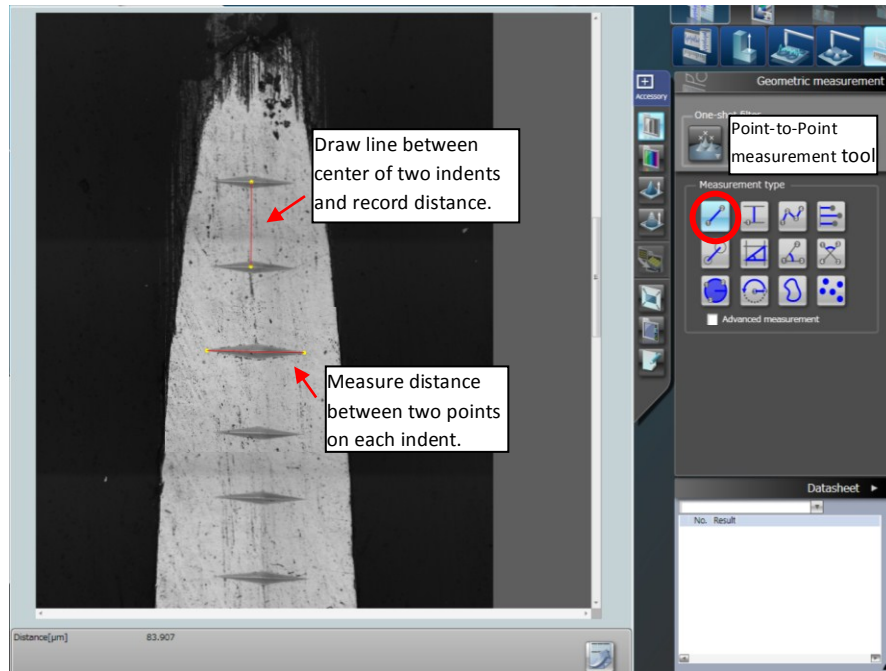


Figure 7: Screenshot of LEXT software showing how to measure length of indents and distance between indents.

The Knoop hardness was plotted against depth for each thread. The mathematical procedure used to calculate depth is shown in Appendix B. The resulting graphs resemble Figure 8. To compare results between each die, box and whisker plots were created for each set of data using a template found online (VERTEX42 LLC, 2012). A downloadable template was used because Excel does not have a straightforward way to make box and whisker plots. The template automatically calculated minimum, maximum, median, Q1, Q2, and IQR. Standard deviation and mean were also calculated.

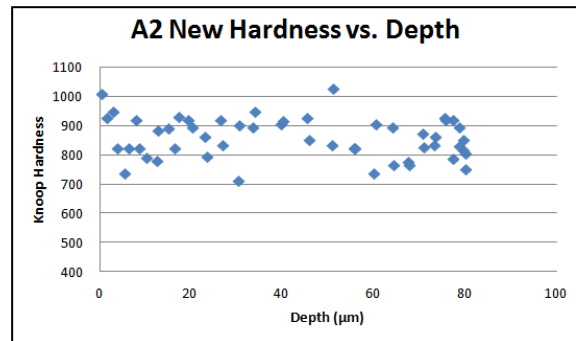


Figure 8: Example of a Depth vs. Hardness graph

2.2.6 Failure Mode

Micrographs of new and used thread crests on each die were taken with a 20x objective lens using a confocal laser scanning microscope. The intensity layer was used as a micrograph of the surface. The macro-scale wear mechanism was determined based on the difference in appearance between the new and used thread crests. The wear mechanisms considered were spalling, galling, abrasive wear, adhesive wear, erosive wear, and continuous wear because they are the most common failure mechanisms for thread rolling dies (Gagg & Lewis, 2007). Fracture surfaces were not examined with an SEM due to unavailability of equipment and users with

fracture surface experience. Because of this, the failure mode cannot be determined with certainty, but a best guess can be made based on the appearance at low magnification.

2.3 Surface Measurement

Ten measurements were taken on one sectioned piece of each die: five measurements in the new region and five in the used region. These regions can be seen in Figure 9. Each measurement was $265 \times 256 \mu\text{m}$ and done using an Olympus LEXT OLS4000 Confocal Laser Scanning microscope. A 50x objective lens with a 0.95 NA created a height map of 1024×1024 points resulting in a 250nm sampling interval.

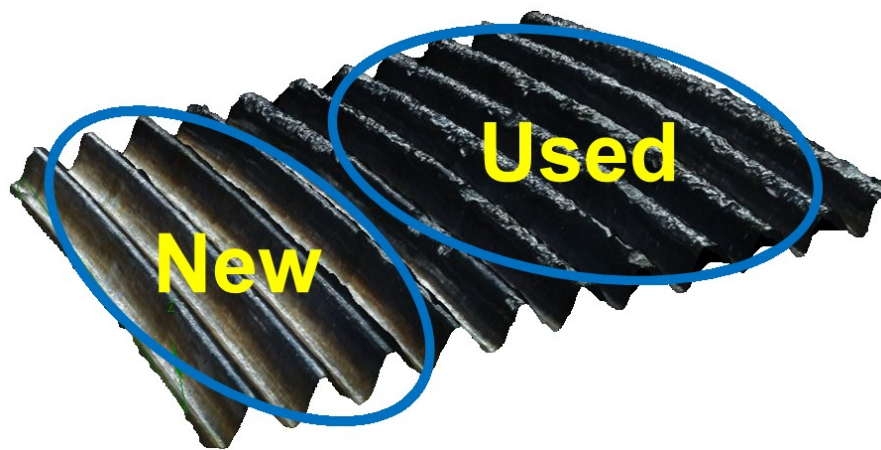


Figure 9: Macro image of the example New and Used thread regions on a die

Post processing of the images was done using a combination of MountainsMap and Sfrax. The raw images were first processed in MountainsMap where a $5\mu\text{m}$ border was cropped to remove the majority of spikes located along the edges of the images. The majority of the remaining spikes were removed using an 85° slope filter in Sfrax. A lower angle was not used to ensure that only spikes, not real data points, would be removed due to the high slope of the thread edges.

The final processing- more cropping, form removal and selective spike removal- was done in MountainsMap. The edges of the measured area were cropped, leaving only the crest of the thread that was used for analysis. The remaining region was $228.5 \times 172.25 \mu\text{m}$. Just prior to form removal, the non-measured points resulting from spike removal were filled in using MountainsMap. A 4th order polynomial fit was used to remove form. A 4th order was the lowest

order found that removed most of the form without potentially removing actual surface features. Finally a 9 x 9 median (denoising) spatial filter was applied to remove any remaining spikes. An overview of the image processing can be seen step by step in Figure 10.

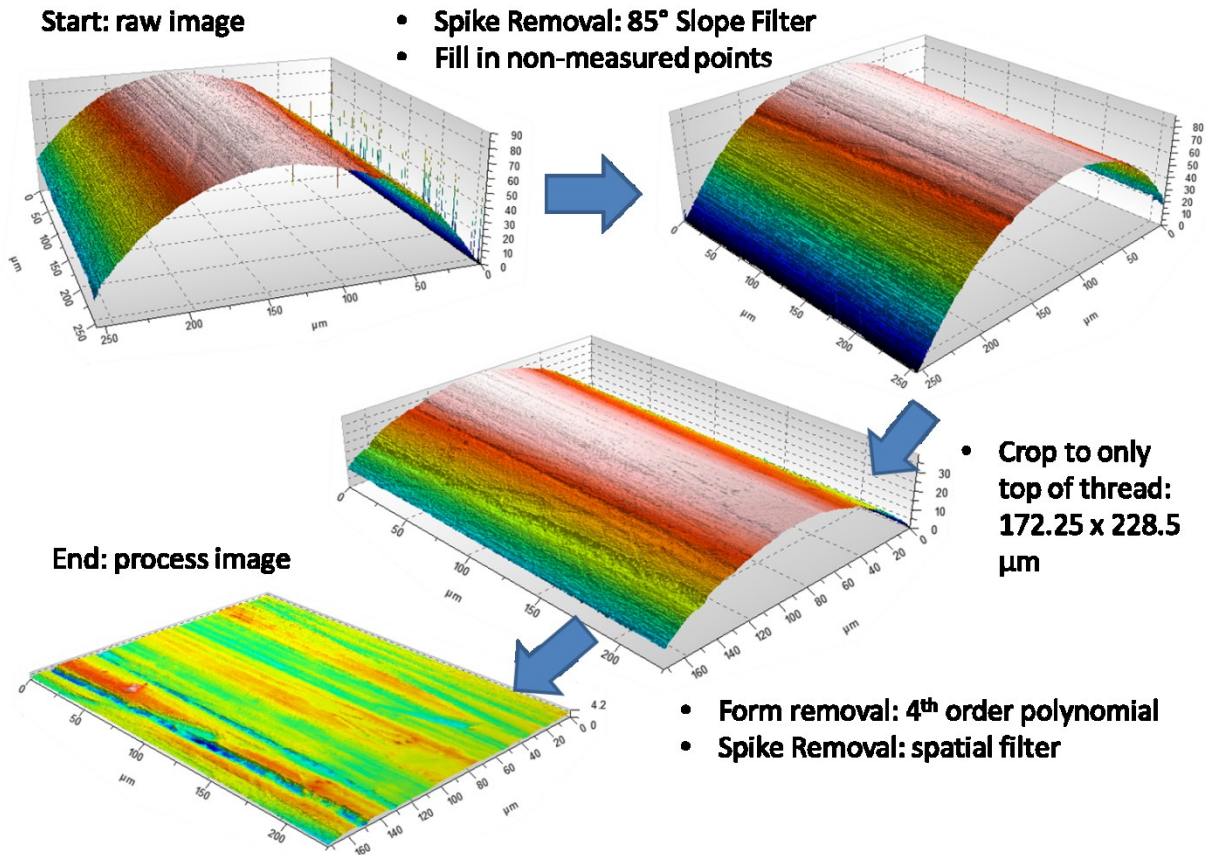


Figure 10: Overview of image processing

2.4 Surface Analysis Methods

Two types of surface analyses were used: multi-scale and conventional height parameters. The height parameters were calculated in MountainsMap according to the ASME B46.01 surface roughness standards. The parameters calculated were St, Sp, Sv, Sq, Sa, Ssk, and Sku. Multi-scale analysis was performed using Sfrac scale-sensitive fractal analysis software. Relative area and complexity were examined. Figure 11 visually displays how the relative area of a surface changes as a function of scale. For the multi-scale analysis, a bottom left tiling

method was used. F-tests were used to determine the level of confidence for discrimination between surfaces. Conventional height parameters were compared using an F-test in Microsoft Excel and a modified F-test in Sfrax was used for the multi-scale analysis.

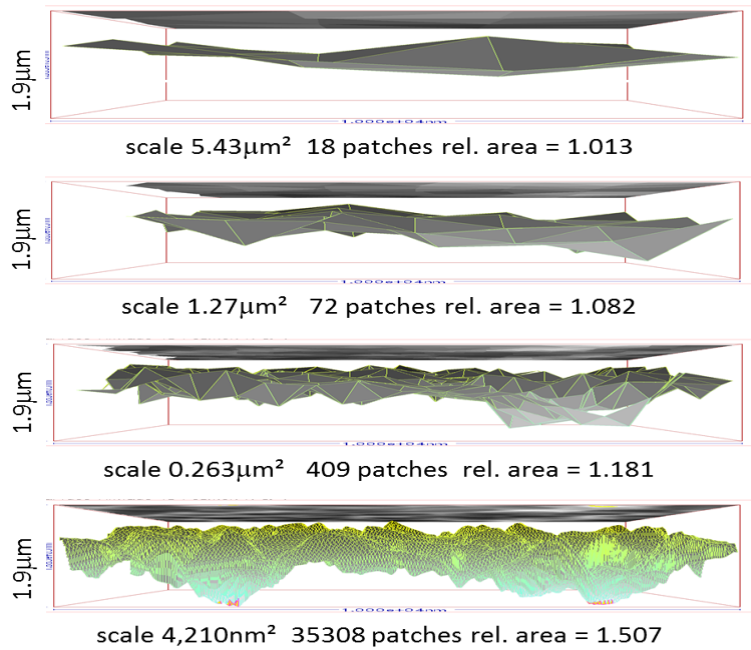


Figure 11: Example of how the relative area of a surface changes as a function of scale (ASME B46.1-2009)

3.0 Results

3.1 Materials Properties

3.1.1 Alloy

The OES results for each die are shown in Tables 1-6, expressed in percent. The composition of the alloy that most closely matched each composition is shown in the bottom row. Alloy compositions are expressed as percentage ranges. A dash (-) in a box indicates a minimal value or a value that was not specified in the Metals Handbook (Davis, 1994). Note that all elements in the OES specimens may not match exactly with the ranges given. The alloy was identified if the element concentrations were close to the specified value and the relative concentrations matched. Table 7 summarizes the alloys found, the lifetime of each die, and some properties of each type of steel.

Table 1: OES composition of die A1

Sample	C%	Mn	Si	Cr	Ni	Mo	W	V	Co	Al	Cu	P	S	Ti	Sn	As	N	Fe
1	1.03	0.343	1.05	6.93	0.194	2.55	0.018	0.391	0.027	0.022	0.035	0.021	0.0055	0.0055	0.0046	<.001	0.024	87.3
2	1.06	0.343	1.06	6.93	0.199	2.56	0.018	0.391	0.028	0.021	0.035	0.023	0.058	0.0056	0.0045	<.001	0.016	87.3
3	1.05	0.344	1.06	6.93	0.189	2.54	0.02	0.39	0.026	0.022	0.037	0.022	0.0052	0.0058	0.0046	<.001	0.012	87.3
4	1.03	0.343	1.07	6.81	0.2	2.52	0.017	0.376	0.028	0.022	0.111	0.025	0.0063	0.0054	0.0045	<.001	0.011	87.4
Alloy: A2	.95- 1.05	1.0 max	.5 max	4.75- 5.5	.3 max	.9- 1.4	-	.15- .5	-	-	-	-	-	-	-	-	-	-

Table 2: OES composition of die A2

Sample	C%	Mn	Si	Cr	Ni	Mo	W	V	Co	Al	Cu	P	S	Ti	Sn	As	N	Fe
1	1.74	0.345	0.64	11.06	0.109	0.439	0.014	0.243	0.027	0.028	0.273	0.033	0.027	0.012	0.0087	<.0016	0.077	84.9
2	1.71	0.339	0.63	11.01	0.107	0.431	0.017	0.236	0.025	0.028	0.178	0.03	0.017	0.011	0.0087	<.001	0.04	85.2
3	1.7	0.337	0.62	10.81	0.112	0.416	0.013	0.227	0.027	0.027	0.105	0.031	0.019	0.011	0.0086	<.001	0.027	85.5
4	1.72	0.338	0.62	10.95	0.108	0.416	0.017	0.231	0.026	0.026	0.106	0.029	0.016	0.011	0.0086	<.001	0.02	85.4
Alloy: D2	1.4- 1.6	.6 max	.6 max	11- 13	.3 max	.7- 1.2	-	1.10 max	1.00 max	-	-	-	-	-	-	-	-	-

Table 3: OES composition of die A3

Sample	C%	Mn	Si	Cr	Ni	Mo	W	V	Co	Al	Cu	Ti	P	S	Sn	As	N	Fe
1	1.71	0.342	0.62	10.79	0.114	0.417	0.015	0.226	0.027	0.028	0.125	0.011	0.032	0.019	0.0089	<.001	0.015	85.5
2	1.73	0.34	0.6	10.85	0.113	0.413	0.007	0.229	0.027	0.026	0.1	0.01	0.031	0.018	0.0089	<.001	0.015	85.5
3	1.71	0.343	0.61	10.96	0.114	0.411	0.0093	0.229	0.027	0.027	0.1	0.01	0.03	0.014	0.0086	<.001	0.014	85.4
4	1.63	0.343	0.61	10.8	0.118	0.411	0.0095	0.223	0.028	0.028	0.148	0.01	0.031	0.018	0.0085	<.001	0.014	85.6
Alloy: D2	1.4- 1.6	.6 max	.6 max	11- 13	.3 max	.7- 1.2	-	1.10 max	1.00 max									

Table 4 OES composition of die A4

Sample	C%	Mn	Si	Cr	Ni	Mo	W	V	Co	Al	Cu	Ti	P	S	Sn	As	N	Fe
1	1.12	0.222	0.409	3.55	0.178	8.74	1.22	0.96	7.51	0.025	0.167	0.0052	0.024	0.031	0.011	0.015	0.097	75.7
2	1.15	0.219	0.409	3.56	0.175	8.88	1.22	0.98	7.47	0.023	0.167	0.0052	0.024	0.027	0.011	0.014	0.096	75.6
3	1.12	0.223	0.412	3.56	0.17	8.75	1.29	0.98	7.57	0.027	0.166	0.0052	0.024	0.027	0.011	0.014	0.096	75.6
4	1.16	0.223	0.414	3.57	0.175	9.04	1.3	1	7.46	0.026	0.165	0.0053	0.025	0.033	0.011	0.014	0.096	75.3
M42	.15- 1.15	.15- .4	.15- .65	3.50- 4.25	.3 Max	9.0- 10.0	1.15- 1.85	.95- 1.35	7.75- 7.75									

Table 5: OES composition of die A5 (Crucible Industries)

Sample	C%	Mn	Si	Cr	Ni	Mo	W	V	Co	Al	Cu	Ti	P	S	Sn	As	N	Fe
1	1.34	0.59	0.55	4.05	0.175	4.74	6.38	3.25	7.74	0.0094	0.135	0.0058	0.025	0.048	0.012	0.001	0.088	70.7
2	1.35	0.59	0.55	4.05	0.167	4.74	6.4	3.26	7.73	0.0093	0.135	0.0058	0.024	0.048	0.012	0.001	0.088	70.7
3	1.36	0.59	0.55	4.04	0.172	4.75	6.45	3.26	7.73	0.0096	0.135	0.0058	0.026	0.048	0.012	0.001	0.087	70.6
4	1.38	0.59	0.55	4.05	0.172	4.74	6.49	3.27	7.7	0.0097	0.135	0.0058	0.024	0.048	0.012	0.001	0.089	70.6
Alloy: CPM Rex 45	1.3	.3-.7	0.5	4.05	-	5	6.25	3.05	8	-	-	-	-	0.06	-	-	-	-

Table 6: OES composition of die A6

Sample	C%	Mn	Si	Cr	Ni	Mo	W	V	Co	Al	Cu	Ti	P	S	Sn	As	N	Fe
1	1.19	0.288	0.35	3.89	0.078	7.32	7.22	1.7	7.7	0.031	0.052	0.006	0.023	0.007	0.009	0.011	0.082	70
2	1.21	0.291	0.347	3.94	0.076	7.24	7.07	1.73	7.72	0.031	0.051	0.0059	0.024	0.0068	0.0091	0.01	0.083	70.2
3	1.2	0.291	0.344	3.95	0.076	7.19	6.92	1.73	7.72	0.03	0.051	0.058	0.023	0.0068	0.0091	0.099	0.082	70.4
4	1.22	0.291	0.344	3.96	0.074	7.32	7.12	1.77	7.68	0.03	0.051	0.0059	0.022	0.0065	0.0091	0.0092	0.083	70
Alloy: M36	.8- .9	.15- .4	.2- .45	3.75- 4.5	.3 max	4.5- 5.5	5.5- 6.5	1.75- 2.25	7.75- 8.75	-	-	-	-	-	-	-	-	-

Table 7: Alloy features. (Roberts et al., 1998), (Crucible Industries, n.d.)

Sample	Lifetime (Pcs)	Alloy	Alloy Type	Wear Resistance	Hardness HRC	Crack Resistance	Toughness
A1	50,000	A2	Air-hardening, medium-alloy, Cold work	High	57-62	Highest	Medium
A2	59,458	D2	High-carbon, high-chromium cold-work	High	54-61	Highest	Low
A3	-	D2		High	54-61	Highest	Low
A4	22,000	M42	High speed tool steel	Very High	65-70	Medium	Low
A5	22,000	Rex 45	Super high speed steel	Very High	52-68	Medium	Low
A6	48,000	M36	High speed steel	Very High	60-65	Medium	Low

3.1.2 Microstructure

Images of the microstructure were taken using the confocal laser scanning microscope using 20x, 50x and 100x objective lenses. To conserve space, only the images taken with the 100x lens are shown in this section. Appendix A contains all images sorted by die. To help identify the constituents of each microstructure, textbook examples of similar materials are displayed next to each image.

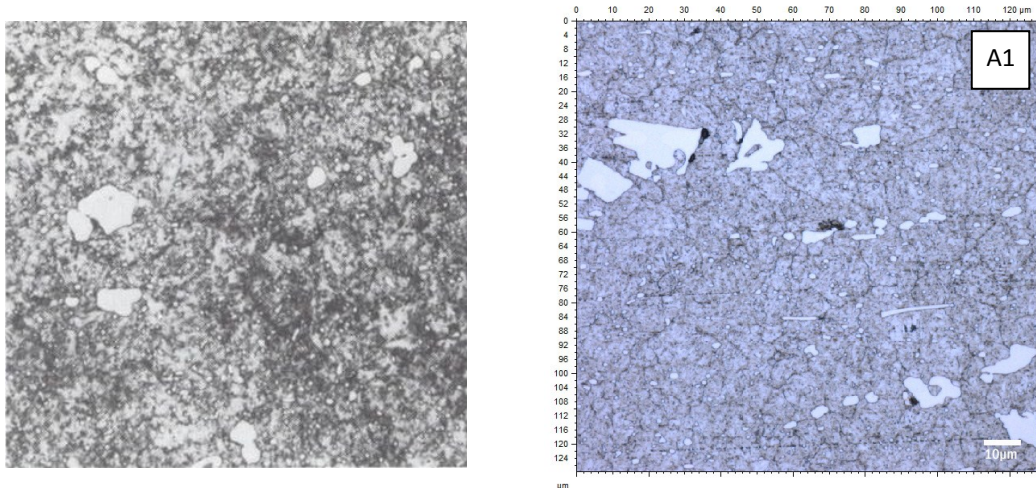


Figure 12: Microstructure of A-type steel. (Left) microstructure of A2 tool steel (Davis, 1995). (Right) Image of die A1, taken with scanning confocal laser microscope.

The large white particles in Figure 12 are carbides. The high alloy content of A2 helps create these carbides which improve wear resistance. Some carbides are large and irregularly shaped, which might act as crack initiation sites in microstructure. There are not a lot of large carbides present, unlike in D2, so wear resistance is somewhat lower than D2 (Davis, 1994).

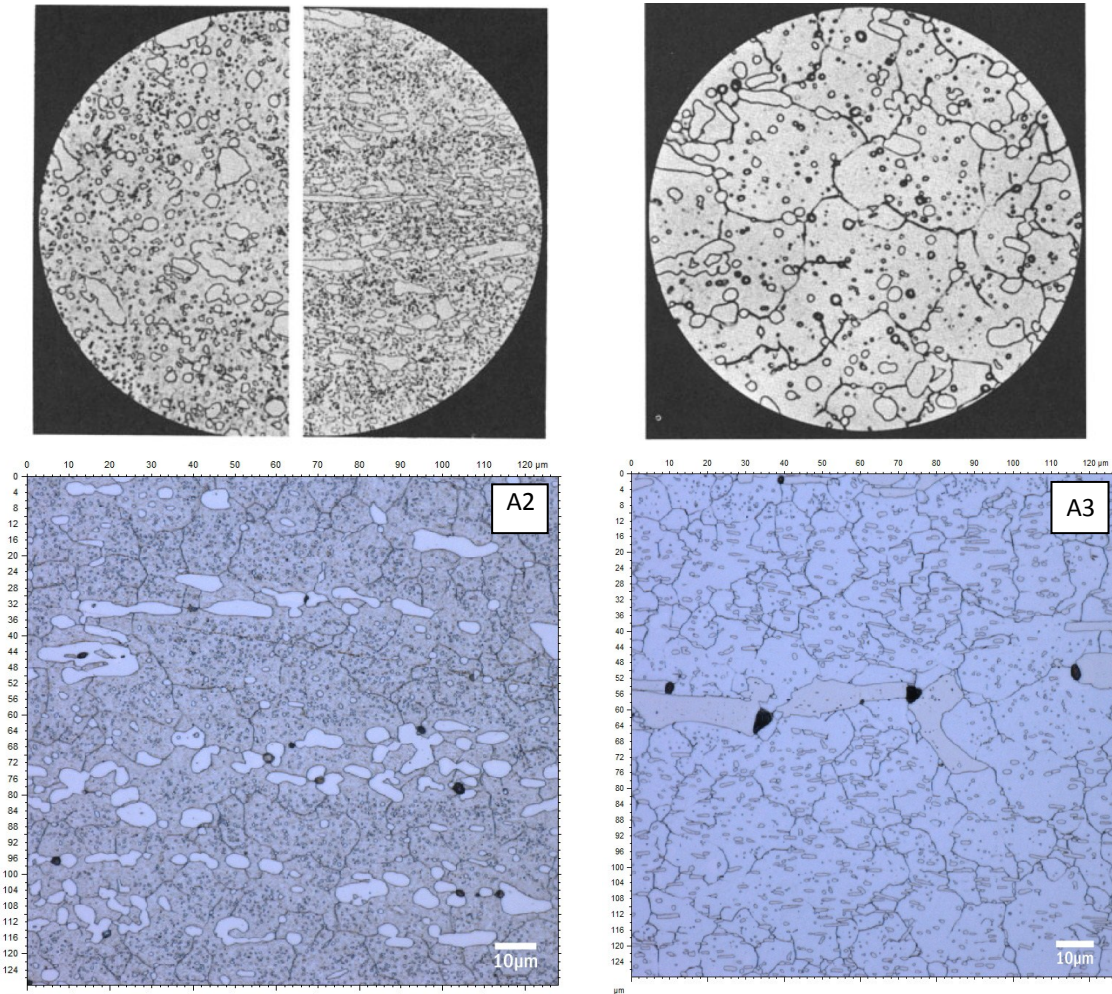


Figure 13: Microstructure of D-type tool steel. (Top Left) annealed microstructure. Left side is transverse section; right side is longitudinal section at 500x (Roberts, Krauss, & Kennedy, 1998). (Top Right) As-quenched, hardened microstructure at 100x (Roberts et al., 1998). (Bottom Left) Microstructure of die A2 etched with 3% nital. (Bottom Right) Microstructure of die A3 etched with 3% nital. Bottom images taken with confocal scanning laser microscope.

Figure 13 shows the microstructure of dies A2 and A3, which are both made of D2 tool steel. This steel is a type of high-carbon, high-chromium cold-work tool steel. The steel is alloyed primarily with chromium, which contributes to the formation of a large number of primary (large white grains) and secondary (smaller white grains) carbides which greatly

improve wear resistance in cold-work operations. The micrographs of die A2 and A3 show small voids associated with the primary carbides, which could contribute to increased susceptibility to cracking of the alloy which could decrease lifetime.

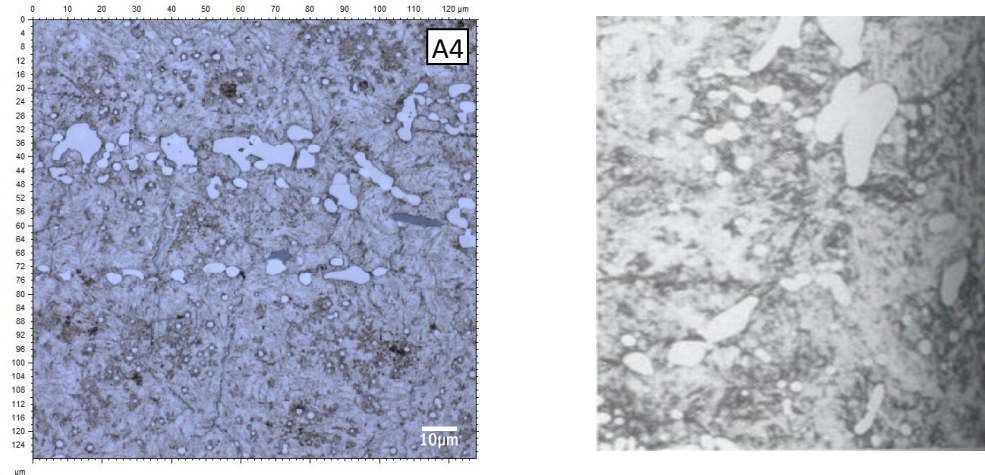


Figure 14: Microstructure of M42. (Left) microstructure of die A4 etched with nital. (Right) textbook example of M42 steel etched with Vilella's reagent. 1000x (Davis, 1995).

Die A4 was identified as M42, a type of high speed tool steel (HSS). This steel is primarily alloyed with molybdenum, with fair amounts of cobalt and chromium as well. M-type HSS maintain good hardness at elevated temperatures, and are often used for applications with a high cutting speed. There are significant amount of alloy carbides throughout the microstructure (large white and grey grains in the left image), which contribute to excellent wear resistance (Roberts et al., 1998).

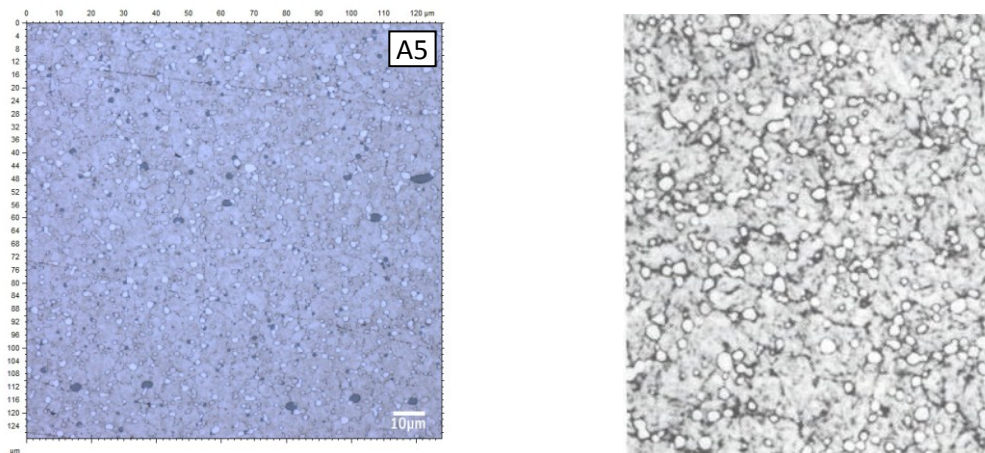


Figure 15: PM microstructure of high speed steel. (Left) CPM Rex 45 in die A5. (Right) Example of T15 powder compact. 1000x (Davis, 1995)

Die A5 is made of CPM Rex 45, which is a type of specialty powder metal high speed steel manufactured by Crucible Industries. The grain structure is very small, uniform, and absent of voids, indicating it was properly sintered. There are no large, segregated alloy carbides like there are in the other five dies. This grain structure makes the material easier to machine or grind when making the die and improves the toughness during use (Davis, 1995). In general, powder metal is being increasingly used because the alloy composition can be altered more freely, producing a wide variety of potential alloys with unique properties. Rex 45 is an alteration of conventional M3 type II chemistry in that 8% cobalt is added, which provides excellent hot hardness, wear resistance, and toughness (Crucible Industries).

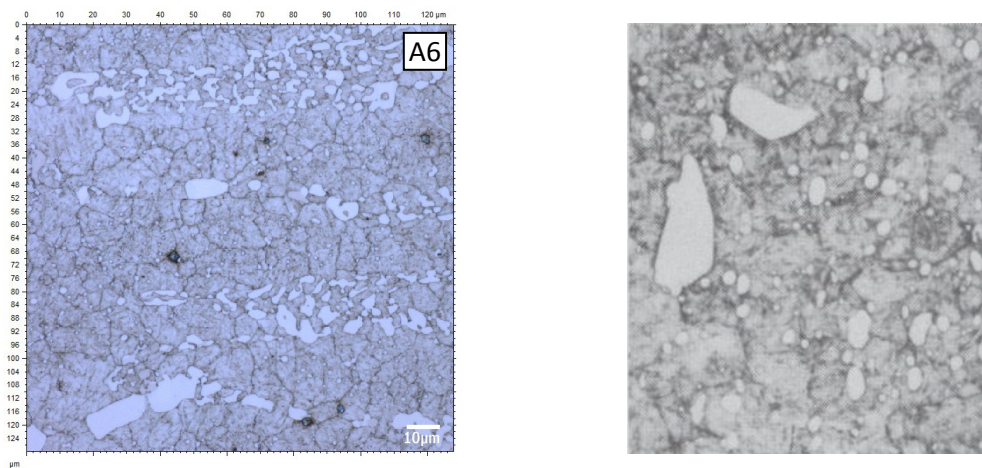


Figure 16: Microstructure of M-type high speed tool steel. (Left) M36 steel in die A6. 3% nital. (Right) M4 steel. Vilella's reagent 1000x. (Davis, 1995).

Die A6 was found to be made of M36 high speed tool steel. Most M-type tool steels are very similar in performance, and there are many alloys available with slightly different compositions. The microstructure of M36 is very similar to that of M42, though there appears to be a more dominant primary carbide phase compared to M42, as there are no secondary, grey grains. M36 has more tungsten but about half the Mo as M42, giving this steel slightly different properties. There was not a micrograph of the grain structure available in reference books, so Figure 16 compares the microstructure of die A6 with M4 tool steel, which has similar properties but a different composition. This composition difference could be the reason why the carbide size and distribution is different between the two images.

3.1.3 Hardness Profiles

Figures 17-22 are hardness vs. depth graphs for each thread that had a hardness profile created. Each die had a used and a new thread hardness profile.

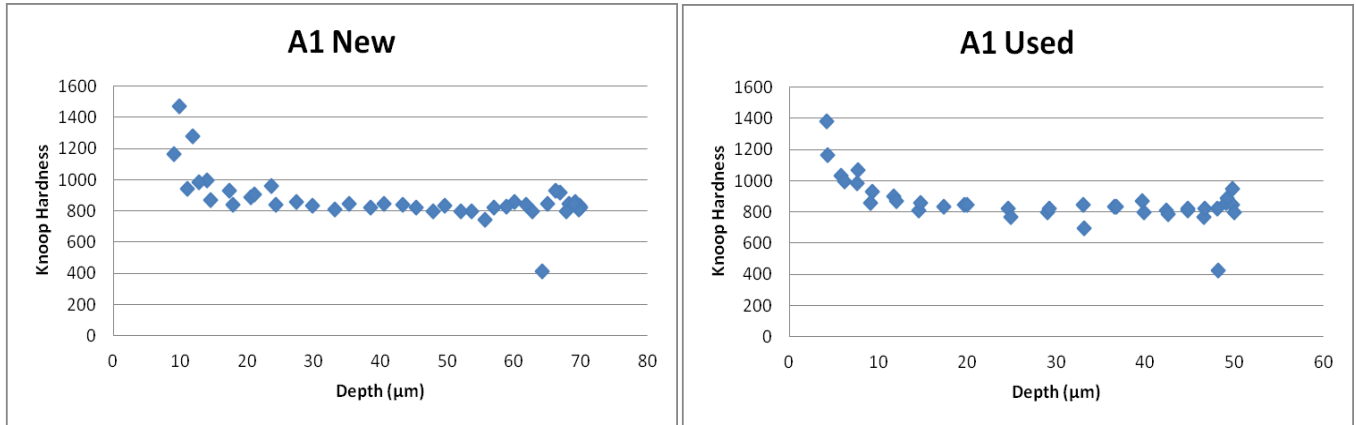


Figure 17. Hardness vs. Depth graph for A1

A1 has a noticeable increase in hardness as the indents get closer to the surface. This could be due to due to carburization at the surface, which is a common feature of A2 steel (Davis, 1994). The change appears to be similar between the used and the new thread.

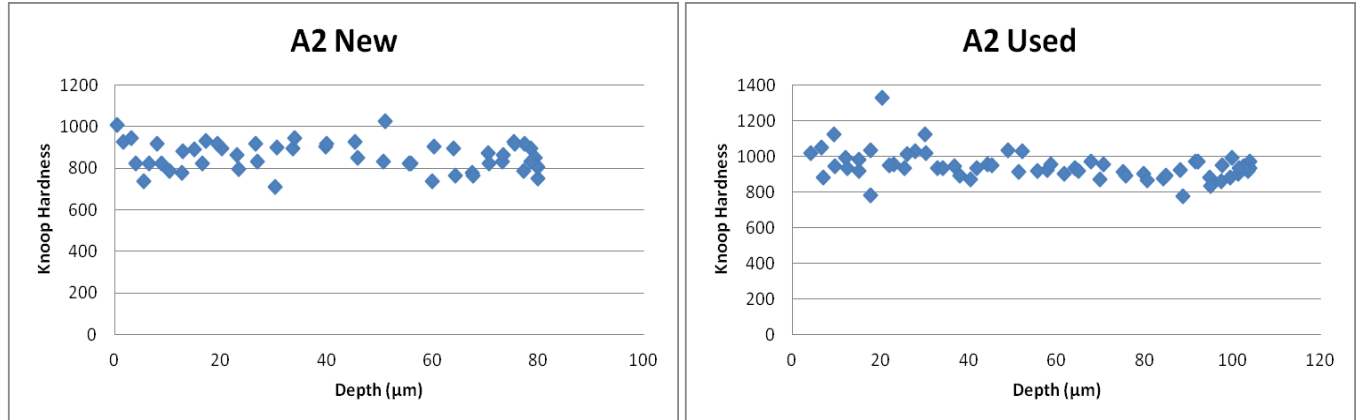


Figure 18. Hardness vs. Depth graph for A2

A2 does not have a noticeable change in hardness as depth changes. There is greater variation in hardness tests taken near the surface of the used thread, which may indicate localized variability in hardness when compared to the new thread. It could also be a result of the specific locations of where the hardness indents were taken.

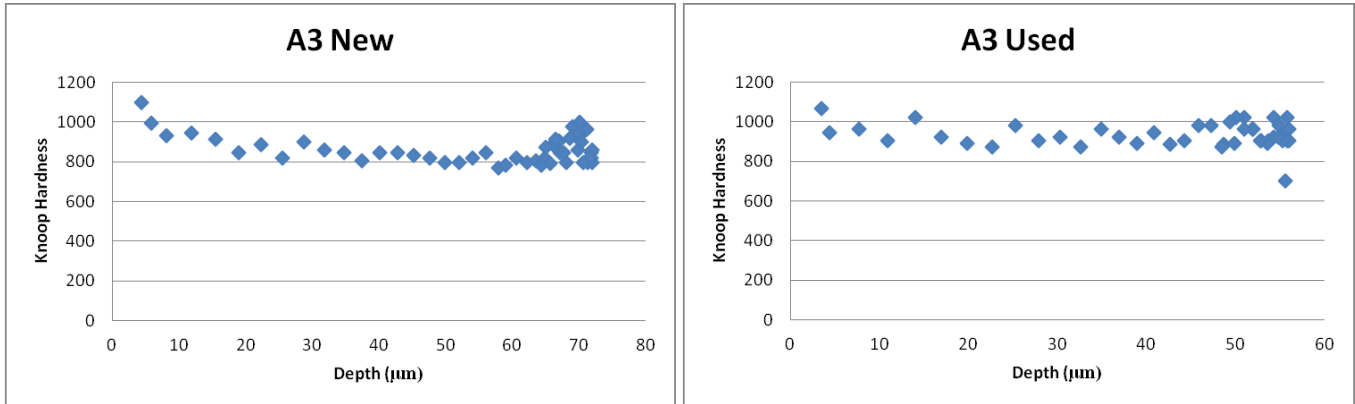


Figure 19. Hardness vs. Depth graph for A3

There is an increase in hardness closer to the surface of A3, particularly with the new thread. The used thread does not have an increase and appears to remain relatively constant throughout the thread, though there appear to be undulations in the data, which could indicate the location of carbide bands with higher hardness.

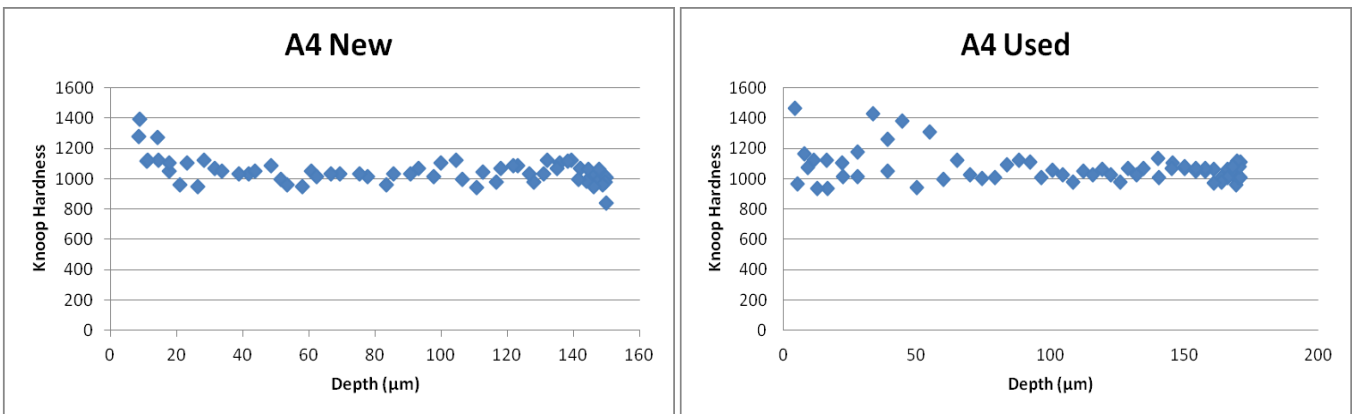


Figure 20. Hardness vs. Depth graph for A4

There appears to be an increase in hardness closer to the surface of the threads in A4. The new thread shows a more consistent trend, while the used thread shows more scattered data that may only indicate certain points of increased hardness. This could be an indication of readings being taken on harder grains such as carbides.

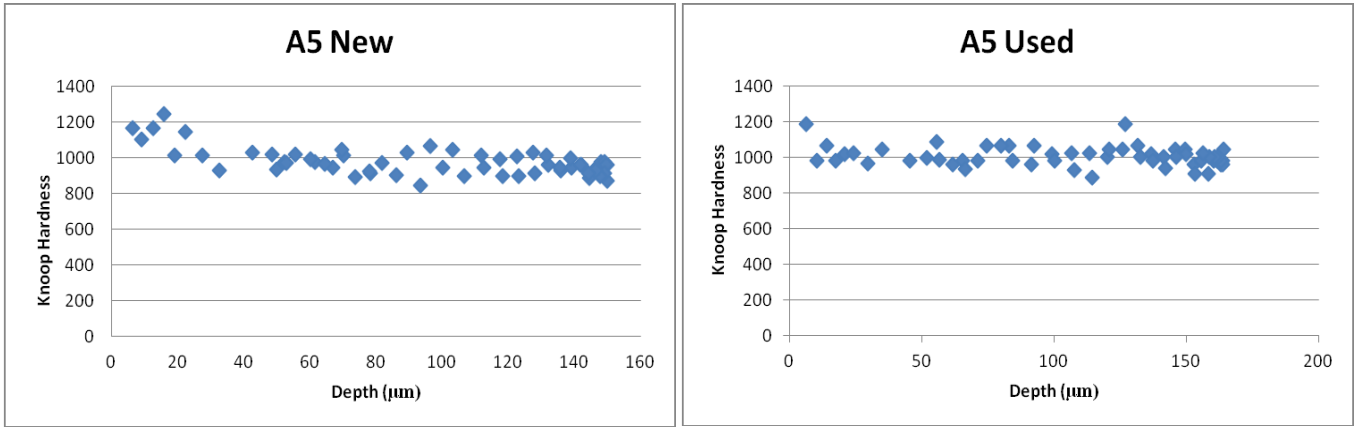


Figure 21. Hardness vs. Depth graph for A5

A5 shows a slight increase in hardness closer to the surface, potentially indicating slight work hardening. The surface hardening is more noticeable in the new thread as opposed to the used thread. This may indicate the die was initially surface hardened, but did not work harden during use. However, the trend is not very noticeable so the increased readings may be caused by a localized condition.

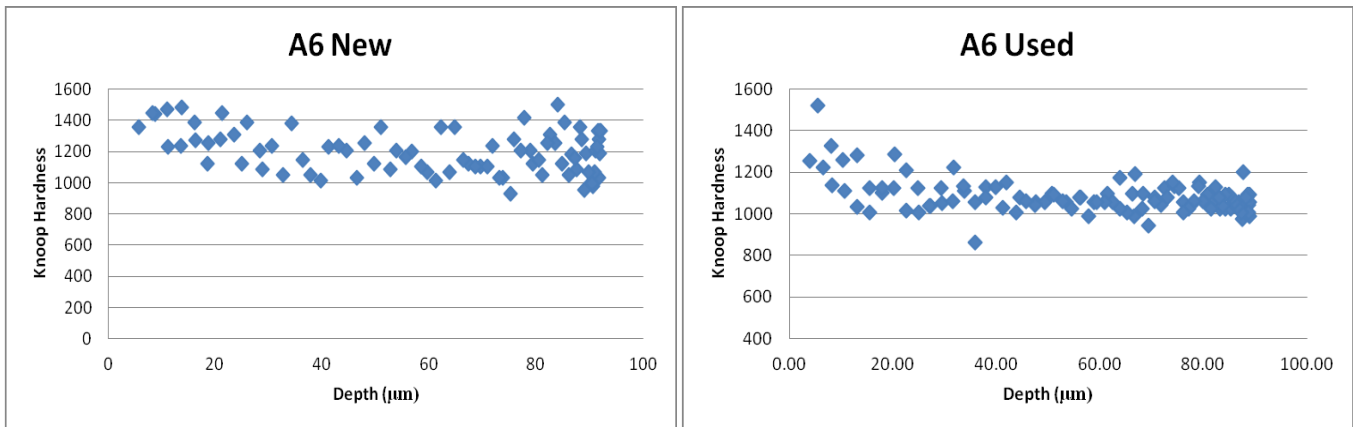


Figure 22. Hardness vs. Depth graph for A6

A6 shows variable readings throughout the depth profile. There is a trend toward harder readings near the surface, especially in the used die. The hardness readings for the new thread appear to have more variability than the readings for the used thread, which may be due to localized around the indent.

To compare the hardness data from the six dies, a box and whisker plot was created of all data sets. Figure 21 plots various statistical values associated with each hardness profile so they can be compared. The plot does not take depth into account.

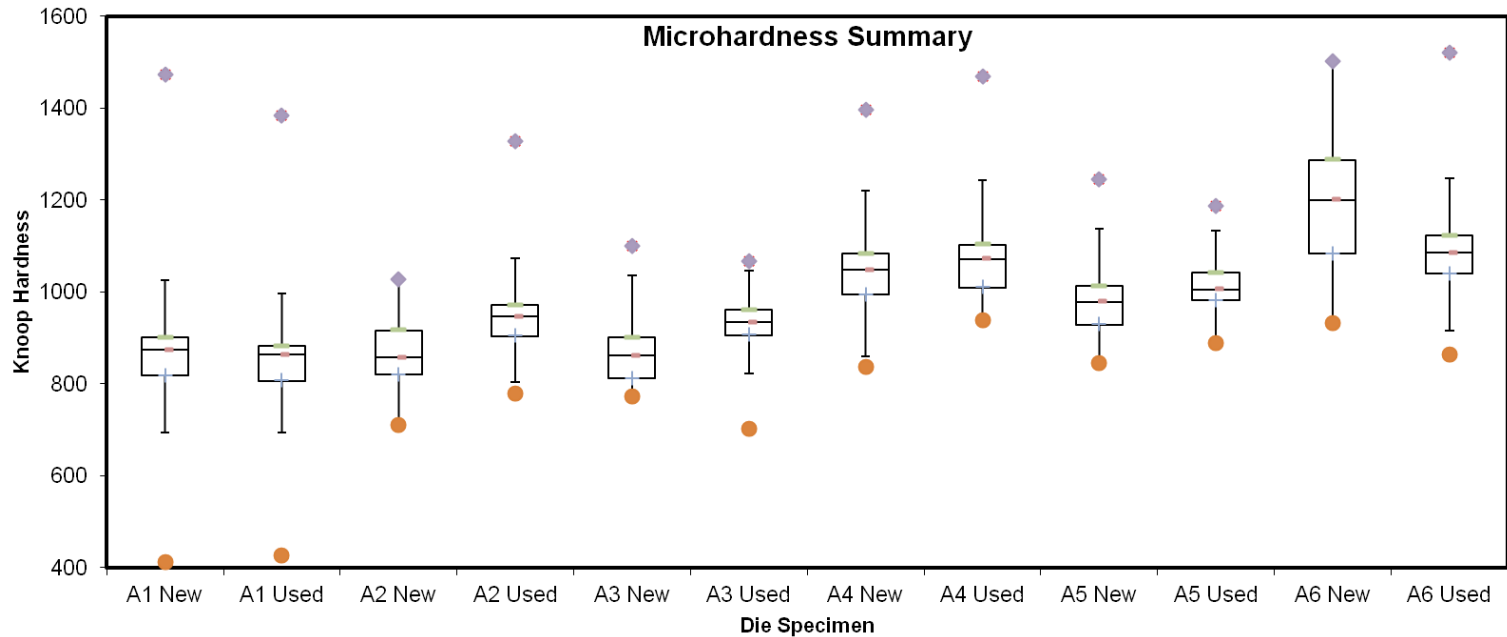


Figure 23: Box and Whisker plot summary of hardness profiles. See ‘Features of a Box and Whisker Plot’ in Appendix B.

Table 8: Summary of statistical values needed to create box and whisker plot in Figure 23. Bottom three rows also show standard deviation, median, and the lifetime of the dies which were not used to create Figure 23.

Labels	A1 New	A1 Used	A2 New	A2 Used	A3 New	A3 Used	A4 New	A4 Used	A5 New	A5 Used	A6 New	A6 Used
Min	411.45	427.55	711.5	778.5	772	703	837	938	846	888	931.5	863
Q ₁	819	807	820.375	904.5	813	906.5	994.625	1010.5	929.625	982.5	1084.5	1040
Mean	874.79	864.48	858.17	947.33	861.91	934.48	1048.91	1072.68	979.04	1006.07	1200.93	1085.46
Q ₃	901.875	882.625	917	972	902.25	962	1084.5	1103.5	1013	1043	1288.125	1123
Max	1473	1384	1028	1328	1100.5	1066	1395.5	1468.5	1245	1187.5	1503	1520.5
IQR	82.875	75.625	96.625	67.5	89.25	55.5	89.875	93	83.375	60.5	203.625	83
Upper Outliers	3	4	0	3	1	1	3	5	4	2	0	6
Lower Outliers	1	1	0	2	0	1	1	0	0	1	0	1
Standard Dev	152.5	142.8	69.2	80.4	69.1	60.1	85.5	106.3	76.2	55.6	138.9	83.5
Median	842.25	839.75	857.25	935.50	846.00	925.00	1030.00	1060.75	965.25	1001.00	1209.50	1060.50
Lifetime	50,000 Pieces		59,458 Pieces		None specified		20,000-22,000 Pieces		20,000-22,000 Pieces		44,000-48,000 Pieces	

3.1.4 Failure Mechanism

Images of each new and used thread crest are presented in this section. The new thread is on the left, the used thread is on the right. The images show the top of the thread, as the angled sides of the threads did not appear clearly on the images. All images were taken with a 20x objective lens on a confocal laser scanning microscope.

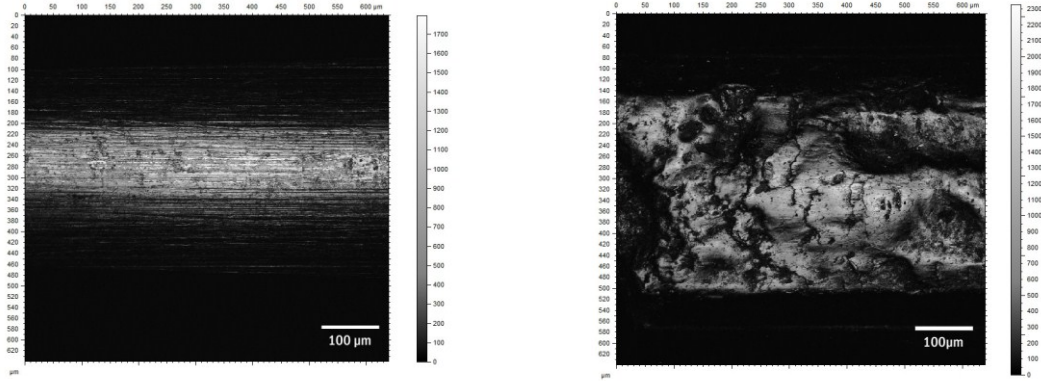


Figure 24 thread crest of die A1. (Left) New thread. (Right) Used thread.

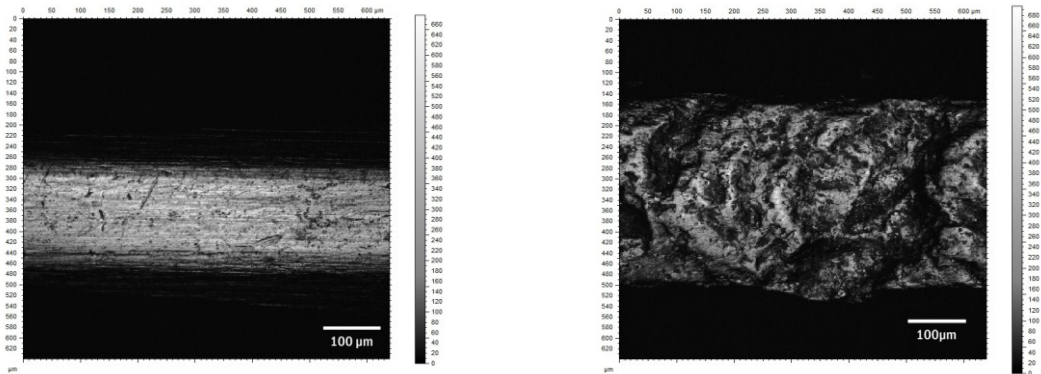


Figure 25: Thread crest of die A2. (Left) New thread. (Right) Used thread.

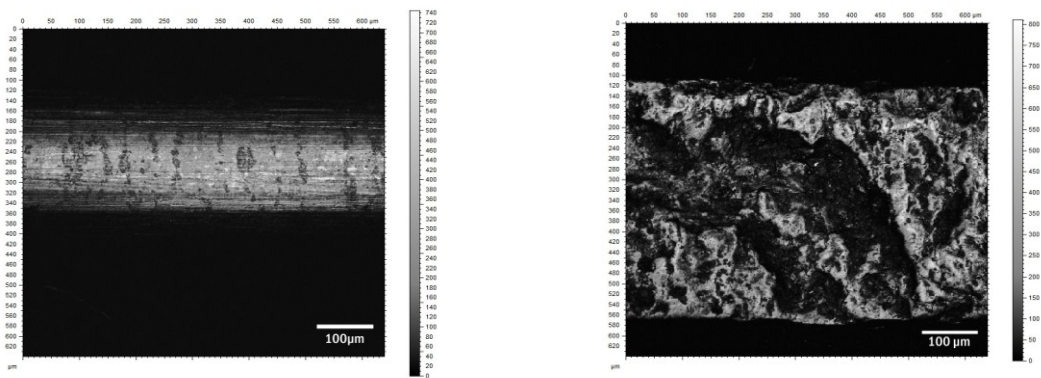


Figure 26: Thread crests of die A3. (Left) New thread. (Right) Used thread.

Figures 24-26 show the thread crests for dies A1, A2, and A3. They are made of A2 or D2 steel and appear to have failed by spalling. Based on the similarity to Figure 25 which shows D2 threads that have failed from spalling. To definitively determine if the fracture occurred through spalling SEM images would be needed to look at the grain-scale fracture surfaces.

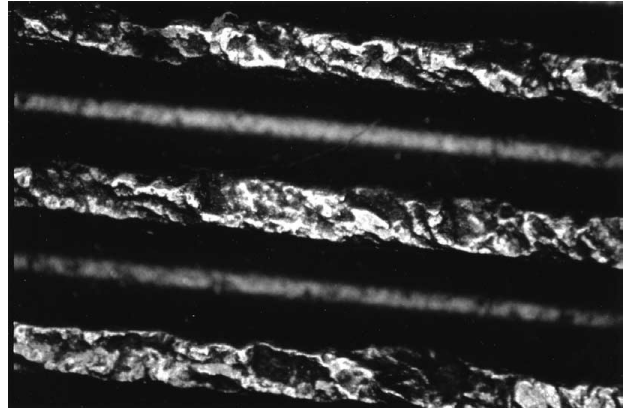


Figure 27: Macro-scale image of spalled thread crests on D2 tool steel (Gagg, 2005).

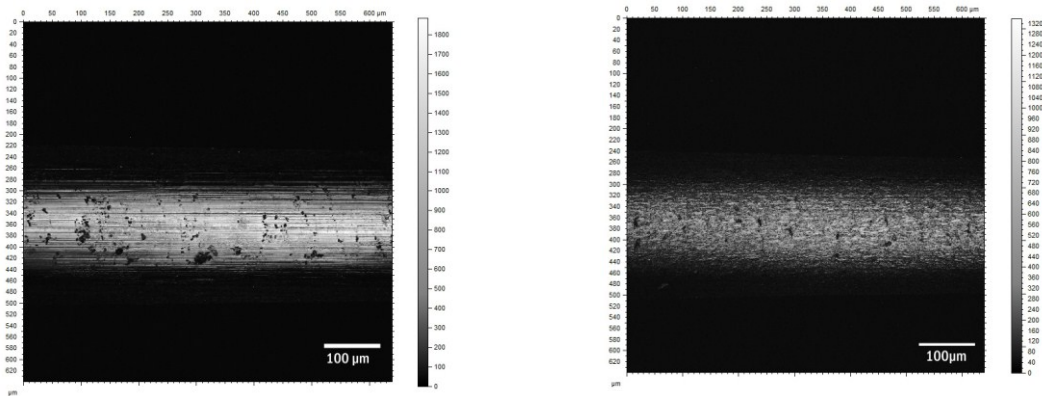


Figure 28: Thread crests of die A4. (Left) New thread. (Right) Used Thread.

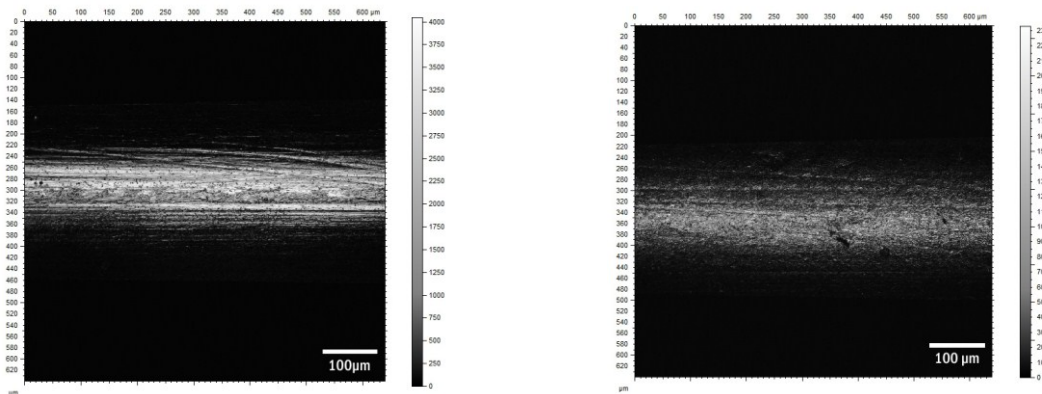


Figure 29: Thread crests of die A5. (Left) New thread. (Right) Used thread.

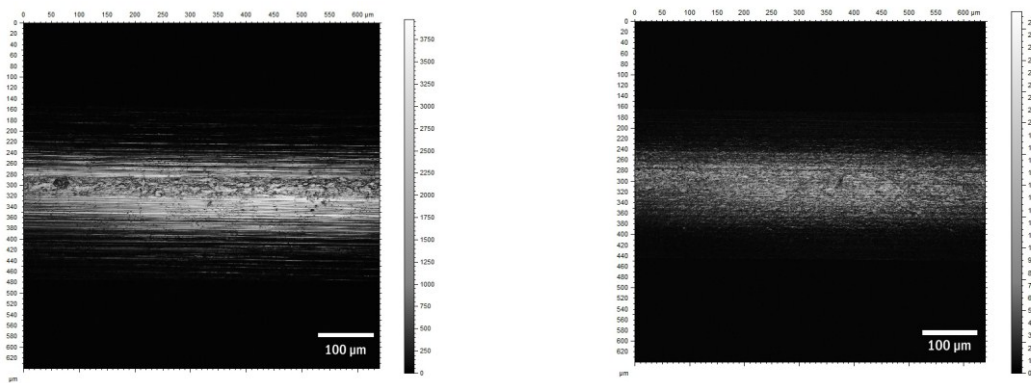


Figure 30: Thread crests of die A6. (Left) New thread. (Right) Used thread.

Figures 28-30 show the thread crests of dies A4, A5, and A6, which are made of high speed tool steel. The most common wear mechanisms for high speed steel are edge chipping, abrasion, adhesive wear, and continuous wear (Soderberg & Hogmark, 1986). The grinding marks on the new threads have become less noticeable and the whole surface of the thread has taken on a more homogenous visual texture, which potentially indicates that the surfaces were subject to abrasive wear. On dies A4 and A5, there are divots in the worn surface, which could have resulted from adhesive wear or indicate locations where cracks are beginning to form. SEM micrographs would reveal the nature of those divots. Without further observation the failure mode cannot be absolutely determined, but at this scale of observation the failure mode appears to be abrasive wear.

3.2 Surface Analysis

3.2.1 New vs. Used

The figure below shows which height parameters are able to discriminate between the new and used regions of each die. For this figure and the following discrimination matrices, green corresponds to a discrimination confidence level greater than 99%, yellow to greater than 90%, and red to less than 90%.

New vs Used: Height Parameters

Dies	St	Sp	Sv	Sq	Sa	Ssk	Sku
A1 New vs Used	Green	Green	Green	Green	Green	Red	Yellow
A2 New vs Used	Yellow	Red	Green	Green	Green	Yellow	Yellow
A3 New vs Used	Green	Green	Green	Red	Red	Red	Yellow
A4 New vs Used	Red	Red	Red	Red	Red	Red	Red
A5 New vs Used	Red	Red	Red	Red	Red	Red	Red
A6 New vs Used	Red	Red	Green	Red	Red	Red	Green

Figure 31: Discrimination by height parameters for new vs. used regions

Figure 32 is an example of an area-scale graph of the new and used region of a die and its correspond F-test. For this F-test and all that follow in this report, the lower blue line represents a confidence level of 90%, the middle line represents 95%, and the top line 99%. As the relative areas of the new and used regions start to converge at the lower scales the confidence level in discrimination between the two goes down. This is reflected in the F-test shown to the right of the relative area plot in Figure 30.

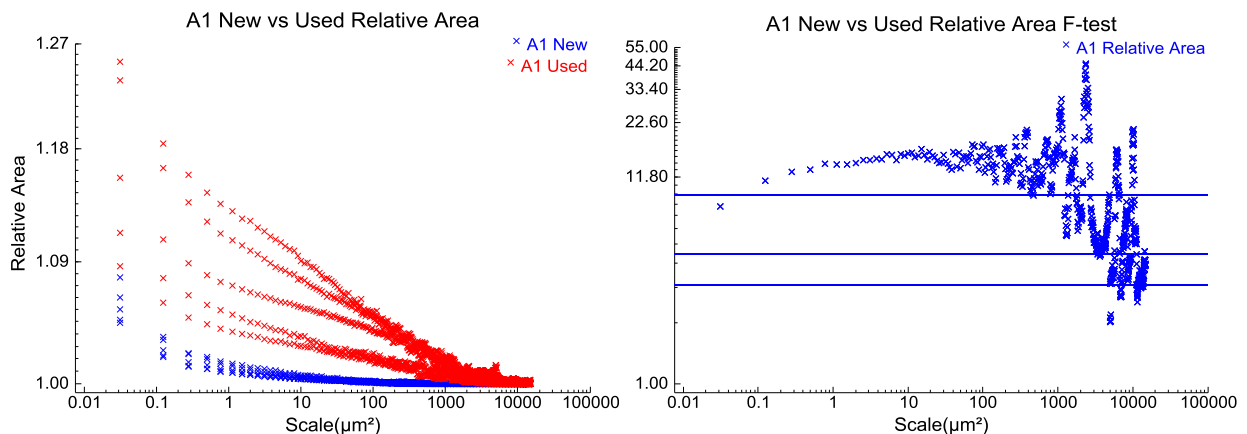


Figure 32: Example relative area graph for a new vs. used section and corresponding F-test graph

Figure 33 summarizes at which scales discrimination is possible between the new and used region of each die using relative area. All new vs. used relative area and F-tests can be found in the appendix. The color of each box represents the level of confidence for discrimination. Green corresponds to greater than 99%, yellow to greater than 90%, and red to less than 90%.

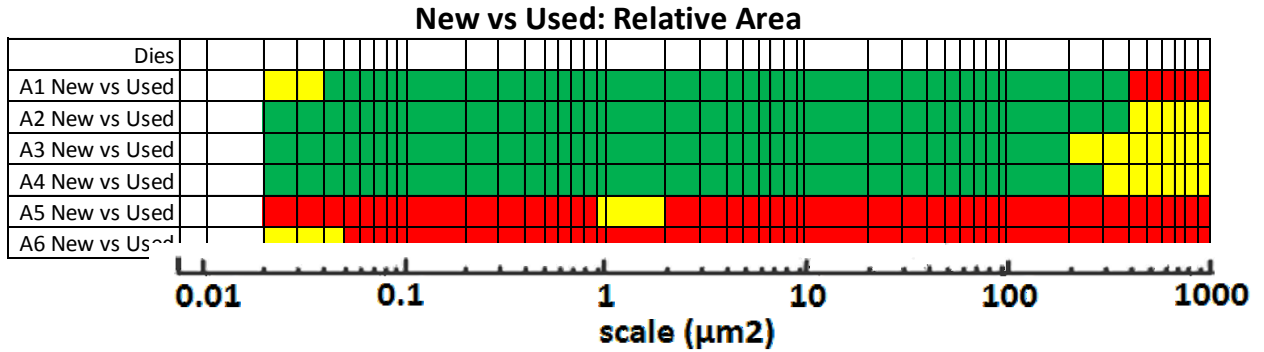


Figure 33: Discrimination by relative area for new vs. used regions

Figure 34 shows the complexity of the new and used regions as a function of scale for the A1 die. The F-test graph to the left of the relative area graph shows at what scales discrimination is possible between the new and used regions of die A1 as well as the level of confidence.

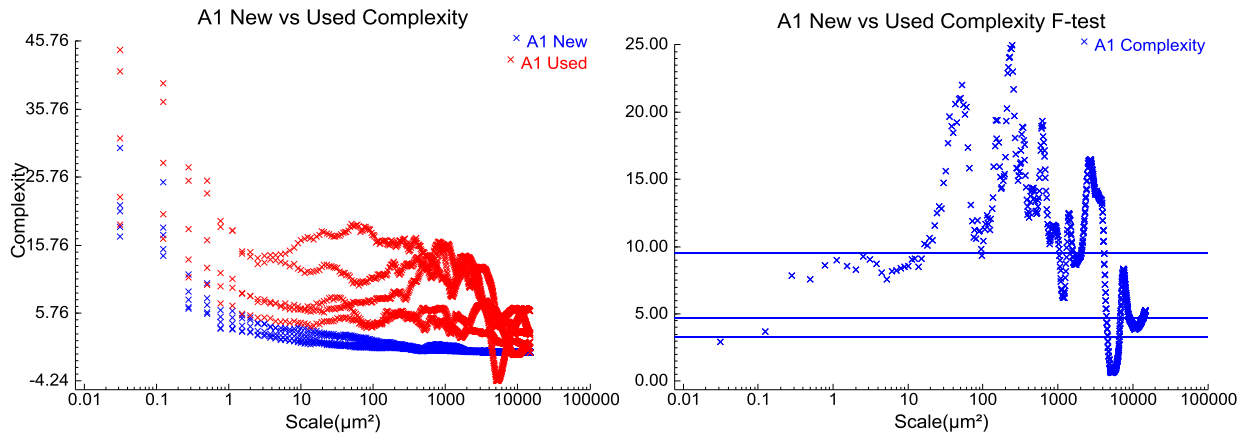


Figure 347: Example complexity-scale plot for a new vs. used region and corresponding F-test graph

Figure 35 below summarizes at which scales we are able to discriminate between the new and used region of each die using complexity-scale. All new vs. used complexity-scale and F-test graphs can be found in the appendix.

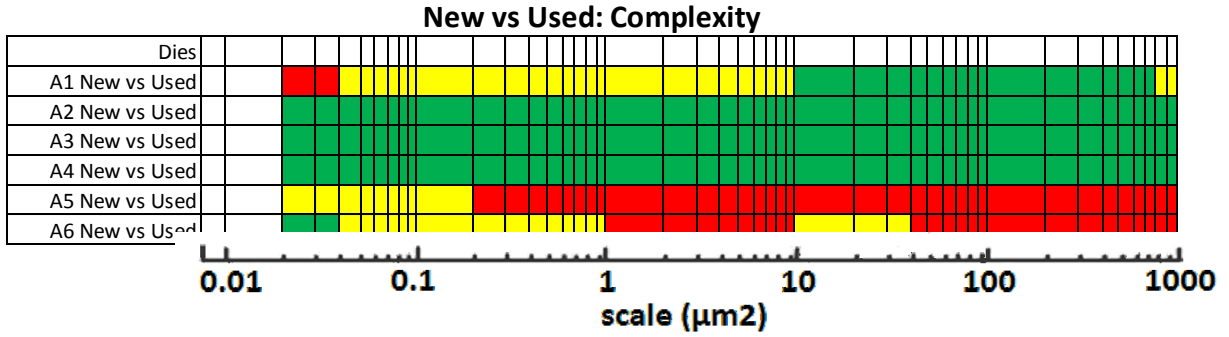


Figure 35: Discrimination by complexity-scale for new vs. used regions

3.2.2 New vs. New

Figure 36 shows the average of the five relative area results of the new regions of each die.

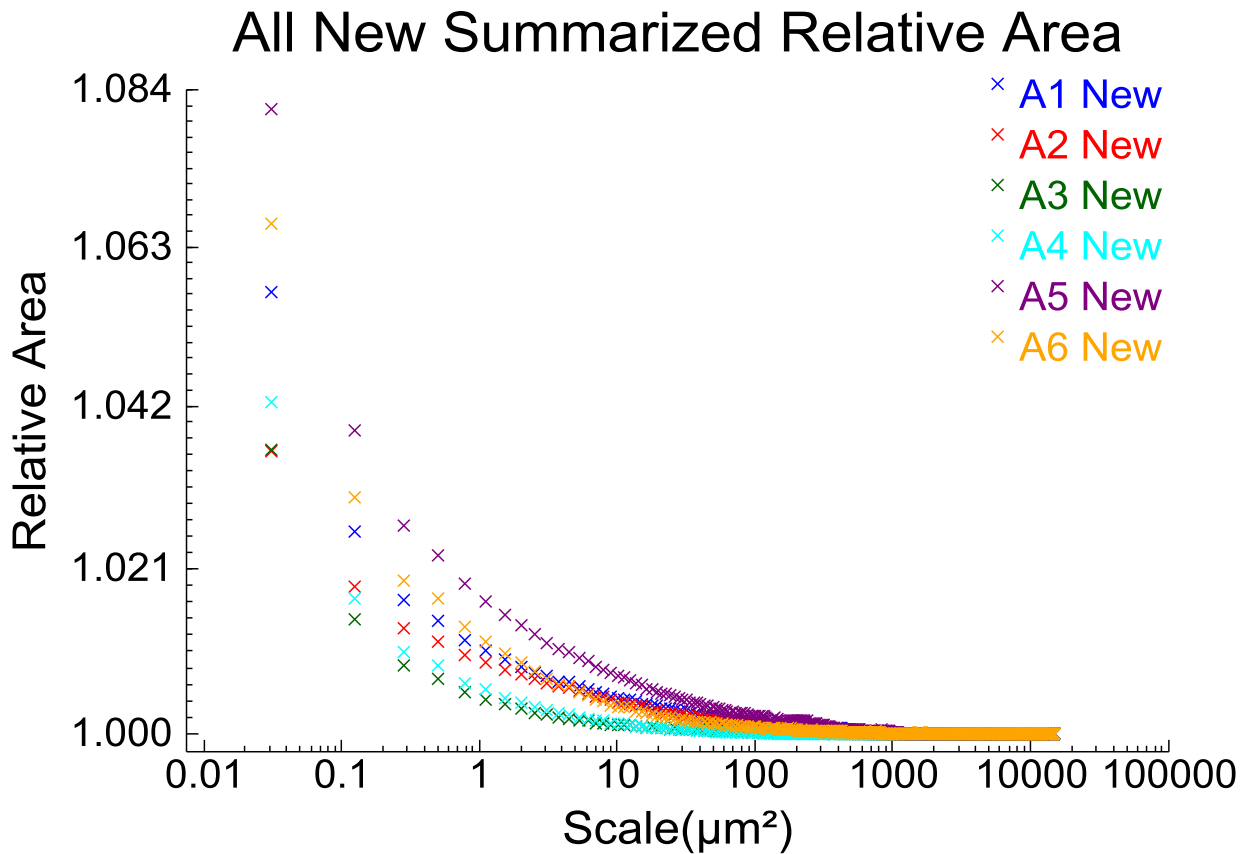


Figure 36: Graph of averaged relative area for the new regions of each die

The height parameters that are able to discriminate between the new regions of each die are shown in Figure 37.

New vs New: Height Parameters

	Dies	St	Sp	Sv	Sq	Sa	Ssk	Sku
A1 vs A2		Yellow	Green	Red	Yellow	Yellow	Green	Green
A1 vs A3		Red	Red	Red	Yellow	Yellow	Yellow	Yellow
A1 vs A4		Red	Red	Red	Red	Red	Yellow	Yellow
A1 vs A5		Red	Yellow	Red	Yellow	Yellow	Red	Red
A1 vs A6		Red	Red	Red	Green	Green	Yellow	Yellow
A2 vs A3		Yellow	Green	Yellow	Red	Red	Red	Red
A2 vs A4		Yellow	Green	Red	Yellow	Yellow	Red	Red
A2 vs A5		Red	Red	Yellow	Red	Red	Green	Green
A2 vs A6		Red	Yellow	Yellow	Red	Red	Red	Red
A3 vs A4		Red	Red	Red	Yellow	Yellow	Red	Red
A3 vs A5		Yellow	Yellow	Red	Red	Red	Yellow	Green
A3 vs A6		Red	Red	Red	Red	Red	Red	Red
A4 vs A5		Red	Green	Red	Green	Green	Red	Green
A4 vs A6		Red	Yellow	Yellow	Green	Green	Red	Red
A5 vs A6		Red	Red	Red	Red	Red	Yellow	Green

Figure 37: Discrimination by height parameters for new regions

Figure 38 is an example of a new vs. new relative area graph and its corresponding F-test graph. All new vs. new area-scale graphs and corresponding F-tests and be found in the appendix.

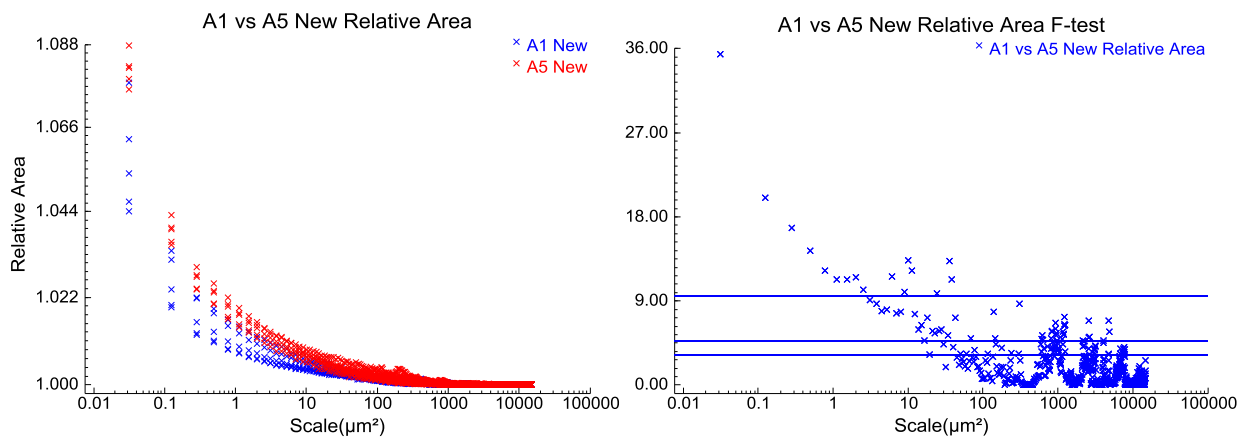


Figure 388: Example relative area graph for new regions and the corresponding F-test graph

Figure 39 summarizes at which scales discrimination between the new regions is possible and to what level of confidence.

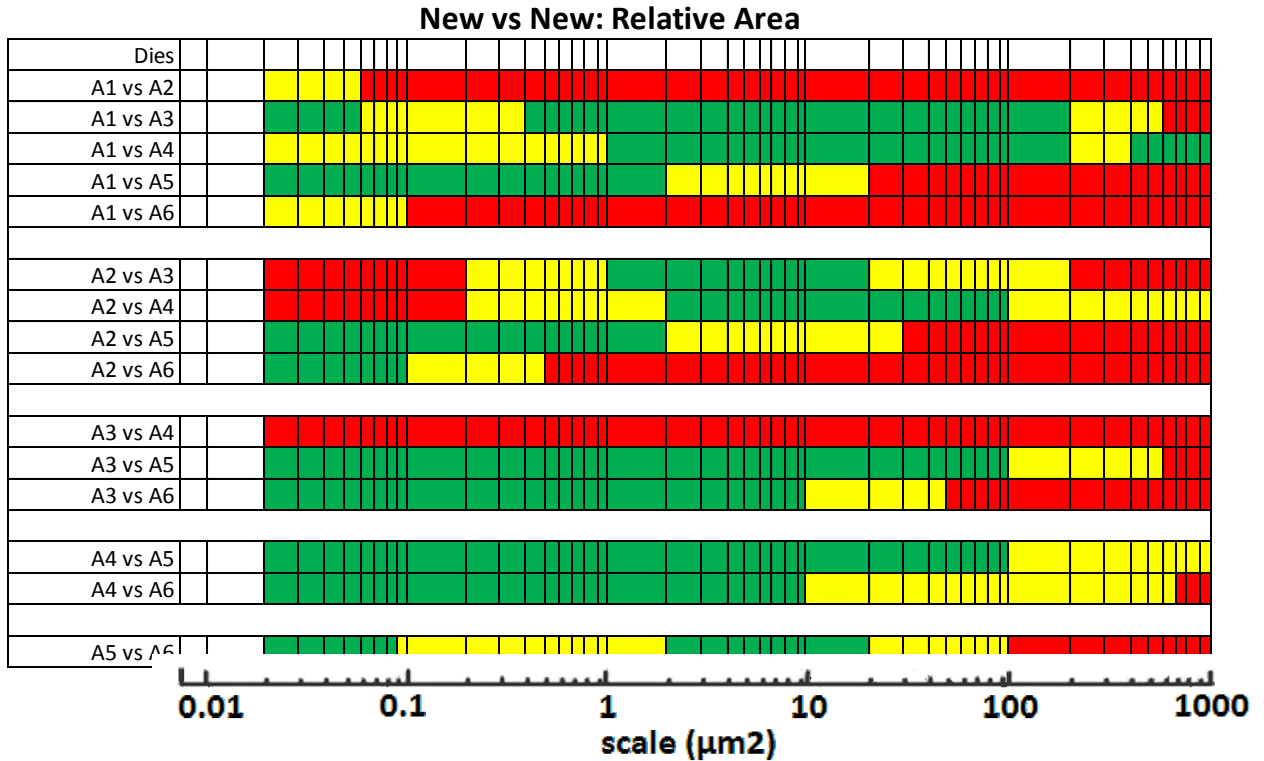


Figure 39: Discrimination by relative area for new regions

An example complexity-scale graph for a new vs. new comparison is shown in Figure 40 below with its corresponding F-test. All of the new vs. new complexity graphs and F-tests can be found in the appendix.

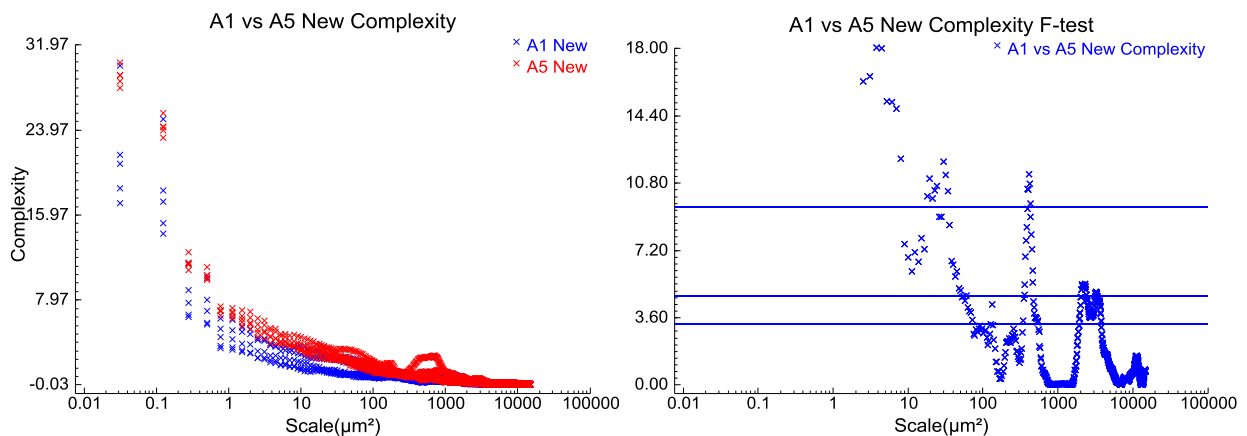


Figure 40: Example Complexity-scale graph for new regions and the corresponding F-test graph

Figure 41 summarizes the ability of complexity to discriminate between the new regions of each die.

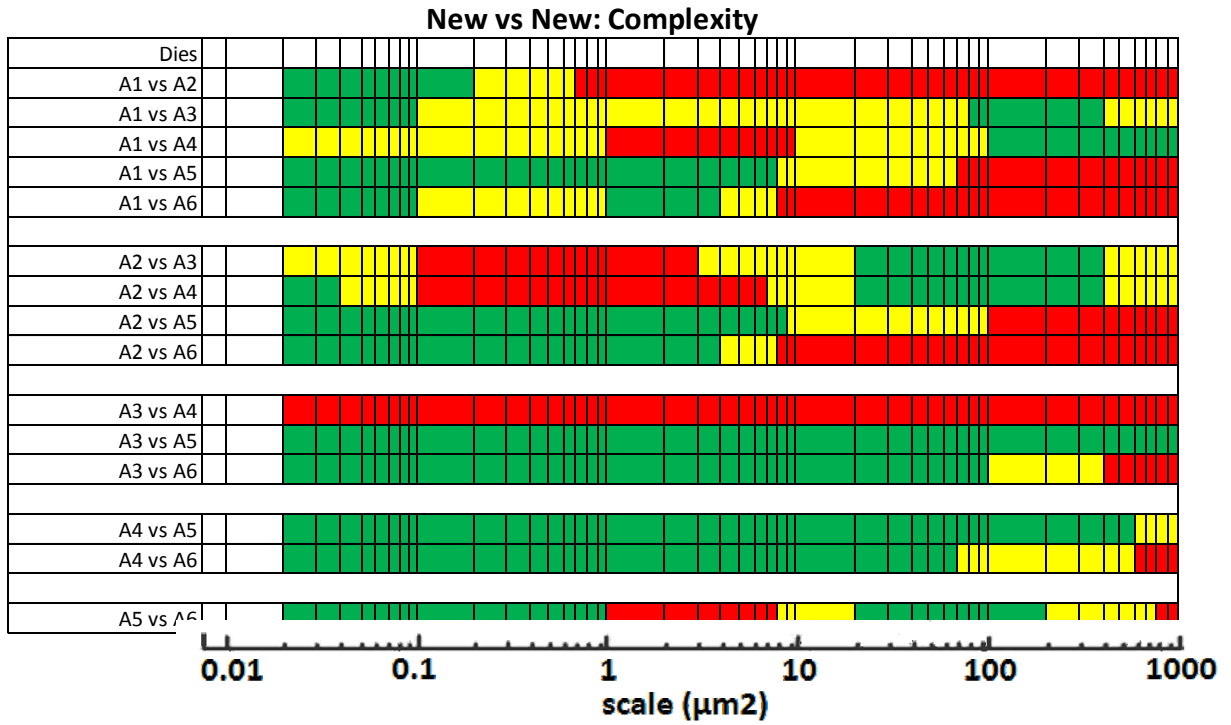


Figure 419: Discrimination by Complexity-scale for new regions

3.2.3 Used vs. Used

Figure 42 shows the height parameters that are able to discriminate between the used regions of each die and with what confidence.

Used vs Used: Height Parameters

Dies	St	Sp	Sv	Sq	Sa	Ssk	Sku
A1 vs A2	Red	Red	Red	Red	Red	Red	Yellow
A1 vs A3	Yellow	Red	Yellow	Green	Green	Green	Red
A1 vs A4	Green	Green	Green	Green	Green	Green	Red
A1 vs A5	Green	Green	Green	Green	Green	Red	Yellow
A1 vs A6	Green	Green	Green	Yellow	Yellow	Red	Green
A2 vs A3	Red	Red	Yellow	Green	Green	Yellow	Green
A2 vs A4	Yellow	Green	Green	Green	Green	Red	Red
A2 vs A5	Green	Green	Green	Green	Green	Red	Red
A2 vs A6	Green	Green	Green	Yellow	Yellow	Red	Red
A3 vs A4	Yellow	Green	Red	Yellow	Green	Yellow	Red
A3 vs A5	Yellow	Yellow	Yellow	Red	Red	Green	Green
A3 vs A6	Red	Green	Red	Red	Red	Yellow	Green
A4 vs A5	Red	Red	Red	Green	Green	Red	Red
A4 vs A6	Red	Red	Red	Green	Green	Red	Yellow
A5 vs A6	Red	Red	Red	Red	Red	Red	Red

Figure 42: Discrimination by height parameters for used regions

The relative area graph for the A1 vs. A3 dies is shown in Figure 43 with the corresponding F-test.

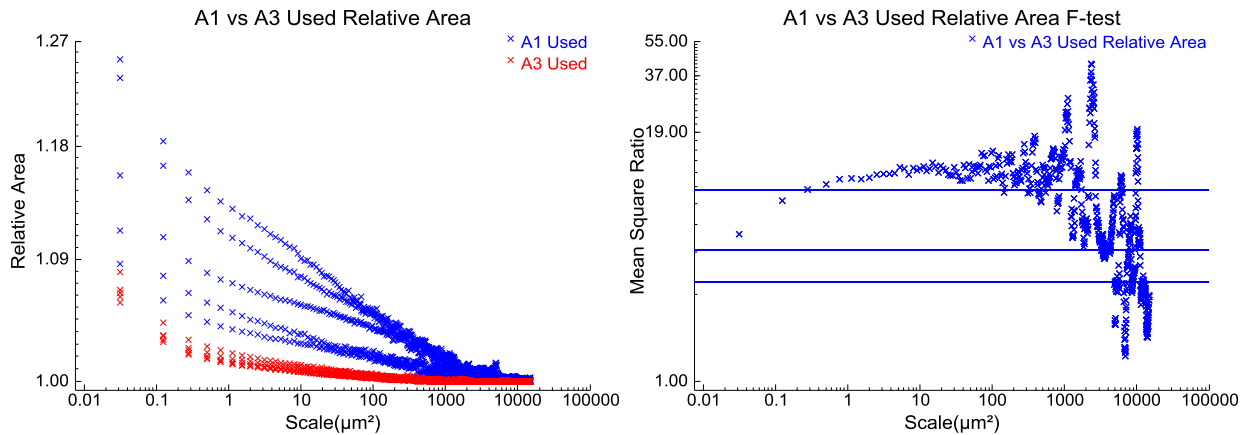


Figure 43: Example relative area graph for used regions and the corresponding F-test graph

The scales are which relative area is able to discriminate between the used regions and with what level of confidence is summarized in Figure 44.

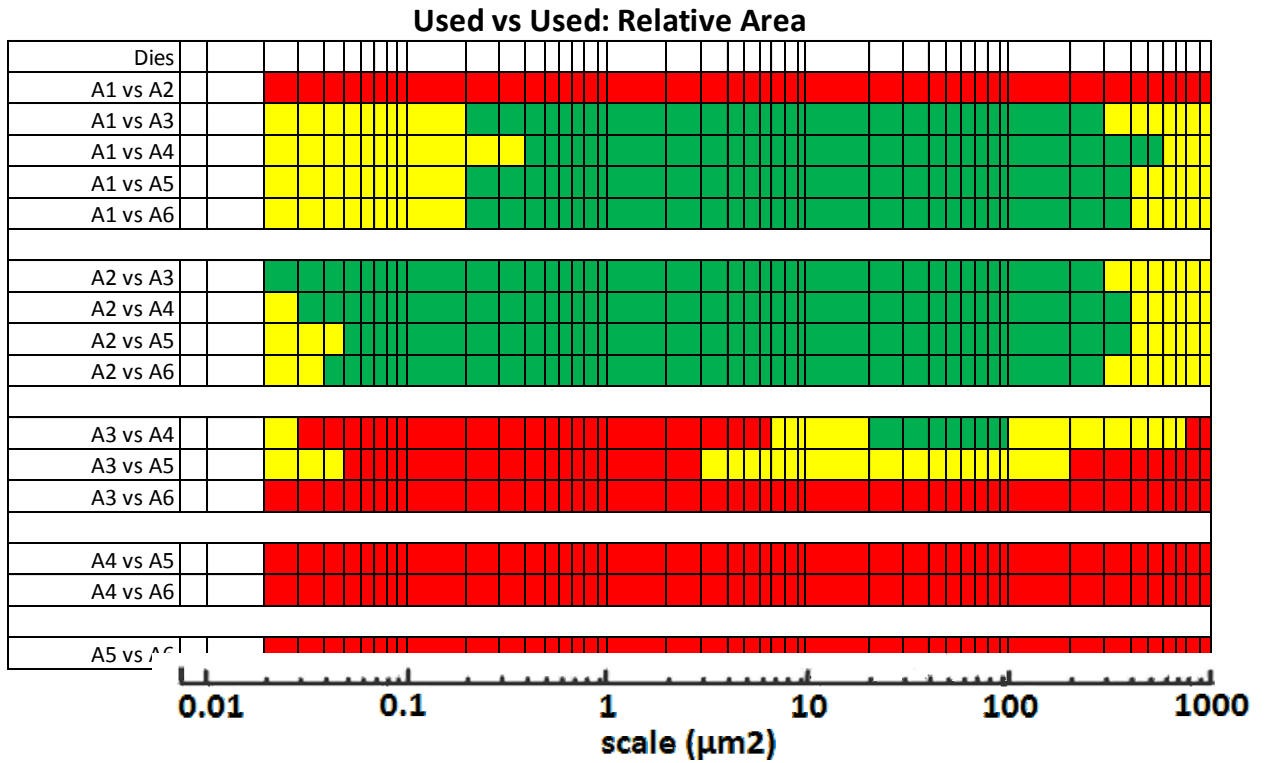


Figure 44: Discrimination by Area-scale for used regions

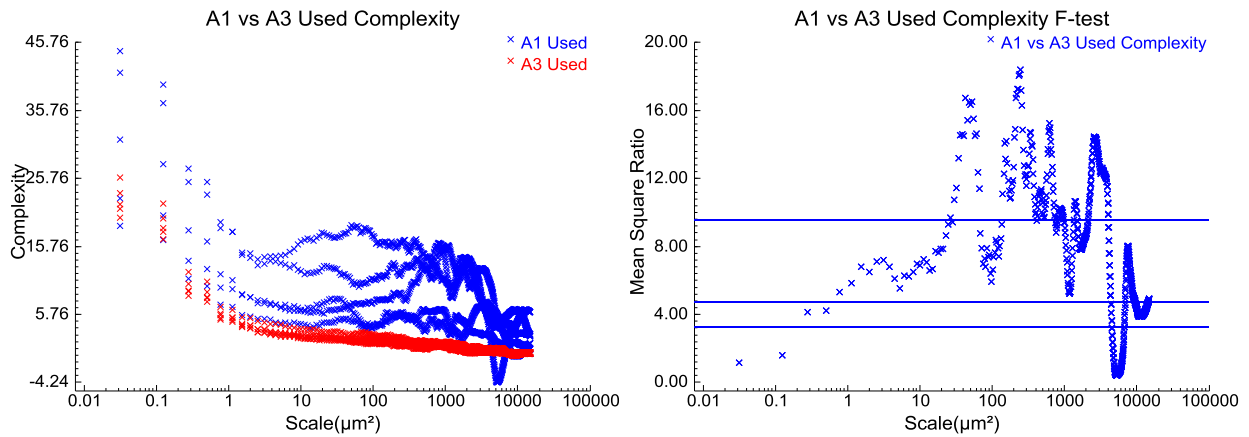


Figure 45: Example complexity-scale graph of used regions and corresponding F-test graph

Figure 46 summarizes the ability of complexity to discriminate between the used regions for all die.

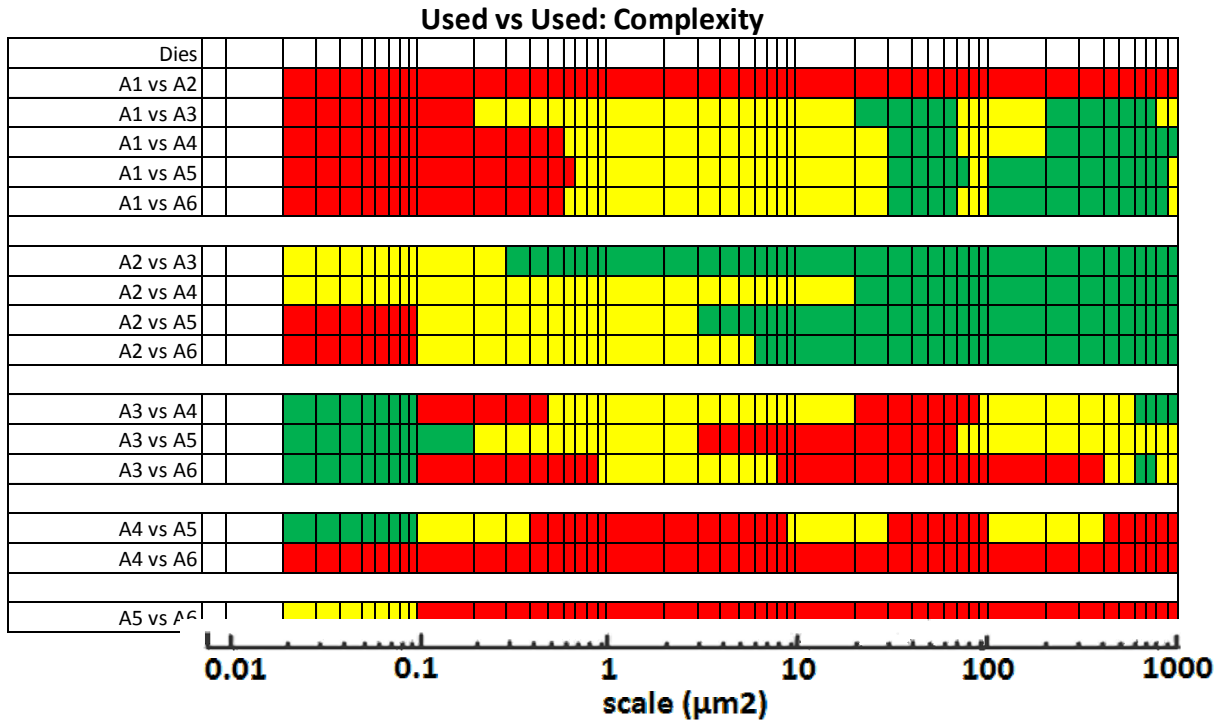


Figure 46: Discrimination by complexity-scale for used regions

4.0 Discussion

4.1 Alloy Type

Dies A1, A2, and A3 (larger dies) are made of A2 or D2 steel which are two of the most commonly used alloys for thread rolling dies (Davis, 1995). These alloys are used because they display good hardness, toughness and wear resistance (Gagg, 2001). They have a high carbon and alloy content which promotes the growth of hard alloy carbides that increase the wear resistance. Though the two steels have similar properties, A2 is known to have slightly lower performance than D2, which might be one of the reasons why die A1 did not last as long as die A2 (Nowicke, 1991). Though A2 steel is known to have slightly lower performance, it is often preferred to D2 because it exhibits higher crack resistance and lower distortion during air hardening, about .04%, and does not require a quenching medium (Davis, 1995). A2 is more susceptible to decarburization than D2, which may further detract from its overall performance. However, die A1 showed a hardness increase closer to the surface, so it is possible that the material was actually slightly carburized, or that there is a higher concentration of carbides closer to the surface. D2 steel has higher chromium content than A2, which contributes to a greater abundance of hard chromium carbides throughout the microstructure that contribute to improved wear resistance. The higher chromium content also provides some protection against oxidation (Roberts, Krauss, & Kennedy, 1998).

The smaller dies, A4, A5, and A6, were made of high speed tool steels. High speed steel (HSS) in general has properties similar to cold-worked steel, but exhibits better hot hardness which is important when rolling at higher speeds and temperatures (Davis, 1995). Die A4 was most likely made of M42, die A5 was CPM Rex 45 (powder metal), and die A6 was made from M36. The fact that each die was made of a different alloy may indicate that there is a wider variety of HSS materials that work for thread rolling than the cold-work materials, though without a larger number of dies to examine that conclusion cannot be reached. Many literature sources suggests using M1 or M2 HSS for rolling dies, which contrasts with a lack of M1 or M2 dies in this study (Gagg, 2001). It is possible that those alloys are common for these types of dies; the team just did not receive one. One source cited that M-type tool steels are better for longer production runs, rolling larger parts with coarser threads, which contrasts directly with the observations in this MQP where the smaller dies were made of HSS (Davis, 1995). Little

information was available about the relative performance of different grades of M-type tool steel, so a conclusion cannot be reached about why none of the dies examined were made from M1 or M2, or why the smaller dies were made from HSS.

4.2 Hardness Profiles

No two threads examined had exactly the same hardness vs. depth profile. Die A1 has a fairly consistent hardness through the deeper sections of the profile, but has a noticeable increase in hardness closer to the surface, which could potentially be due to carburization of the surface, a common feature of A2 steel (Roberts, Krauss, & Kennedy, 1998). Die A2 has a fair amount of variation between data points but appears to keep a relatively constant average hardness throughout the hardness profile, which could be a result of the uniform hardening of D2 steel (Roberts, Krauss, & Kennedy, 1998). For both A2 and A3 there appear to be small regions of increase and decrease, like waves of hardness throughout the profile. This could be due to measuring the bands of carbides in the microstructure that are oriented parallel to the die surface. These bands are highlighted by drawn-in white stripes in Figure 44. Carbide size and distribution impacts the wear resistance of tool steels, and it appears that hardness tests could potentially reveal how the bands are oriented.

Die A4 shows similar behavior, though the variation between the highs and lows of the waves appear to be smaller, possibly due to smaller carbides and thinner bands. A4 also shows a hardness increase at the surface of the die, though that increase is less noticeable in the used thread because of the increased scatter in

the points near the surface. A5 has little variation between the hardness tests, which might potentially be due to the fine, homogenous grain structure characteristic of powder metal. Powder metal sintering makes it such that each phase is small grained and cannot segregate into bands like a conventionally wrought piece of metal. This could create a more consistent hardness profile. The hardness profile of A6 appears to be relatively constant with a slight increase near the surface, though there is a large amount of variation between the points at any given depth so that apparent trend might be caused by local variations. The material of A6 has a similar carbide distribution as A4, though the carbide bands are bigger and more regular.

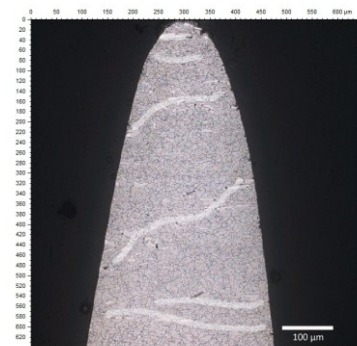


Figure 47: Highlighted carbide bands in A3

4.3 Failure Mode

The different appearance between used thread crests on dies A1, A2, A3 and dies A4, A5, A6 is very obvious. The first set of dies most likely fail due to spalling, while the second set appear to have abrasive wear on the thread crests.

Different types of materials are known to fail in a characteristic way, so an apparent relation between alloy type and failure mode is not surprising. Spalling is characterized by pieces of the thread crest breaking off and leaving a very irregular surface behind, which is consistent with the appearance of the failed threads. Additionally, D2 and A2 tool steels are known to have low toughness and often fail from spalling in thread rolling dies (Brezler, 1983). The second set of dies may have failed through abrasive wear due to the ‘smoothing’ of the grinding marks seen on the new thread crests and the more uniform appearance of the surface at low magnification. More examination, especially on an SEM, would provide more information about the fracture surfaces and the wear mechanism. HSS often fails through edge chipping, abrasion, adhesive wear, and continuous wear (Soderberg & Hogmark, 1986). Images for these failure modes were difficult to find so the failure mode of A4, A5, and A6 could not be identified with certainty.

4.4 New vs. Used Surfaces

The new and used regions of each die were noticeably different but the difference between the regions for the first set of dies was much more than that of the second set. This was very apparent in our analysis. The height parameters did well at discriminating between dies A1 through A3 but out of dies A4 through A6, the height parameters were only able to discriminate between the regions of the A6 die. However, relative area and complexity were both able to discriminate between the regions of all six dies. Both relative area and complexity were able to discriminate between the regions of dies A1 through A4 over most scales. For dies A5 and A6, relative area was only able to discriminate at a few scales but complexity was able to discriminate over most of the finer scales. This shows that multi-scale analysis may provide better insight into quantifying a surface than the conventional height parameters are able to in some cases.

4.5 New Surfaces

For the comparison between the new regions of each die, the discrimination ability of the conventional parameters varied. Relative area was most successful at discriminating at the lower to middle scales. This shows that if there is a difference between how the dies are made, it may affect the finer scale characteristics of the die's surface. Complexity, however, appears to be successful in two ranges: $0.03 - 0.8 \mu\text{m}^2$ and $20 - 300 \mu\text{m}^2$.

4.6 Used Surfaces

The different level of wear between the two sets of dies is also apparent when looking at the comparison of the used regions. Discrimination between the used sections of the 2nd set of dies is most difficult because of the dies are not as noticeably worn as the first set is. In the first set where the wear is a lot more noticeable, discrimination is more successful. Discrimination by relative area and complexity was most successful at scales over $0.2 \mu\text{m}^2$. This shows that the wear mechanisms are affecting the larger topographic features and that wear at the small scales is virtually the same.

4.7 Relative Area of New Dies & Lifetime

Once it was found that there is a difference between the regions of the dies, it was possible to start connecting these differences to potential factors that could play a role in the lifetime of the dies. When the average relative area for each new region was examined, it was found that there appears to be a middle range that corresponds to the dies with better lifetime. Looking at the scale range $0.3 - 10 \mu\text{m}^2$, there is a clear grouping of the relative areas of dies that have the longest lifetimes. A similar pattern was found to also correlate well to the friction coefficient between milled steel dies and steel sheet (Berglund et al., 2010). This correlation between friction and roughness provides support for a hypothesis that manufacturing a die with the proper surface roughness, not too rough but not too smooth, could increase the lifetime of the dies. It is therefore possible that a similar hypothesis would apply in the context of die life as well.

4.8 Study Expansion

Die wear is complex and takes into account thread pitch, accuracy of die setup, blank material, blank dimensions, blank hardness, lubricant, rolling speed, number of revolutions per

blank, and surface condition of the die and blank, among many other things (Davis, 1995). It is hard to account for all of these factors in a single, year-long project with a limited budget, especially when only six dies were provided for examination. Rolling dies are known to have a very wide variation in lifetime, even between near-identical dies (Brezler, 1983). This means that the lifetime for the dies examined in this project may not be typical of that type of die and any patterns found with lifetime in this study may not hold true for a larger set of dies. There is likely not a single factor that will drastically improve the lifetime of all dies, but small improvements can be made for a particular situation. In order to get a statistically significant idea of what alloys or surface characteristics seem to work well, many more than six dies are required.

5.0 Conclusions and Hypothesis

5.1 Conclusions

This study only examined six individual dies, which is too few to make generalizations. This project is a case study encompassing only six individual dies and the conclusions stated may not apply to a larger set of dies.

1. The OES readings indicated that the composition of all dies but A2 and A3 were different. The composition of the larger dies was consistent with A2 or D2 steel. The smaller dies appeared to be M42, CPM Rex 45, and M36 which are all grades of high speed tool steel.
2. Each die had a different hardness profile. New and used threads on each die often showed similar hardness trends, which included increased hardness near the surface and periodic fluctuations in hardness with depth.
3. Appearance of used thread crests changed between the larger and the smaller dies. The larger dies had significant fracture and material loss on the thread crest which is consistent with spalling, while the smaller dies showed minimal material loss and more homogenous surface appearance which could be consistent with abrasive wear.
4. New vs. used regions can be discriminated with 99% confidence either by relative area or complexity at scales between 0.05 and 300 μm^2 .
5. New regions can be discriminated either by relative area or complexity area scales less than 1 μm^2 .
6. Used regions can be discriminated with 99% confidence at scales greater than 0.2 μm^2 by either relative area or greater than 10 μm^2 using complexity.
7. At scales between 1 and 10 μm^2 , relative area appears to correlate well with lifetime. This scale range overlaps closely with scales at which friction and relative area correlate well (Berglund, et al., 2010).

5.2 Hypothesis

1. A more expansive study is needed to determine what factors impact the lifetime of a die, and how those features interact. Some potential features to consider are surface roughness and complexity, alloy, hardness, thread dimensions, rolling speed, lubricant, and blank material.

6.0 References

- Altan, T., Oh, S.-I. & Gegel, H., 1983. *Metal forming: fundamentals and applications*. Materials Park: American Society for Metals.
- Berglun, J., Brown, C. A., Rosen, B. & Bay, N., 2010. Milled die steel surface roughness correlation with steel sheet friction. *CIRP Annals - Manufacturing Technology*, Volume 59, pp. 577-580.
- Brezler, R., 1983. Getting the most from thread-rolling dies. *Tooling & Production*.
- Buehler, 2004. *The Science Behind Materials Preparation*, Lake Bluff, IL: Buehler LTD.
- Chandler, H., 1999. *Hardness Testing*. Materials Park, OH: ASM International.
- Craig, B., 2005. Material Failure Modes, Pt II. *AMPTIAC Quarterly*, 9(1), pp. 11-15.
- Crucible Industries, n.d. *CPM REX 45*. [Online] Available at:
[Http://www.crucible.com/eselector/prodbyapp/highspeed/cpm45.html](http://www.crucible.com/eselector/prodbyapp/highspeed/cpm45.html)
- Davis, J., 1994. Tool Steels. In: *Surface Engineering of Specialty Steels*. Materials Park, OH: ASM International, pp. 762-775.
- Davis, J., 1995. Selection of Material for Thread Rolling Die. In: *Tool Materials*. Materials Park, OH: ASM International, pp. 195-197.
- Davis, J., 1995. *Tool Materials*. Materials Park, OH: ASM International.
- DeGarmo, E., Black, J. & Kohser, R., 2003. *Materials and Processes in Manufacturing*. s.l.:Wiley.
- Dennies, D. P., 2005. *How to Organize and Run a Failure Investigation*. Materials Park (OH): ASM International.
- Edgar, C., 1965. *Fundamentals of manufacturing processes and materials*. Reading, MA: Addison-Wesley.
- Gagg, C., 2001. Premature failure of thread rolling dies: material selection, hardness criteria and case studies. *Engineering Failure Analysis*, 1 February, 8(1), pp. 87-105.
- Gagg, C., 2005. Failure of Components and Products by 'engineered-in' defects: Case Studies. *Engineering Failure Analysis*, December, 12(6), pp. 1000-1026.
- Gagg, C. & Lewis, P., 2007. Wear as a product failure mechanism. *Engineering Failure Analysis*, pp. 1618-1640.
- Nowicke, J., 1991. Why Didn't my Thread Rolling Dies Last Longer?. *Fastern Technology International*, pp. 18-22.
- Roberts, G., Krauss, G. & Kennedy, R., 1998. *Tool Steels*. Materials Park, OH: ASM International.
- Soderberg, S. & Hogmark, S., 1986. Wear Mechanisms and tool life of high speed steels related to microstructure. *Wear*, pp. 315-329.
- Statharas, D., Sideris, J., Medrea, C. & Chicinas, I., 2011. Microscopic examination of the fracture surface of a cold working die due to premature failure. *Engineering Failure Analysis*, 18(2), pp. 759-765.
- Stavridis, N. et al., 2011. Failure analysis of cutting die used for the production of car racks. *Engineering Failure Analysis*, 18(2), pp. 783-788.
- Tukey, J. W., 2008. *How to read (and Use) a Box-and-Whisker Plot*. [Online] Available at: <http://flowingdata.com/2008/02/15/how-to-read-and-use-a-box-and-whisker-plot/>
- Twardowski, P., Wojciechowski, S., Wiczorowski, M. & Mathia, T., 2011. Surface Roughness Analysis of Hardened Steel After High Speed Milling. *Scanning*, pp. 1-10.

- VERTEX42 LLC, 2012. *Box and Whisker Plot*. [Online]
Available at: <http://www.vertex42.com/ExcelTemplates/box-whisker-plot.html>
[Accessed 10 April 2012].
- Voort, G. V., 2004. Metallographic Techniques for Tool Steel. In: *ASM Handbook, Volume 9: Metallography and Microstructures*. Materials Park, OH: ASM International, pp. 644-669.
- Voort, G. V. & Manilova, E., 2009. *Metallographic Characterization of the Microstructure of Tool Steels*, Lake Bluff, IL: Buehler LTD.
- Wright, J., 2008. *When D2 Doesn't Work*. s.l.:Crucible Specialty Metals.

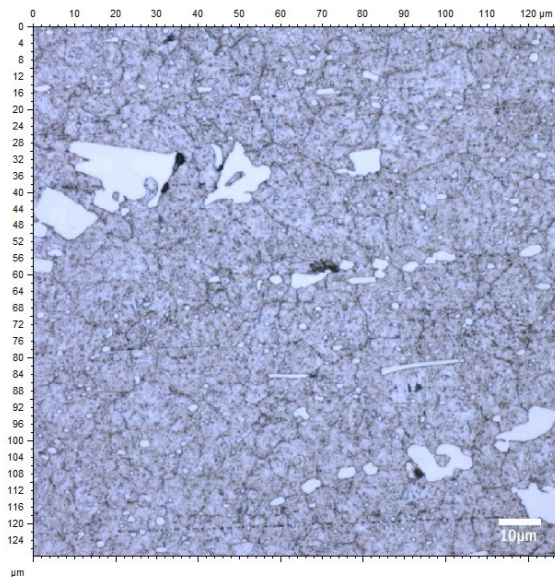
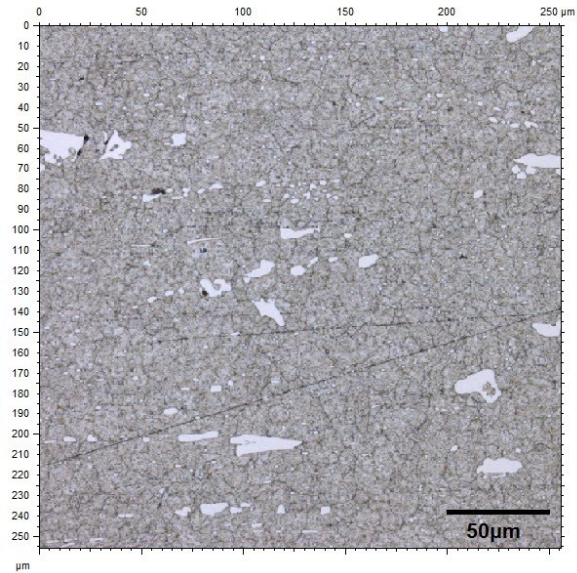
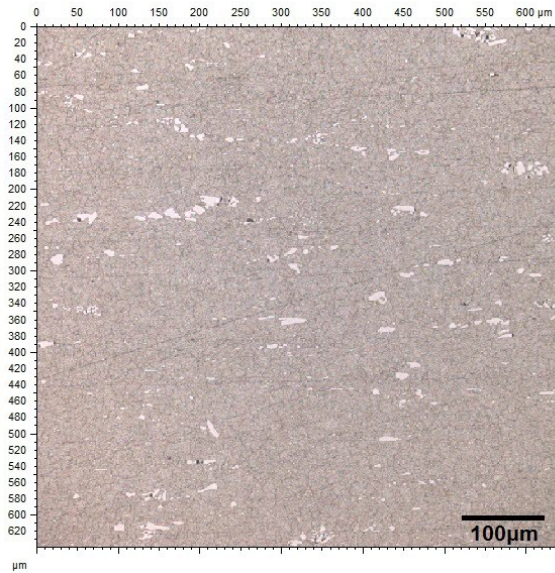
7.0 Appendices

7.1 Appendix A: Microstructure Images

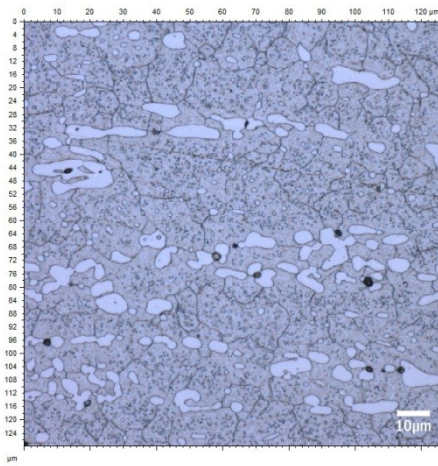
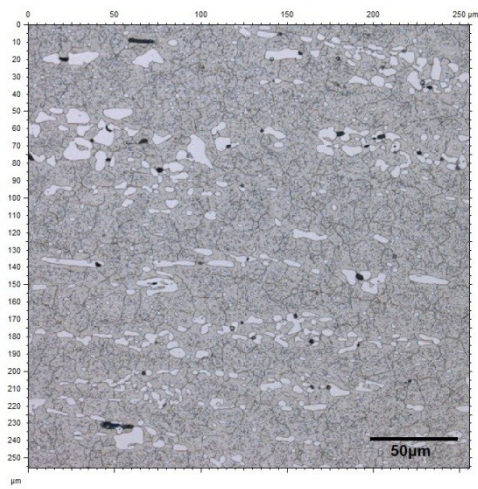
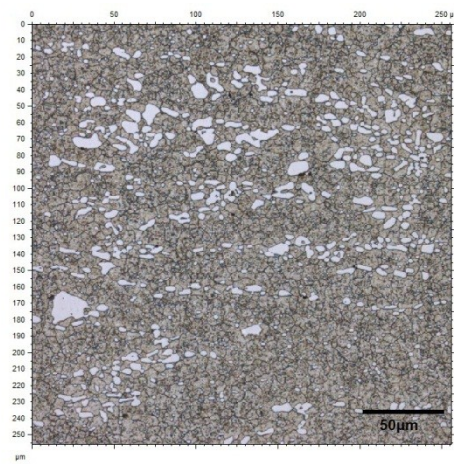
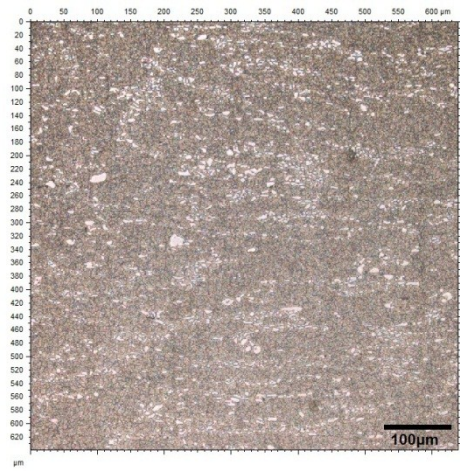
All specimens etched with 3% nital and imaged using a confocal laser scanning microscope.

7.1.1 Die A1

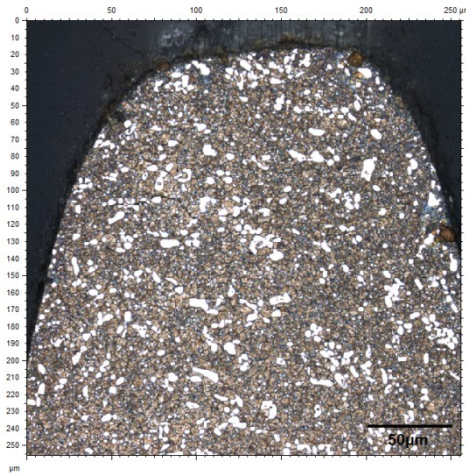
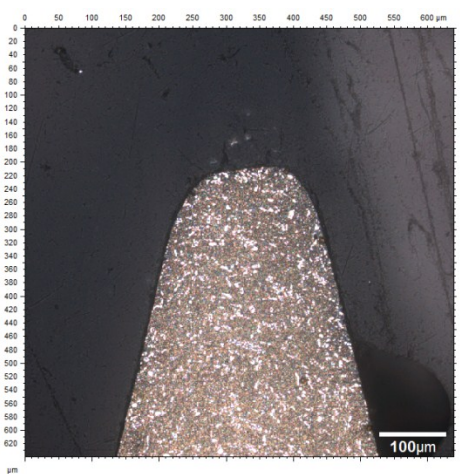
Microstructure a few millimeters below the root of the threads.



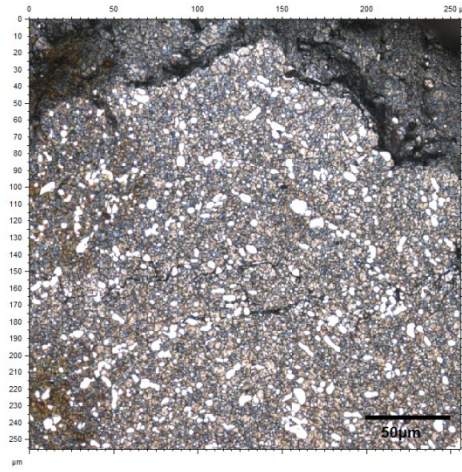
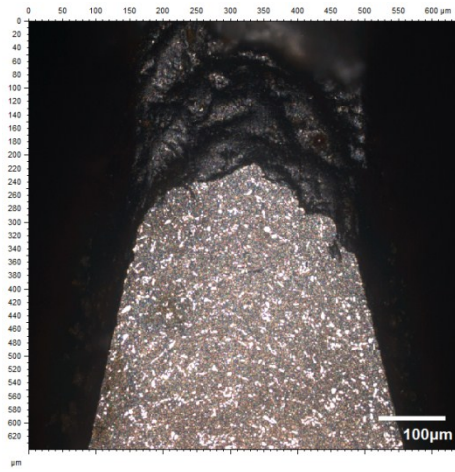
7.1.2 Die A2



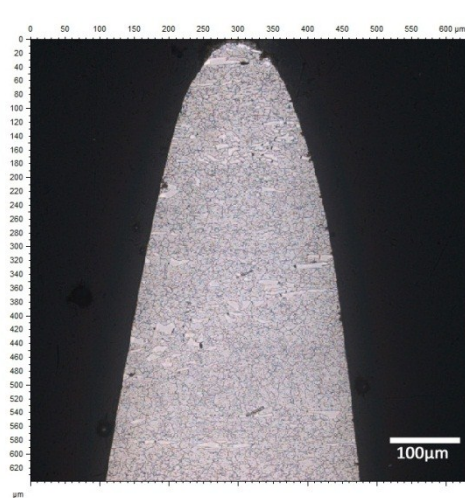
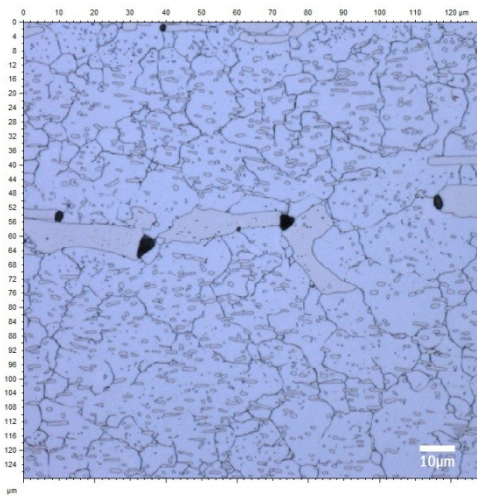
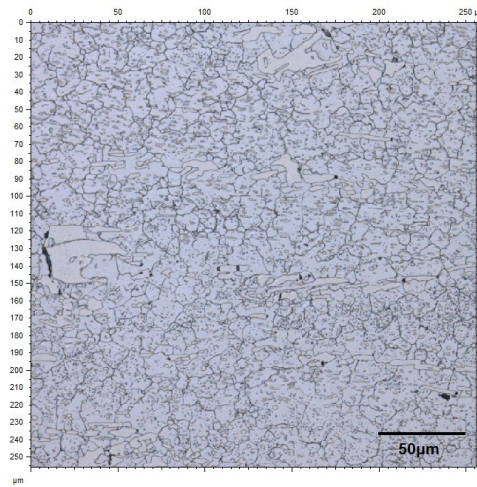
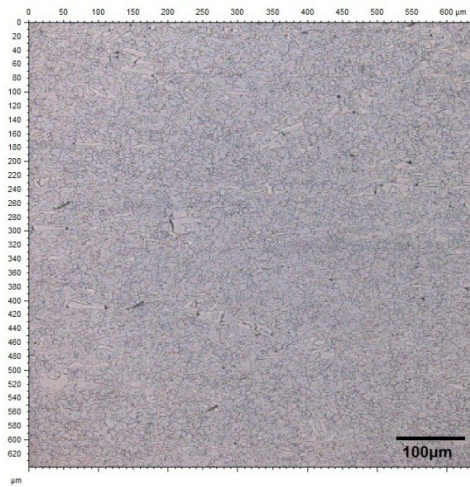
New Thread

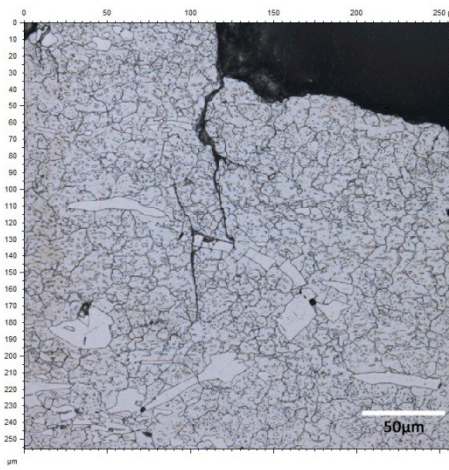
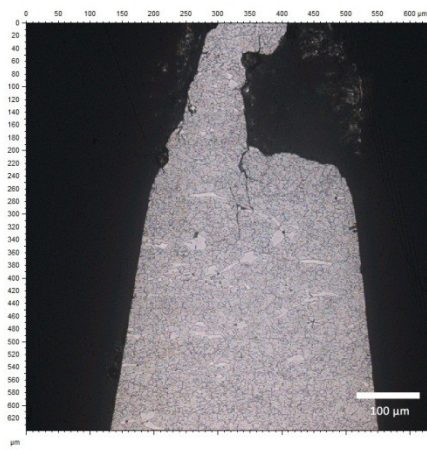
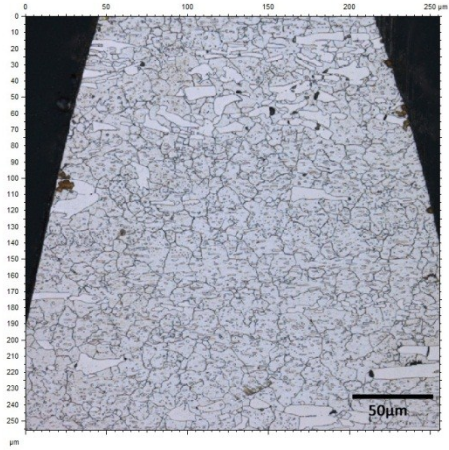


Used Thread

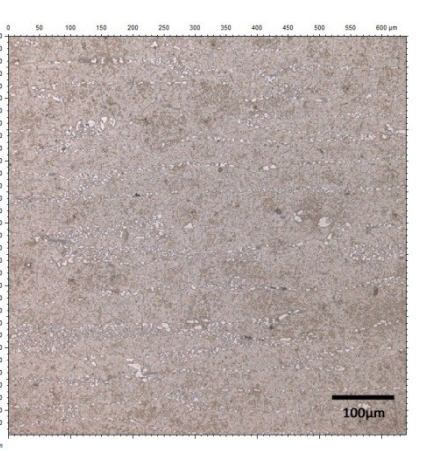
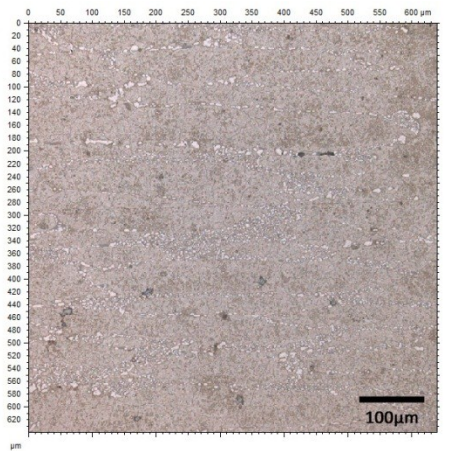


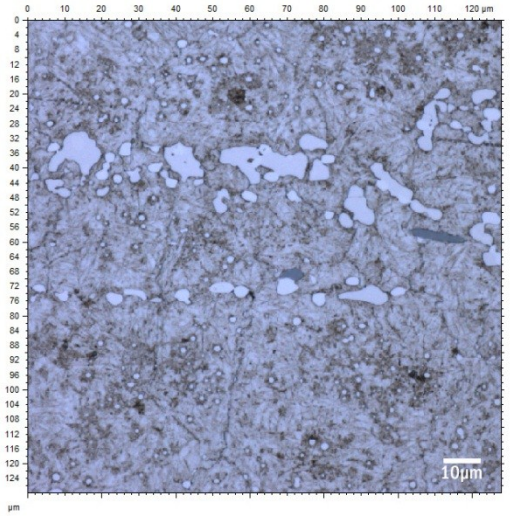
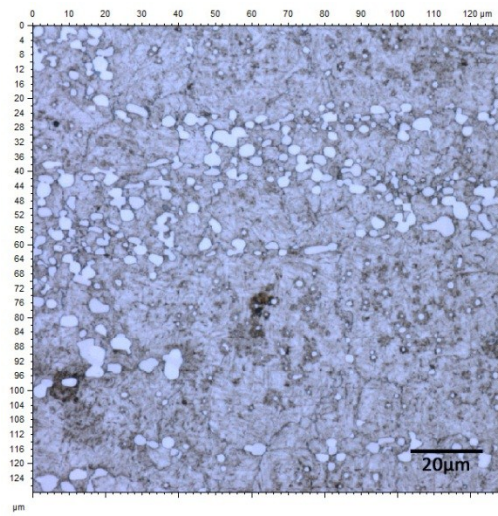
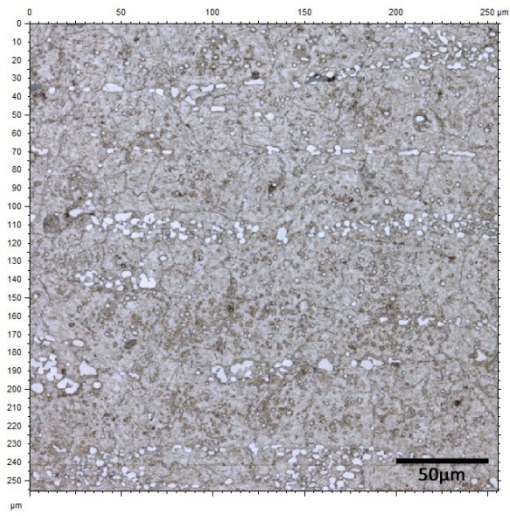
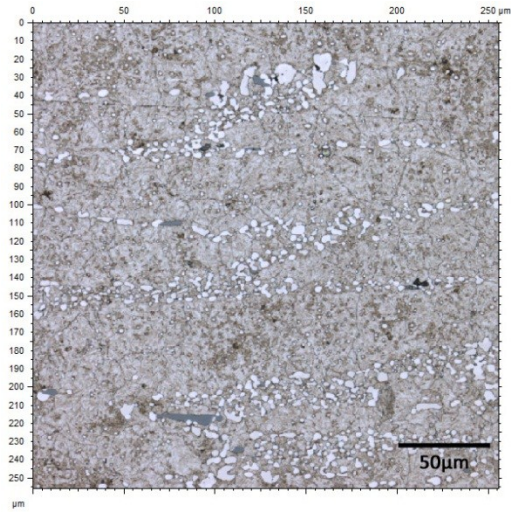
7.1.3 Die A3



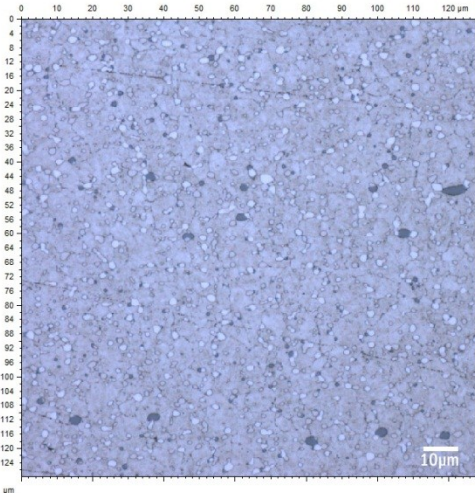
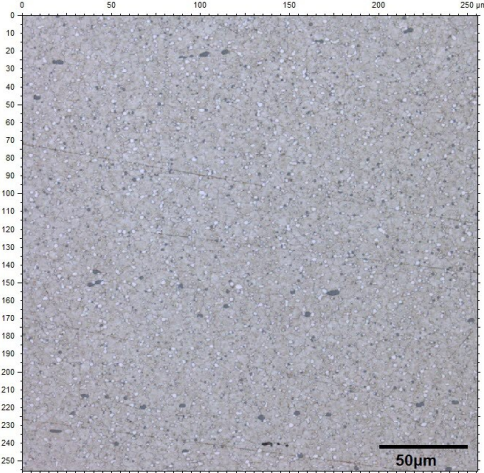
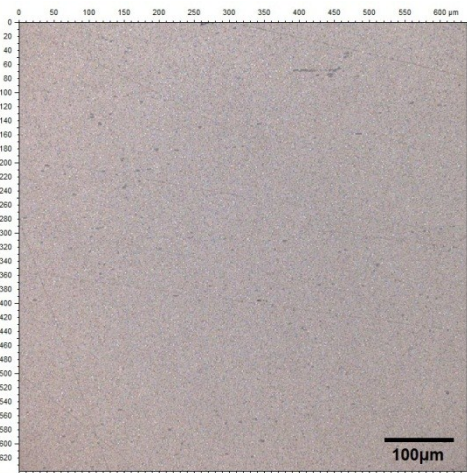


7.1.4 Die A4

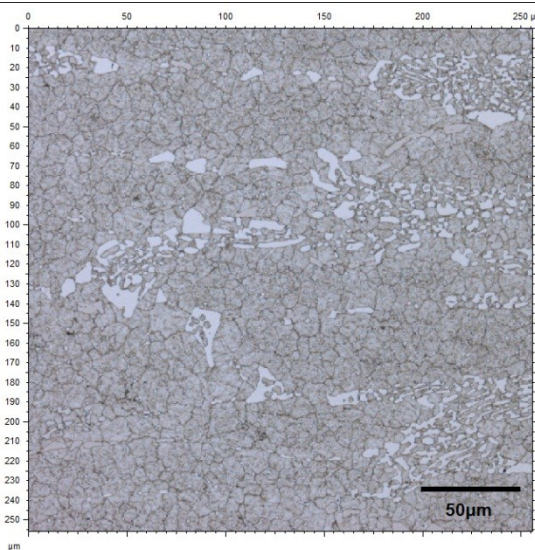
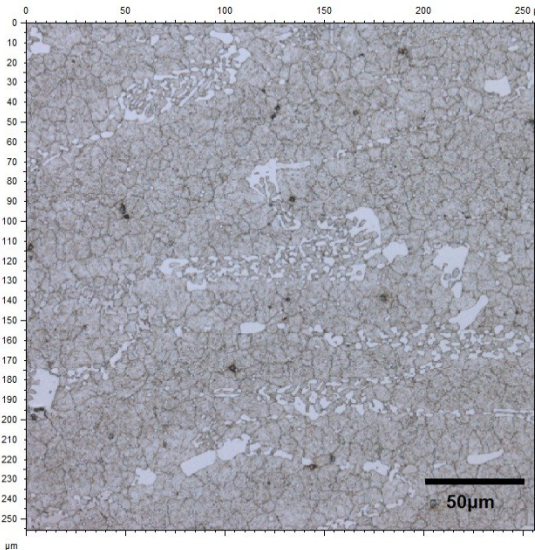
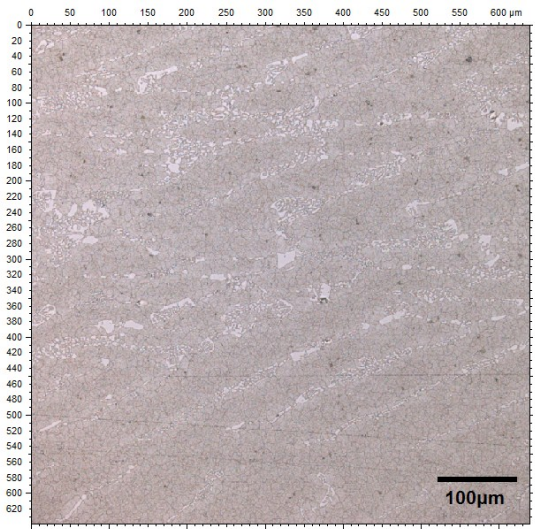
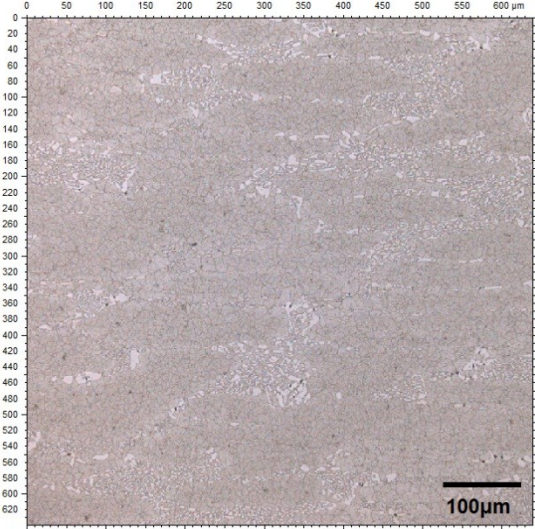


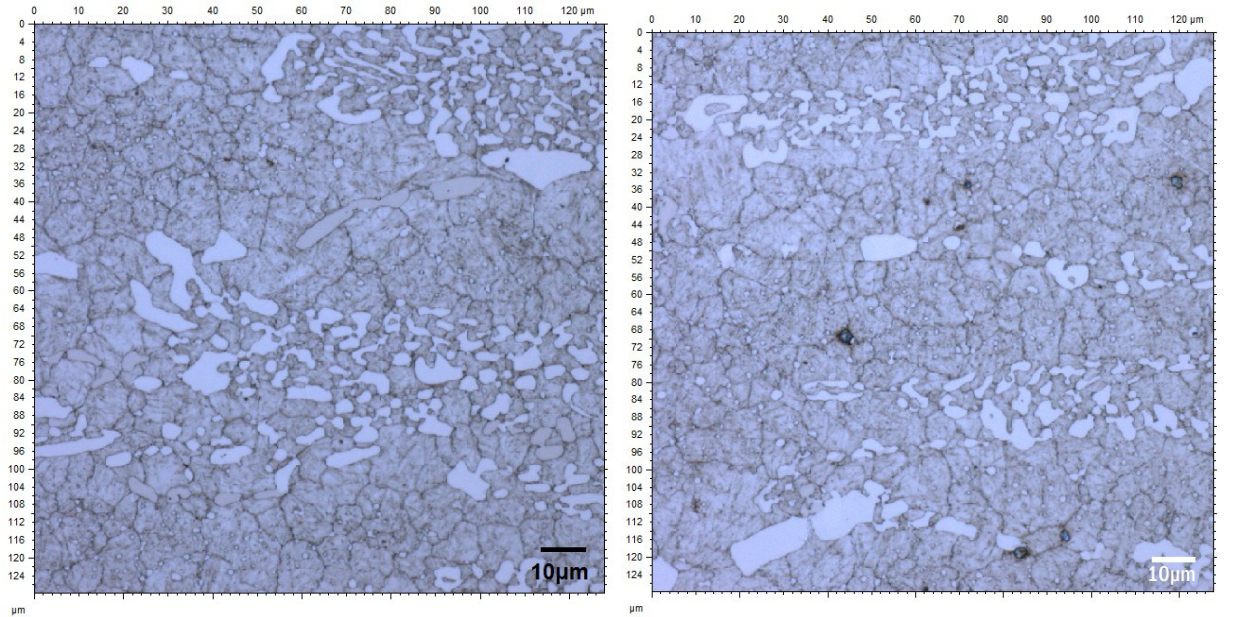


7.1.5 Die A5



7.1.6 Die A6





7.2 Appendix B: Depth Calculation for Hardness Tests

How to find the height of an arc at any point along a chord.

Equation of a circle in general form

$$(x - x_0)^2 + (y - y_0)^2 = R^2$$

To find (0,0)

$$(x - x_0)^2 + (y - y_0)^2 = R^2$$

$$(0 - x_0)^2 + (0 - y_0)^2 = R^2$$

$$x_0^2 + y_0^2 = R^2$$

To find (C,0)

$$(C - x_0)^2 + (0 - y_0)^2 = R^2 \quad \text{Expand}$$

$$C^2 + 2 \cdot C \cdot x_0 + x_0^2 + y_0^2 = R^2$$

For (c/2, s)

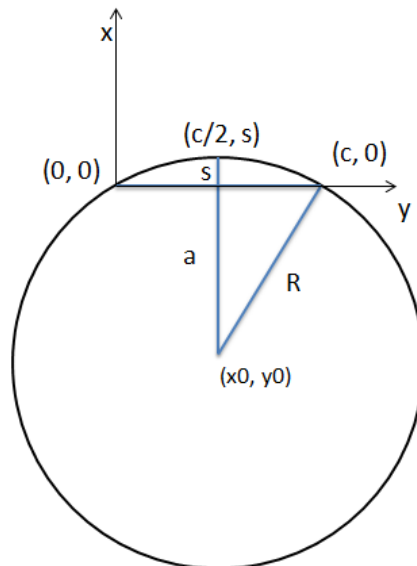
$$\left(\frac{C}{2} - x_0\right)^2 + (s - y_0)^2 = R^2$$

$$\frac{C^2}{4} - C \cdot x_0 + x_0^2 + s^2 - 2 \cdot s \cdot y_0 + y_0^2 = R^2$$

All equations are equal to R^2 , and therefore all equations are equal to each other.

$$x_0^2 + y_0^2 = C^2 - 2 \cdot C \cdot x_0 + x_0^2 + y_0^2 \quad x_0 \text{ and } y_0 \text{ cancel out.}$$

$$0 = C^2 - 2 \cdot C \cdot x_0 \quad x_0 = \frac{C}{2}$$



$$y_0 \quad x_0^2 + y_0^2 = \left(\frac{c}{2} - x_0\right)^2 + (s - y_0)^2$$

Now you know x_0, y_0

$$\left(\frac{c}{2}\right)^2 + y_0^2 = \left(\frac{c}{2} - x_0\right)^2 + (s - y_0)^2$$

$$\left(\frac{c}{2}\right)^2 + y_0^2 = s^2 - 2 \cdot s \cdot y_0 + y_0^2$$

$$y_0 = \frac{\left(s - \frac{x_0^2}{s}\right)}{2}$$

center of the circle $(x_0, y_0) = \frac{c}{2}, \frac{\left(s - \frac{x_0^2}{s}\right)}{2}$

Equation of a circle in general form

$$(x - x_0)^2 + (y - y_0)^2 = R^2 \quad \text{Expand}$$

$$y^2 - 2 \cdot y_0 \cdot y + y_0^2 + (x - x_0)^2$$

solve using quadratic formula

$$y = \frac{-b + \sqrt{b^2 - 4 \cdot a \cdot c}}{2 \cdot a} \quad a \cdot y^2 + b \cdot y + c = 0$$

$$y^2 + (-2 \cdot y_0) \cdot y + [y_0^2 + (x - x_0)^2 - R^2] = 0$$

$$a = 1 \quad b = -2 \cdot y_0 \quad c = y_0^2 + (x - x_0)^2 - R^2$$

neglect negative portion of equation

$$y = \frac{2 \cdot y_0 + \sqrt{2 \cdot y_0^2 - 4 \cdot c}}{2}$$

$$y = y_0 + y_0 + \sqrt{y_0^2 - c}$$

$$y = y_0 + \sqrt{y_0^2 - [y_0^2 + (x - x_0)^2 - R^2]}$$

can use this equation to find depth at any given x value. need chord length and sagitta to use.

$$x_0 = \frac{c}{2} \quad y_0 = \frac{\left(s - \frac{x_0^2}{s}\right)}{2} \quad R^2 = x_0^2 + y_0^2$$

Example

Given x value $x := 125.94$

Radius $R := 143680$

Chord Length $C := 10135.72$ $x_0 := \frac{C}{2} = 5.068 \times 10^3$

Sagitta $s := R - \sqrt{R^2 - x_0^2} = 89.404$

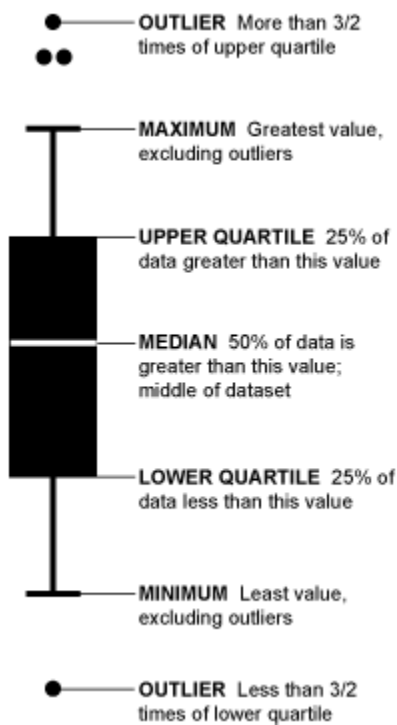
$$y_0 := \frac{s - \frac{x_0^2}{s}}{2} = -1.43591 \times 10^5$$

depth at the given x, chord length, and radius

$$y := y_0 + \sqrt{y_0^2 - [y_0^2 + (x - x_0)^2 - R^2]}$$

$$y = 4.39$$

Features of a box and whisker plot



(Tukey, 2008)

7.3 Appendix C: Rough data for Hardness Tests

A1 New		A1 Used		A2 New		A2 Used	
HK	Depth	HK	Depth	HK	Depth	HK	Depth
1473	9.818452	1384	4.219622	927	1.544305	1018	4.17919
1278.5	11.87803	1030	5.842295	822.5	4.030124	880.5	7.004913
994	13.9588	1066	7.688742	822.5	6.426646	946.5	9.697773
929	17.33606	931.5	9.363042	822.5	8.816196	935.5	12.46153
888	20.60852	900	11.70915	884	12.81342	982.5	15.113
962	23.68824	807	14.49162	822.5	16.5555	781.5	17.77812
831.5	29.84535	846	19.68467	894	20.21907	1328	20.38567
844	35.38102	821	24.54611	795	23.47693	957.5	22.98786
844	40.53465	798.5	28.98212	833.5	26.93255	935.5	25.54998
819	45.3491	846	33.01487	711.5	30.30889	1030	27.98671
831.5	49.66501	833.5	36.52438	894	33.59876	1018	30.43381
795	53.61793	872.5	39.70259	904.5	39.80297	935.5	32.90481
819	57.07916	807	42.41173	927	45.47981	946.5	36.85165
859	60.17042	807	44.73176	833.5	50.84258	872.5	40.56556
795	62.83974	770.5	46.61064	822.5	55.60779	957.5	44.3491
844	65.06996	819	48.09108	736.5	60.07042	912.5	51.40059
916.5	66.88057	859	49.14711	894	64.01189	923	57.99615
844	68.28873	846	49.77972	777	67.51946	935.5	64.11536
857.5	69.27072	795	49.99992	872.5	70.60586	872.5	69.94069
831.5	69.84727	946.5	49.80043	833.5	73.27938	914.5	75.09307

819	69.99598	886	49.18373	927	75.49362	904.5	79.84759
807	69.7241	427.55	48.15675	786.5	77.28006	876.5	84.25613
844	69.03791	819	46.69856	894	78.60377	925	88.14507
795	67.92214	819	44.78906	851.5	79.49869	971	91.65894
929	66.20832	783.5	42.52996	751.5	79.94081	882.5	94.76896
411.45	64.23406	795	39.82414	805	79.94783	863	97.36893
840.5	61.81095	833.5	36.69194	814	79.52648	882.5	99.42697
826	58.94401	697.5	33.14916	831.5	78.65252	904.5	101.1998
741	55.7185	821	29.19033	918.5	77.35414	946.5	102.5405
795	52.01567	770.5	24.87682	918.5	75.60062	946.5	103.4591
795	47.901	846	20.00437	863	73.41077	971	103.9258
840.5	43.39427	831.5	17.38358	826	70.80316	935.5	103.9625
824.5	38.50498	857.5	14.72739	767	67.73483	918.5	103.5673
810.5	33.24064	872.5	11.98382	767	64.26568	935.5	102.7512
857.5	27.42841	859	9.123206	904.5	60.32037	935.5	101.5027
840.5	24.33118	984.5	7.56145	824.5	55.90816	991.5	99.80071
906.5	21.08194	994	6.157482	1028	51.07716	953	97.68942
840.5	17.85495	1166.5	4.31304	850	45.86493	837	95.10341
872.5	14.57009			916.5	40.06197	973	92.12835
982.5	12.76204			946.5	33.92197	778.5	88.70018
944.5	11.11191			902	30.56361	893	84.87772
1162.35	9.054587			918.5	26.53335	868.5	80.5865
				863	23.05331	893	75.81002

				918.5	19.48272	955.5	70.64526
				931.5	17.25656	973	67.86369
				890	15.02696	918.5	64.93057
				778.5	12.67839	904.5	61.84351
				790	10.28958	955.5	58.74221
				918.5	7.940417	918.5	55.61662
				736.5	5.512591	1030	52.29973
				946.5	3.108211	1032.5	48.9409
				1010.5	0.398153	953	45.35705
						935.5	41.83118
						893	38.04821
						935.5	34.15874
						1123	30.13125
						1013	26.18067
						953	22.04074
						1032.5	17.82474
						918.5	15.11046
						991.5	12.05894
						1123	9.372548
						1053	6.649324

A3 New		A3 Used		A4 new		A4 Used	
HK	Depth	HK	Depth	HK	Depth	HK	Depth

1100.5	4.403693	1066	3.445971	1395.5	8.930808	1468.5	4.354
996.5	5.921399	944.5	4.387817	1114.5	11.02384	1166.5	7.865
931.5	8.121604	962	7.671443	1275	14.37796	1125.5	11.61
946.5	11.89976	906.5	10.90918	1048	17.76547	1120	16.28
914.5	15.5205	1023	13.99453	962	21.11094	1103.5	22.19
846	19.02837	923	16.98975	946.5	26.38639	1015.5	27.96
886	22.38648	890	19.88309	1066	31.65729	1048	38.99
821	25.59874	872.5	22.67426	1030	41.83512	944.5	49.82
900	28.70345	980	25.28316	994	51.52928	994	59.98
859	31.83653	906.5	27.91969	1048	60.76724	1028	70
846	34.75445	925	30.29313	1030	69.43008	1010.5	79.25
807	37.51497	872.5	32.63857	1013	77.78862	1120	88.21
846	40.18379	962	34.90103	1030	85.55839	1010.5	96.64
846	42.75969	925	36.96527	1066	93.04756	1025.5	104.7
831.5	45.29645	890	38.94937	1106	99.97937	1048	112.2
819	47.69293	944.5	40.89808	994	106.5146	1063.5	119.3
795	49.95001	888	42.64761	1045.5	112.5282	975.5	125.9
795	52.07334	906.5	44.31193	1066	118.1687	1028	132.1
821	54.12281	982.5	45.87538	1084.5	123.2381	1010.5	140.5
846	56.08305	982.5	47.33095	978	127.9439	1103.5	145.6
772	57.93845	888	48.66121	1125.5	132.2066	1066	150.1
783.5	59.03887	890	49.88827	1103.5	135.9716	1048	154.2
821	60.65444	1020.5	50.99601	1123	139.3153	1048	157.9

795	62.19541	962	52.00603	1066	142.2129	1063.5	161.1
807	63.61655	906.5	52.8913	1060.5	144.6056	1010.5	164
821	64.94054	906.5	53.67054	1028	146.6317	1063.5	166.2
886	66.1633	923	54.32914	994	148.1339	1025.5	168.1
846	67.22949	982.5	54.87535	1028	149.2142	959.5	169.5
795	68.19343	925	55.31368	837	149.8312	1008.5	170.4
978	69.06687	925	55.65373	1010.5	149.9959	1111.5	170.9
859	69.81888	906.5	55.87413	978	149.7034	1008.5	171
900	70.45966	906.5	55.98609	962	148.9696	1079	170.6
959.5	70.99468	962	55.9851	1060.5	147.7737	1114.5	169.6
795	71.41609	1023	55.87226	946.5	146.1331	1079	168
819	71.72081	703	55.64313	987	144.0388	1008.5	166.2
846	71.91591	906.5	55.31719	996.5	141.4368	975.5	163.9
795	71.99706	925	54.86635	1114.5	138.4286	971	161.1
859	71.96703	1020.5	54.31798	1066	134.9784	1066	157.8
819	71.83134	890	53.63285	1030	131.0674	1066	154.1
819	71.57182	906.5	52.85933	1030	126.7427	1079	150
962	71.21528	962	51.95113	1084.5	121.8738	1066	145.4
795	70.73379	962	50.96308	978	116.6173	1137	140.3
999	70.15927	1023	50.08614	940	110.8301	1066	134.9
938	69.46501	1001	49.3618	1125.5	104.5785	1066	128.8
916.5	68.65626	872.5	48.53424	1013	97.86551	1025.5	122.4
846	67.76215			1030	90.73177	1025.5	115.6

904.5	67.10924			962	83.31493	975.5	108.3
914.5	66.47188			1030	75.22929	1058	100.6
793.5	65.79548			1030	66.8007	1111.5	92.28
874.5	65.075			1013	62.44345	1095	83.56
785	64.34096			946.5	57.97526	1003.5	74.44
				962	53.34283	1125.5	64.93
				1084.5	48.48878	1310	54.87
				1048	43.79301	1380	44.41
				1030	38.79185	1261.5	39.02
				1048	33.61759	1431.5	33.46
				1125.5	28.35578	1175.5	27.93
				1106	23.12855	1015.5	22.33
				1103.5	17.75476	938	16.47
				1125.5	14.53043	938	12.75
				1125.5	11.14029	1073.5	9.146
				1282	8.474694	966.5	5.513

A5 New		A5 Used		A6 New		A6 Used	
HK	Depth	HK	Depth	HK	Depth	HK	Depth
1166.5	6.396001	1187.5	6.452696	1439.5	8.7044	1254.5	3.98
1103.5	9.245121	980	10.3876	1231.5	11.17503	1222	6.57
1166.5	12.53337	1066	13.99888	1481.5	13.72852	1140	8.18
1245	15.78344	982.5	17.49021	1275	16.30948	1111.5	10.65

1013	19.05415	1020.5	20.90381	1258	18.77981	1032.5	13.14
1146	22.22554	1023	24.23794	1448	21.25285	1008.5	15.52
1013	27.4519	968.5	29.79361	1306.5	23.61676	1103.5	17.99
929	32.71791	1043	35.12703	1388	25.91906	1288.5	20.33
1028	42.70198	984.5	45.67872	1209.5	28.37369	1015.5	22.61
978	52.29314	1089.5	55.77928	1235	30.61424	1008.5	25.03
978	61.50951	982.5	65.36478	1384	34.26692	1040	27.25
1013	70.10714	1066	74.47598	1048	37.8075	1050.5	29.54
914.5	78.37463	1066	83.11636	1231.5	41.23647	1222	31.70
902	86.12525	959.5	91.45344	1209.5	44.57045	1111.5	33.87
846	93.35386	1020.5	99.21018	1254.5	47.89792	1058	35.95
946.5	100.166	1023	106.6239	1357.5	50.95136	1131.5	37.99
900	106.6648	1023	113.4971	1209.5	53.94395	1030	41.32
946.5	112.5951	1001	120.0786	1203	56.77567	1081.5	44.56
900	118.1791	1045.5	126.0438	1066	59.57364	1055.5	47.69
900	123.298	1066	131.61	1357.5	62.28512	1098	50.68
916.5	127.9185	1020.5	136.7016	1357.5	64.79545	1055.5	53.57
962	132.1028	1001	141.4182	1125.5	67.27399	1081.5	56.30
931.5	135.8758	1043	145.7018	1106	69.55899	1055.5	58.89
946.5	139.1588	1043	149.4627	1235	71.7926	1098	61.50
962	142.0305	962	152.8125	1030	73.84075	1172.5	63.94
888	144.4913	982.5	155.7521	1282	75.86547	1098	66.23
942	146.4809	906.5	158.2439	1415.5	77.72348	1098	68.45

978	148.0221	982.5	160.2829	1123	79.43665	1081.5	70.55
978	149.2027	982.5	161.8686	1048	81.09308	1123	72.53
962	149.814	959.5	163.0223	1306.5	82.64062	1134	74.36
872.5	149.9982	980	163.7304	1503	84.0096	1058	76.13
962	149.7339	1043	163.9977	1388	85.33253	1043	77.78
914.5	149.034	962	163.8168	1181.5	86.52366	1151.5	79.32
900	147.8828	982.5	163.2	1084.5	87.55796	1043	80.73
931.5	146.3111	1001	162.1178	1282	88.50946	1058	82.05
914.5	144.2231	1001	160.5967	1187.5	89.34252	1025.5	83.27
962	141.7834	1001	158.6437	996.5	90.07271	1025.5	84.33
996.5	138.8884	1023	156.2407	978	90.67664	1025.5	85.29
944.5	135.4964	906.5	153.4348	1209.5	91.16742	1043	86.16
1013	131.6416	1020.5	150.0422	1331.5	91.54327	1058	86.89
1030	127.3841	1003.5	146.3395	1282	91.81405	975.5	87.52
1010.5	122.6498	942	142.1712	1187.5	91.96109	1008.5	88.04
994	117.3804	982.5	137.5458	1331.5	91.99823	1081.5	88.45
1013	111.777	1001	132.5301	1331.5	91.92163	1043	88.74
1048	103.2313	1187.5	126.9814	1030	91.7331	1058	88.93
1066	96.54663	1045.5	120.9002	1231.5	91.42046	991.5	89.00
1028	89.4993	888	114.5277	1066	90.99889	1095	88.96
971	81.88746	931.5	107.6522	996.5	90.46282	1008.5	88.81
925	77.92048	982.5	100.3535	1066	89.83516	1095	88.53
892	73.82562	1066	92.53058	955.5	89.06422	1081.5	88.17

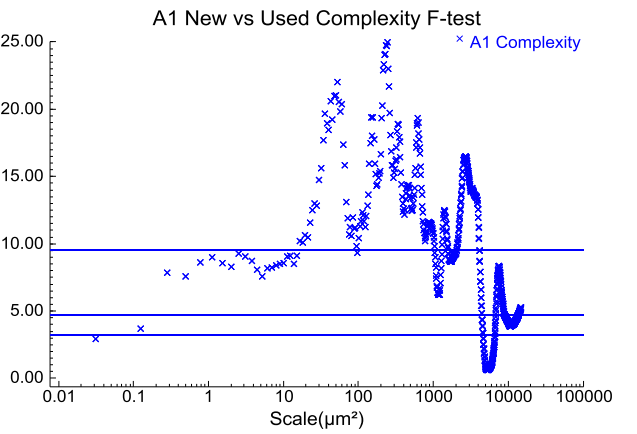
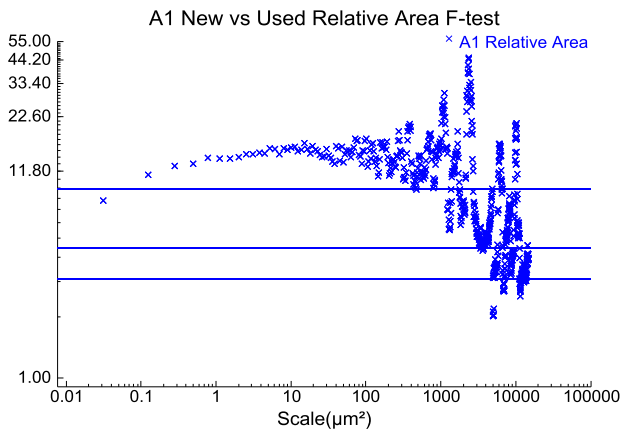
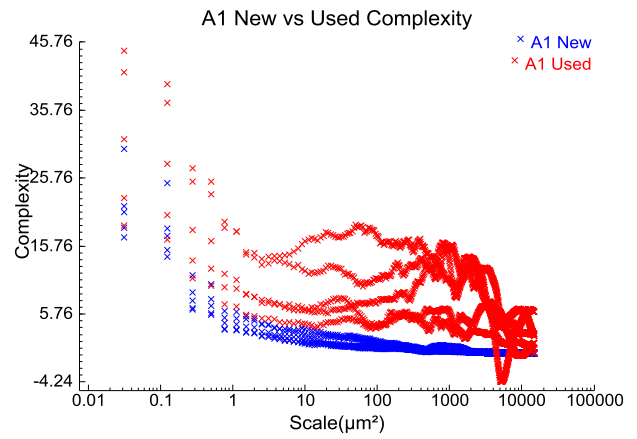
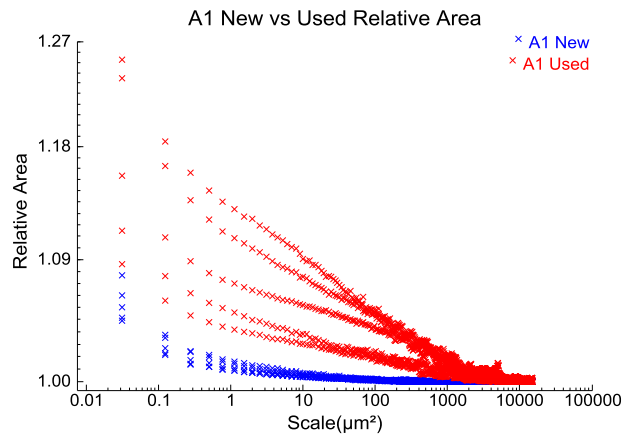
1043	69.582	982.5	84.28198	1357.5	88.18199	1200	87.66
946.5	67.06029	1066	80.0728	1157.5	87.18378	1008.5	87.31
968.5	64.50029	982.5	71.21339	1048	86.10904	1043	86.91
994	60.11618	935.5	66.58586	1123	84.87612	1032.5	86.48
1018	55.60364	962	61.68304	1258	83.57274	1058	86.01
971	52.83571	987	56.82445	1258	82.10052	1081.5	85.49
935.5	49.98922	999	51.82101	1146	80.55507	1095	84.92
1018	48.64475			1209.5	78.88818	1095	84.34
				1209.5	77.08784	1040	83.71
				931.5	75.22475	1081.5	83.04
				1030	73.19591	1131.5	82.31
				1106	70.92323	1025.5	81.57
				1106	68.68204	1095	80.76
				1146	66.32742	1060.5	79.95
				1066	63.84473	1134	79.04
				1013	61.23365	1060.5	78.16
				1106	58.52067	1025.5	77.24
				1163.5	55.7107	1008.5	76.20
				1084.5	52.82095	1123	75.20
				1125.5	49.69771	1151.5	74.12
				1030	46.54523	1081.5	72.96
				1235	43.13003	1043	71.80
				1013	39.70778	1060.5	70.64

				1146	36.32933	946.5	69.38
				1048	32.65958	1025.5	68.14
				1084.5	28.87293	1193.5	66.78
				1125.5	25.05663	991.5	66.65
				1282	21.0334	1008.5	65.26
				1125.5	18.62528	1025.5	63.86
				1388	16.17694	1058	62.43
				1235	13.61687	1058	60.88
				1473	11.06292	1058	59.37
				1448	8.272399	991.5	57.78
				1357.5	5.758087	1081.5	56.18
						1025.5	54.54
						1060.5	52.86
						1092.5	51.08
						1058	49.37
						1043	47.52
						1060.5	45.71
						1008.5	43.81
						1151.5	41.98
						1131.5	39.88
						1081.5	37.93
						863	35.83
						1134	33.71

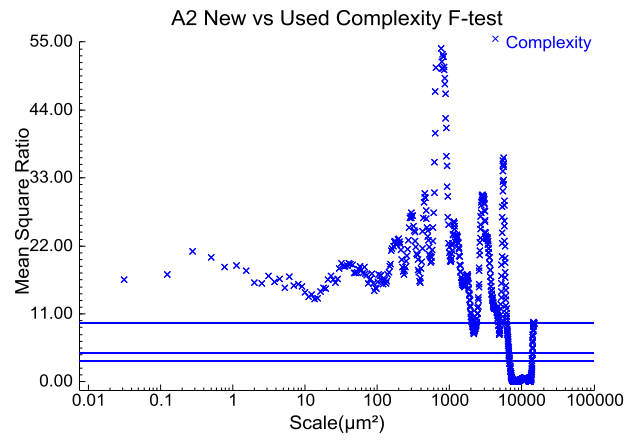
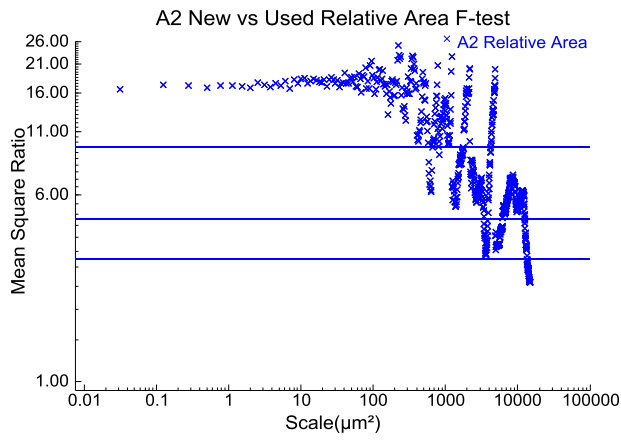
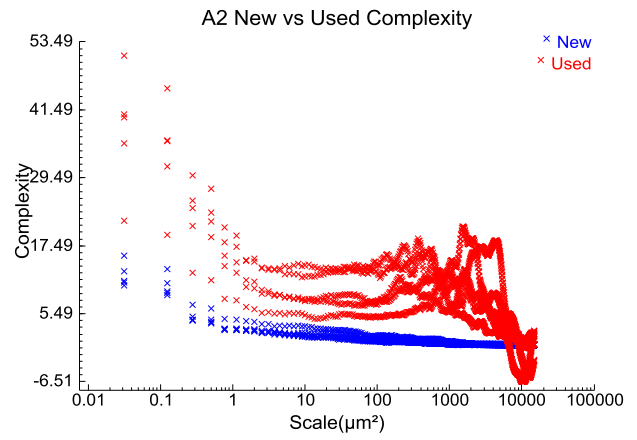
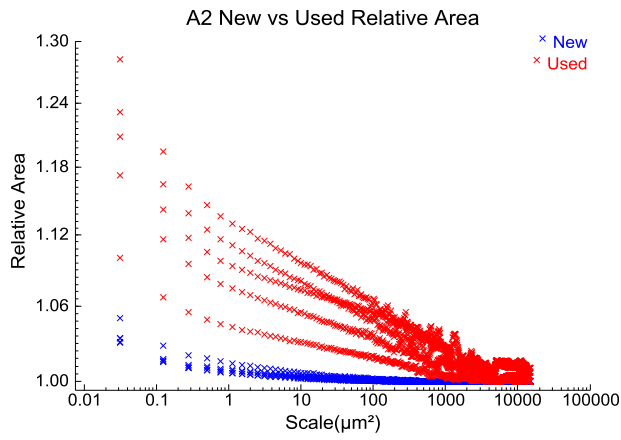
						1060.5	31.53
						1123	29.33
						1040	27.04
						1123	24.91
						1212.5	22.59
						1123	20.18
						1123	17.90
						1123	15.43
						1282	13.02
						1258	10.38
						1328	8.06
						1520.5	5.56

7.4 Appendix D: New vs. Used – Graphs

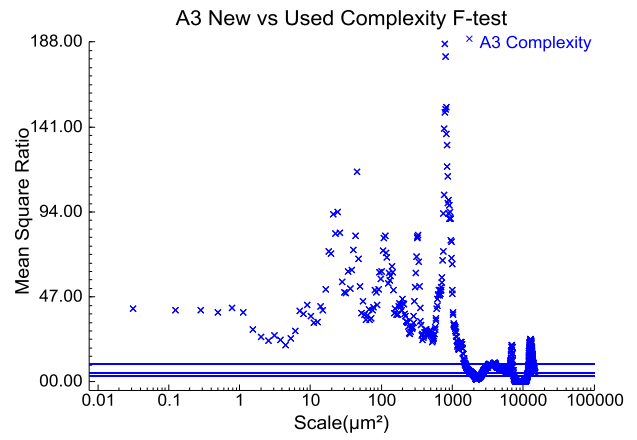
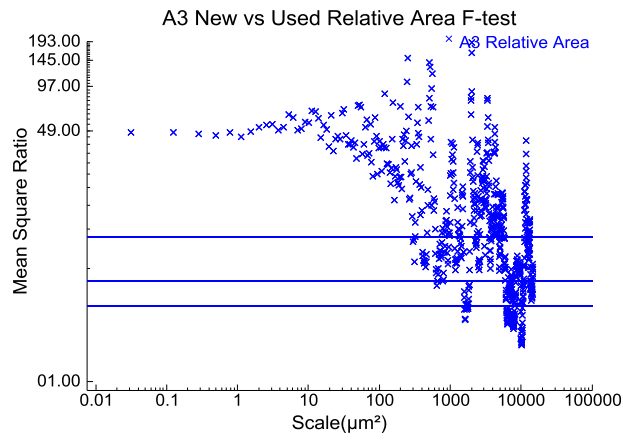
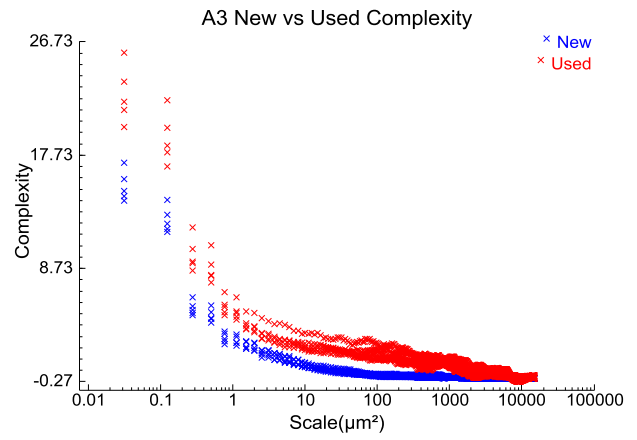
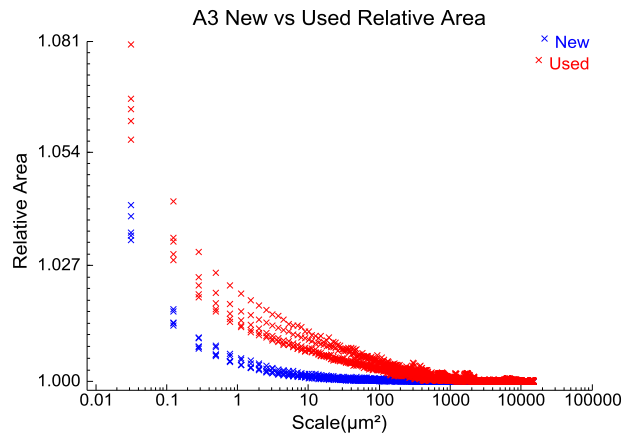
A1



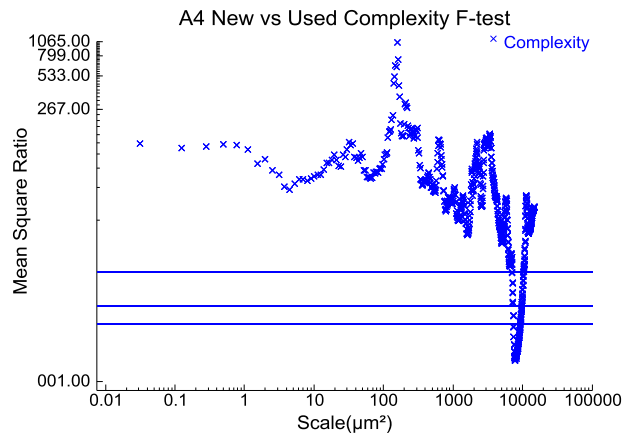
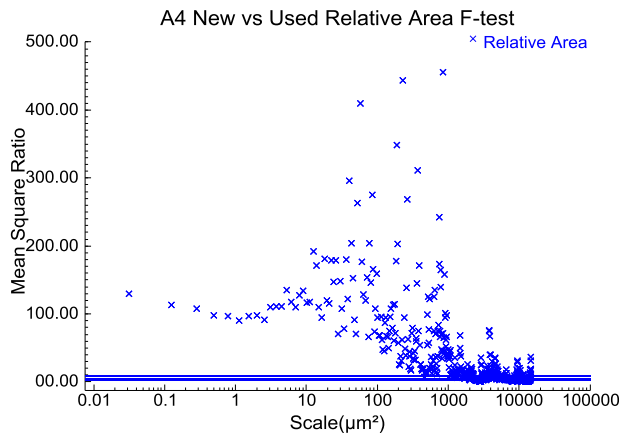
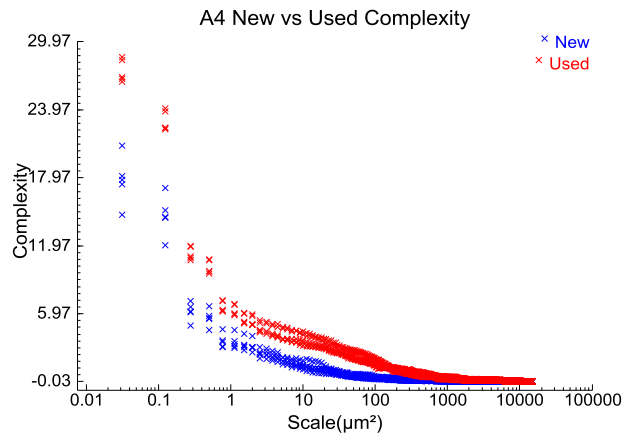
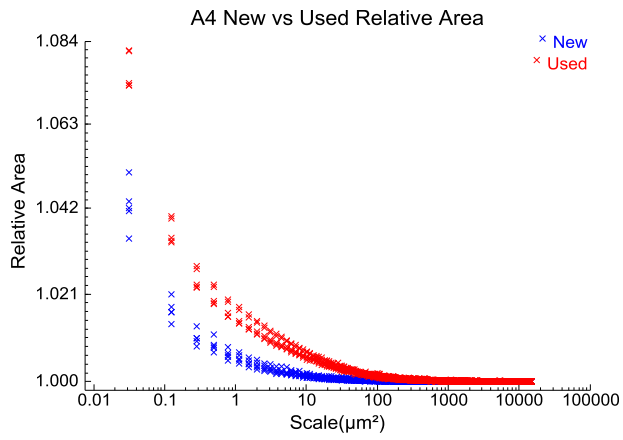
A2



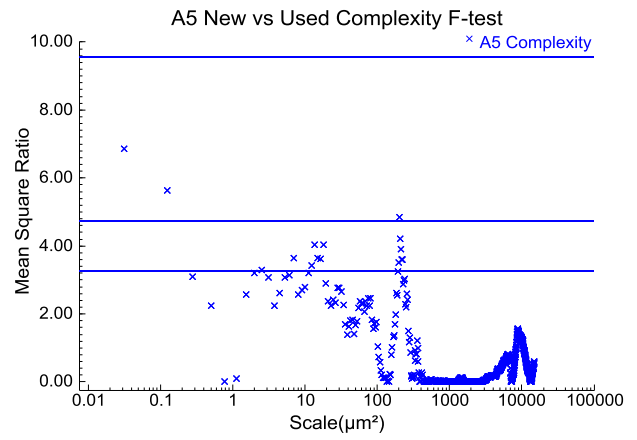
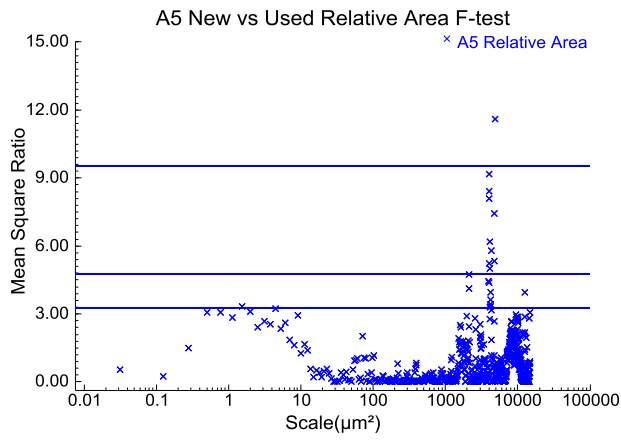
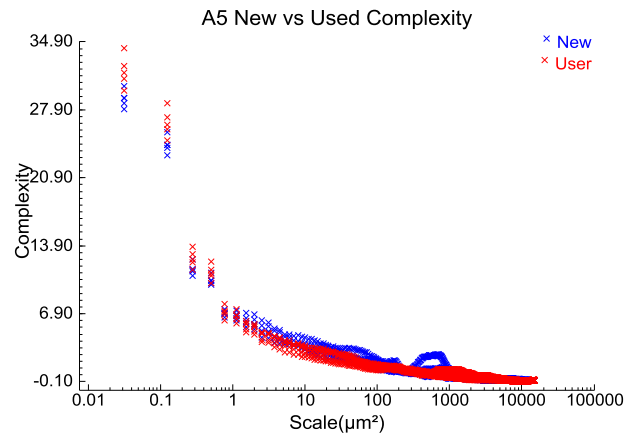
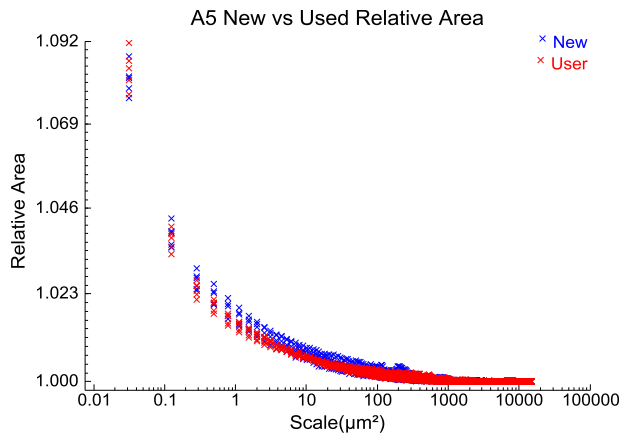
A3



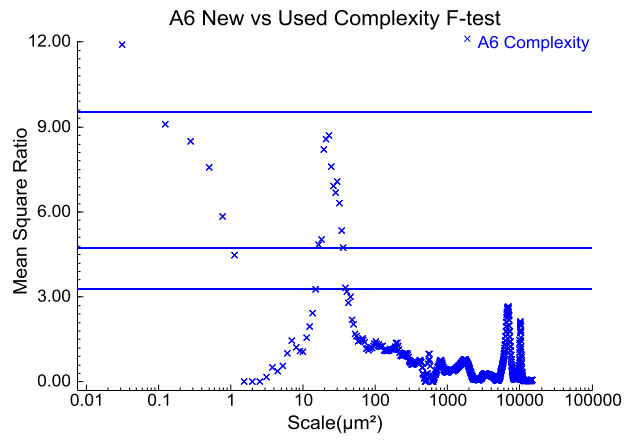
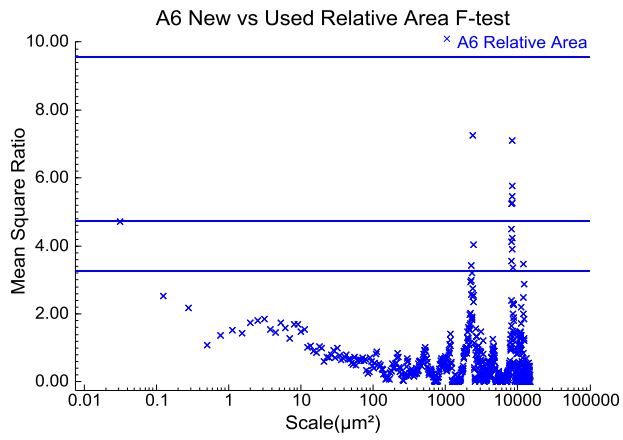
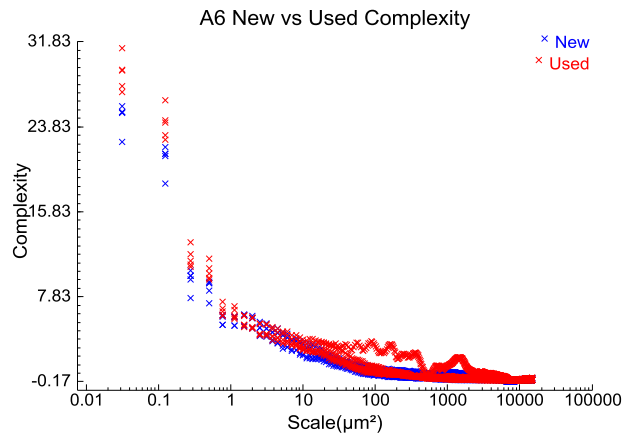
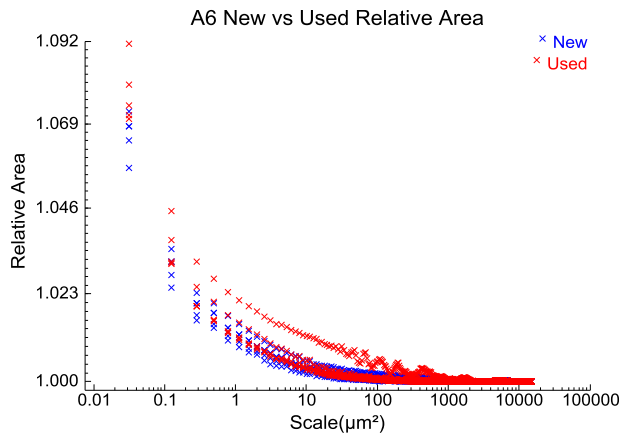
A4



A5

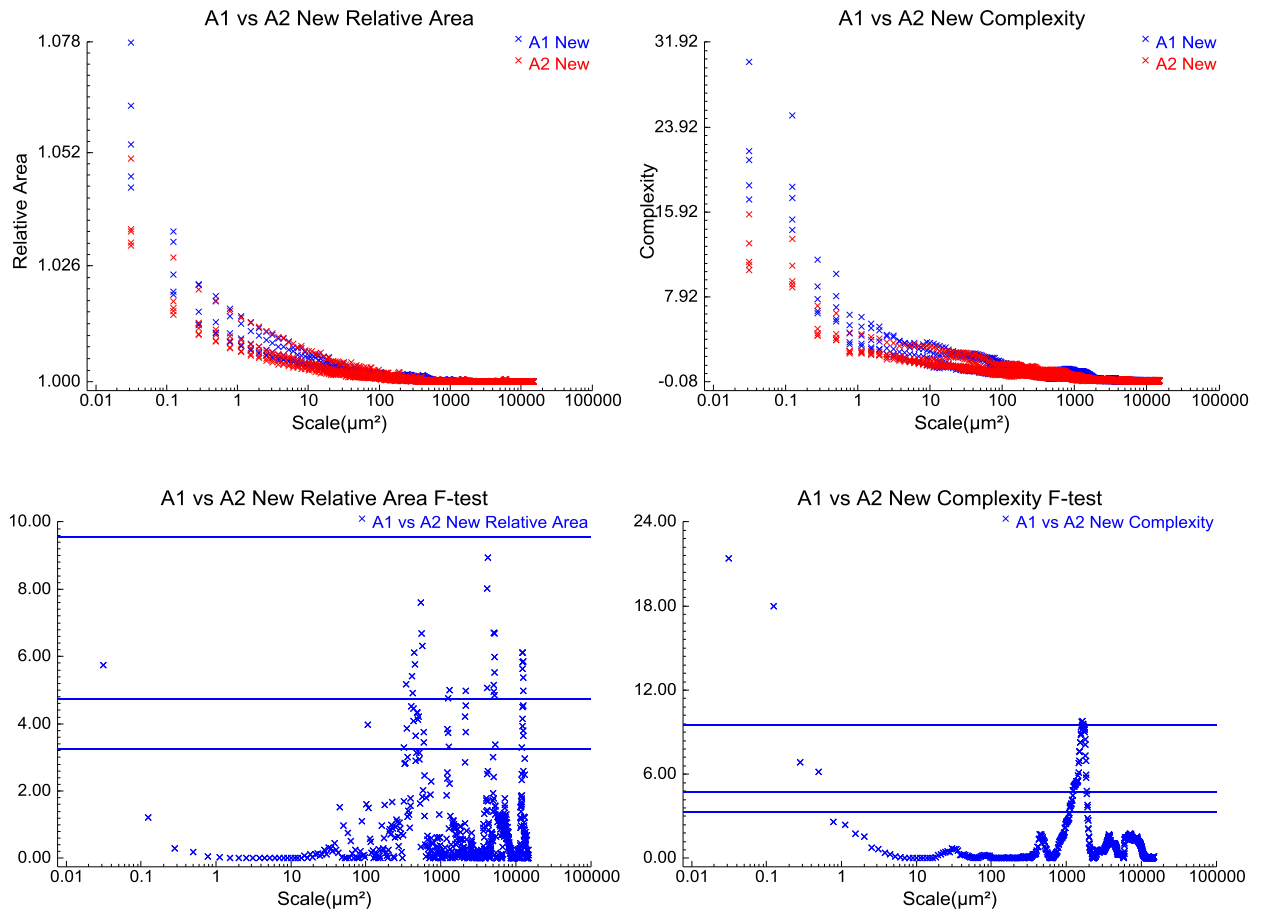


A6

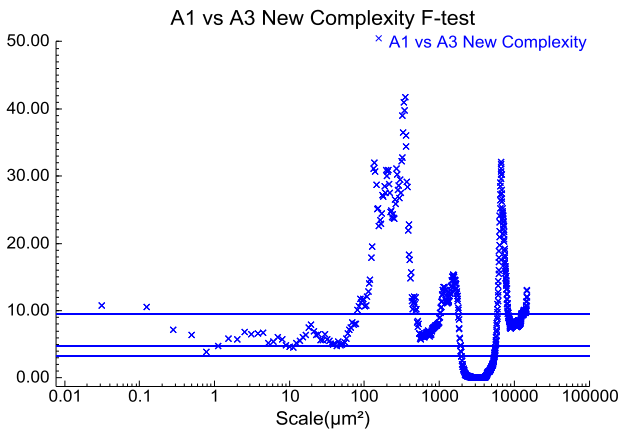
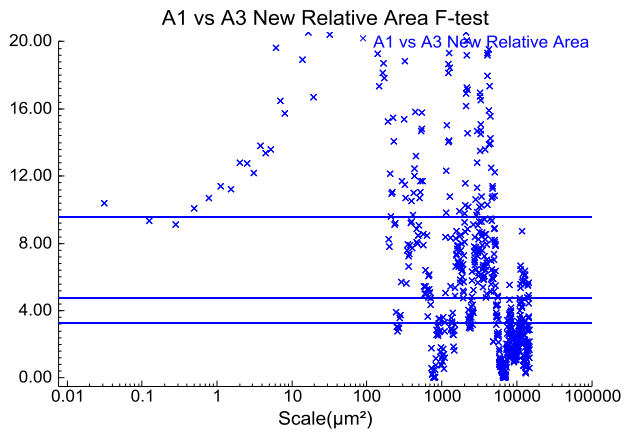
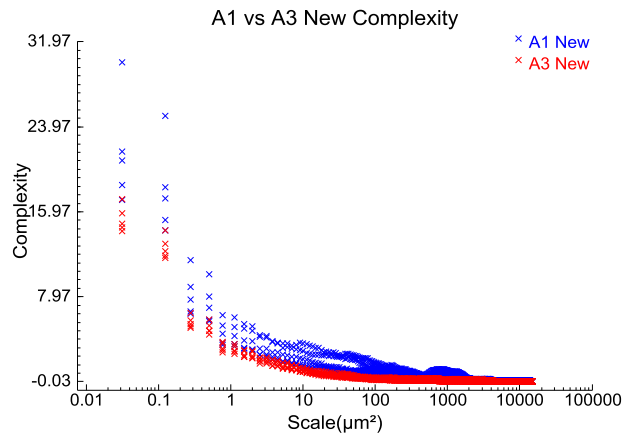
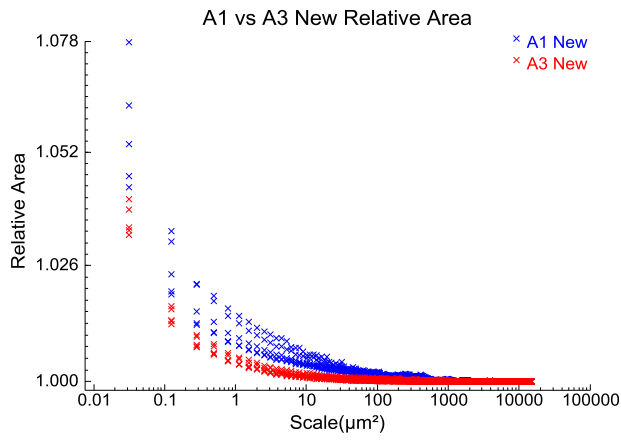


7.5 Appendix E: New vs. New - Graphs

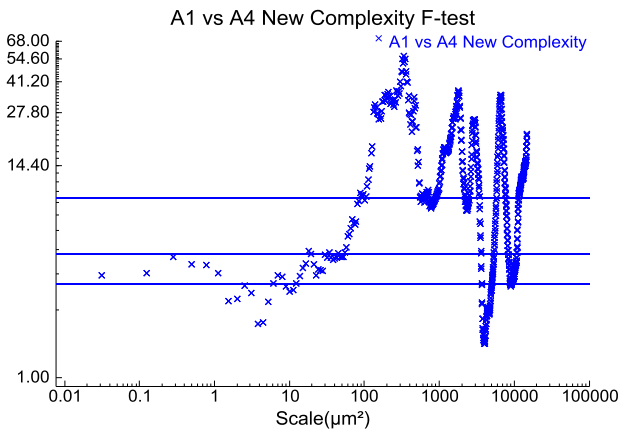
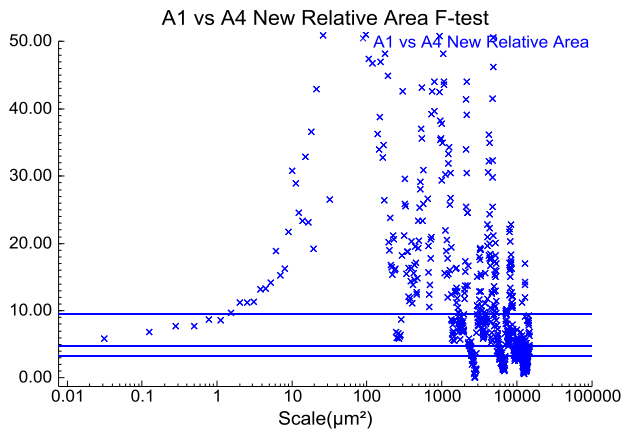
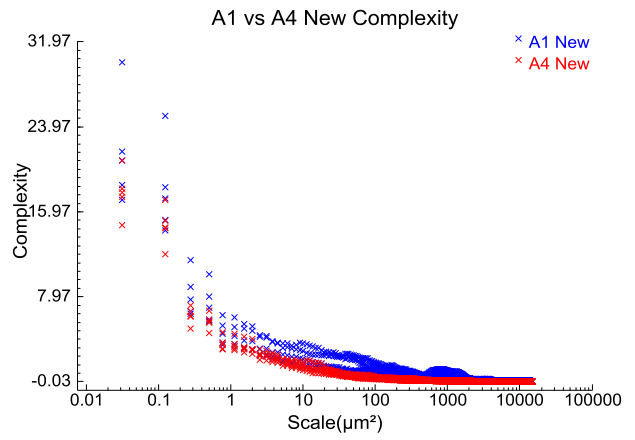
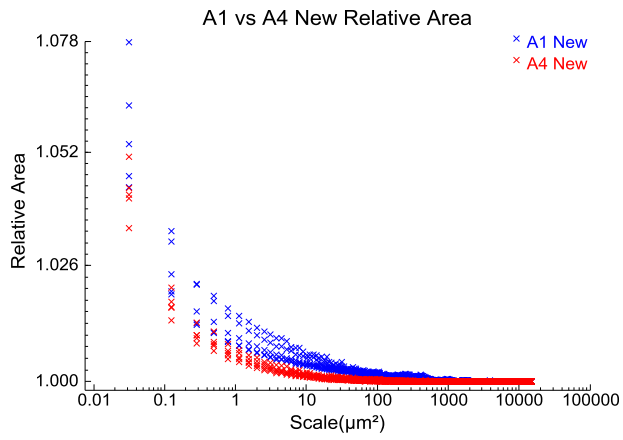
A1 vs. A2



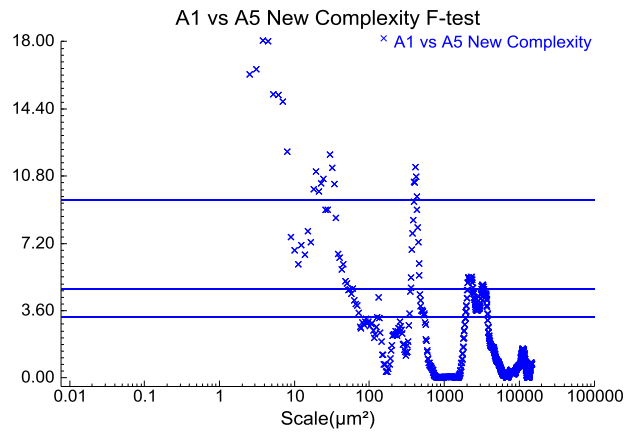
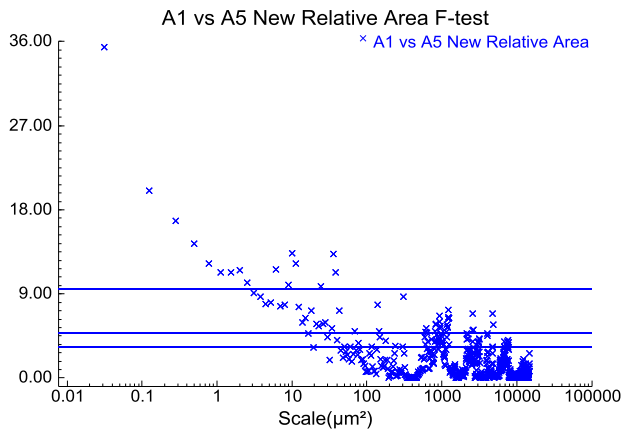
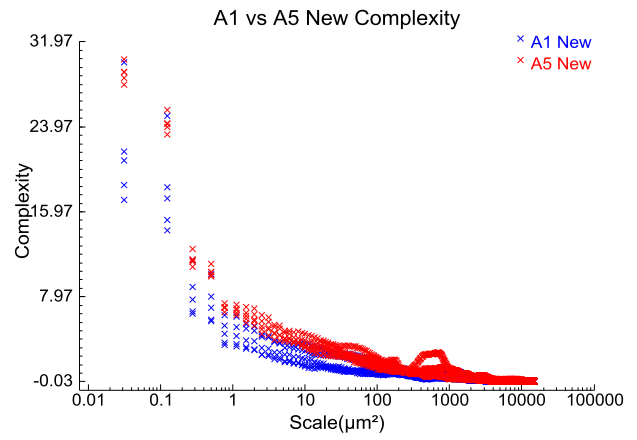
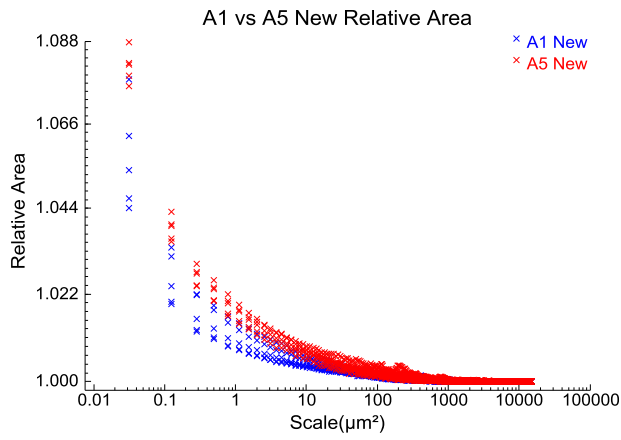
A1 vs. A3



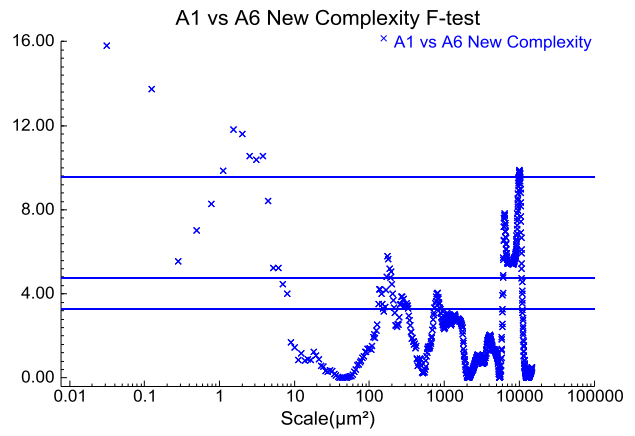
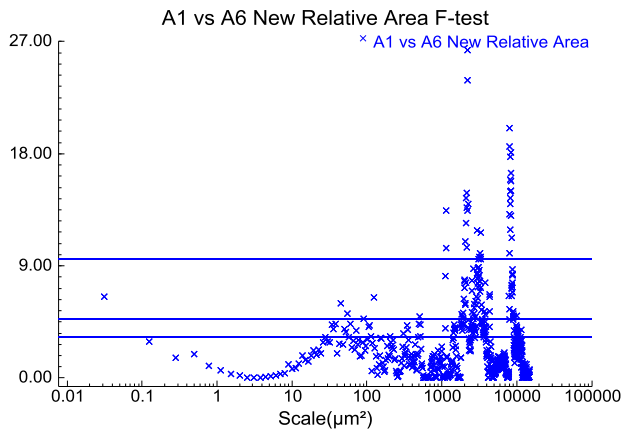
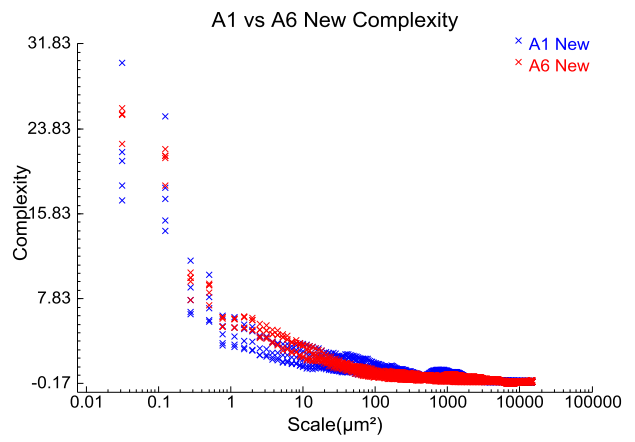
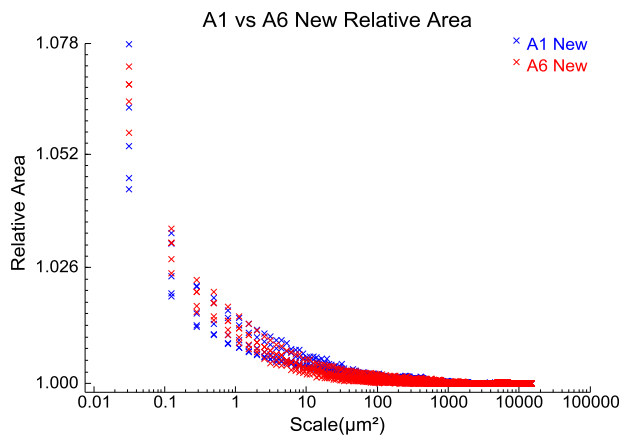
A1 vs. A4



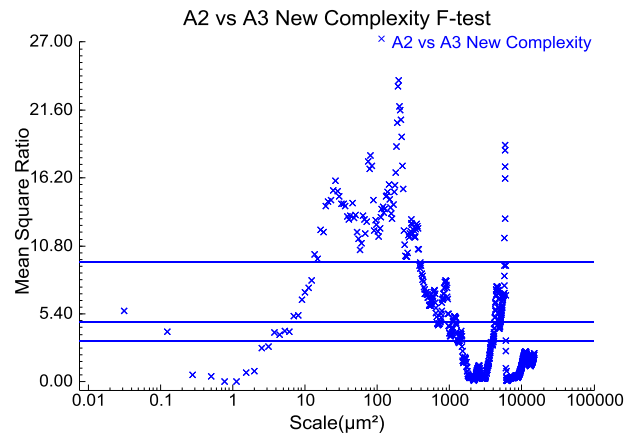
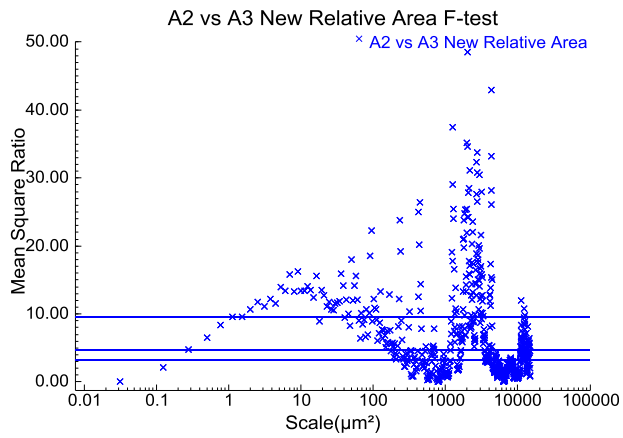
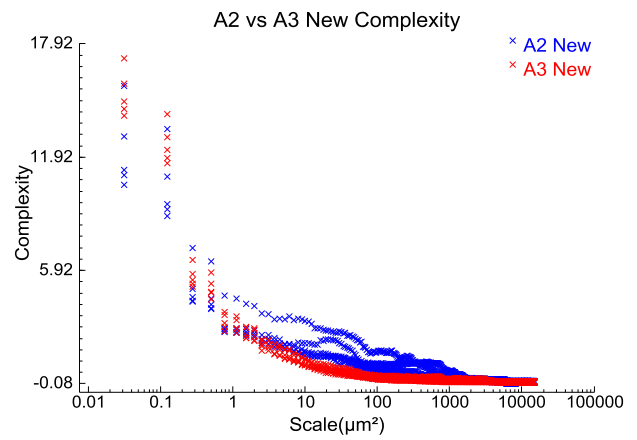
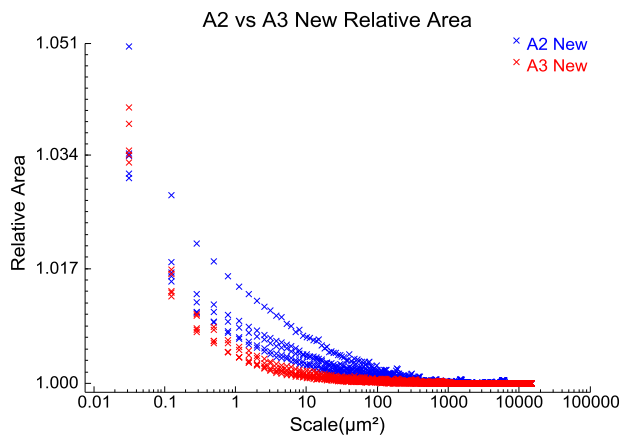
A1 vs. A5



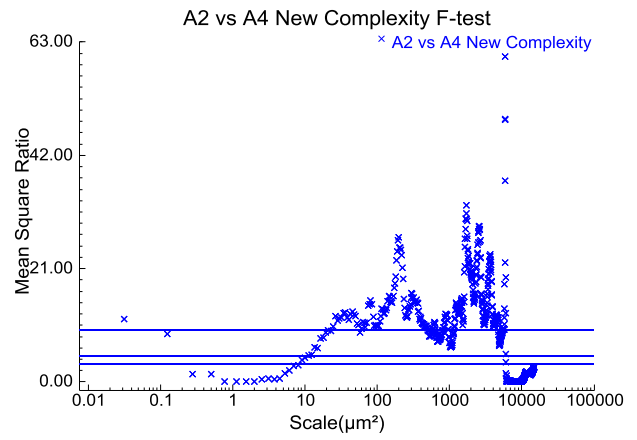
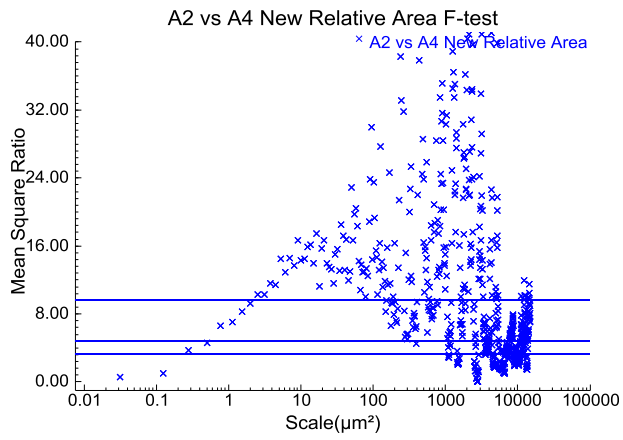
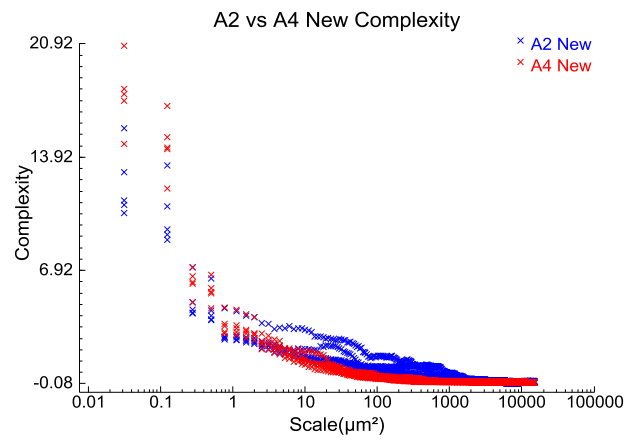
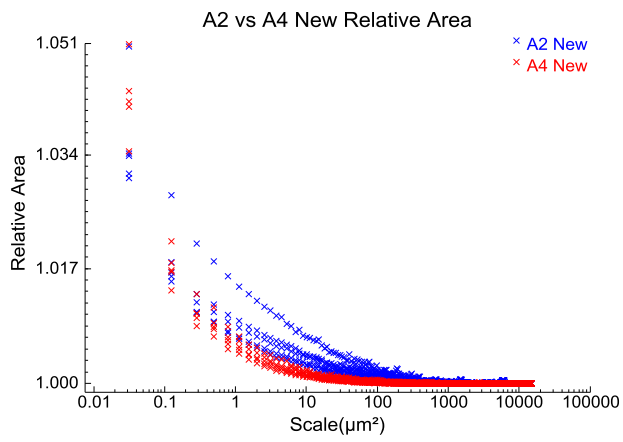
A1 vs. A6



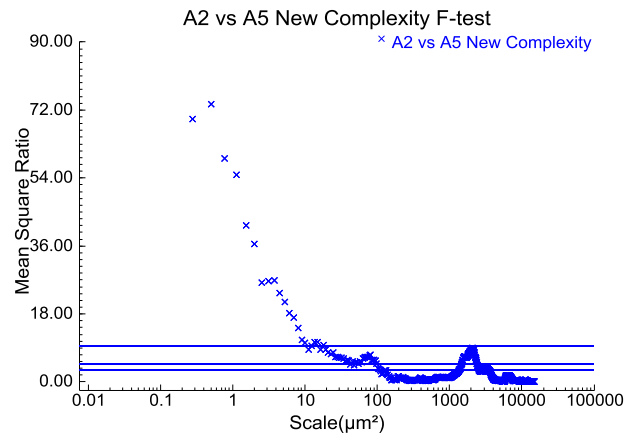
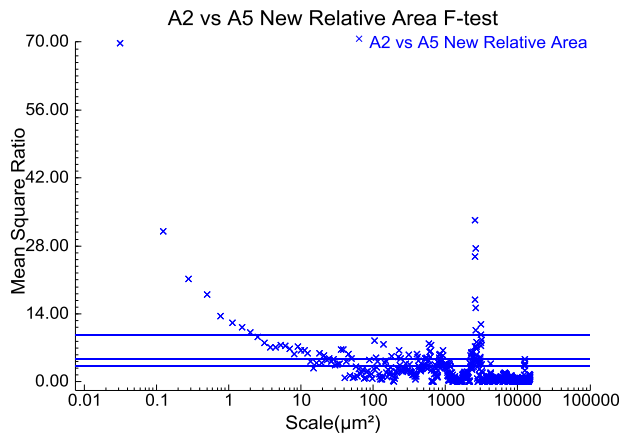
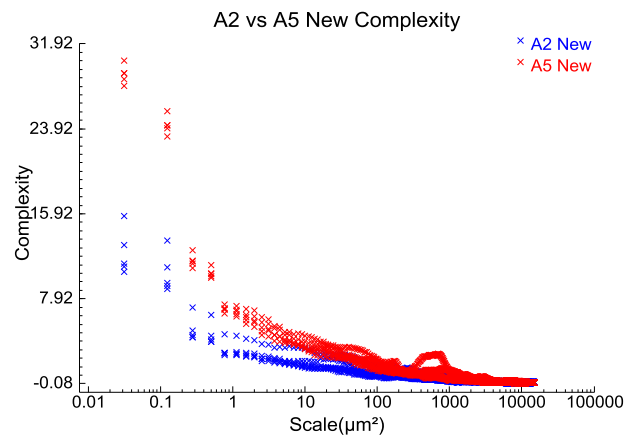
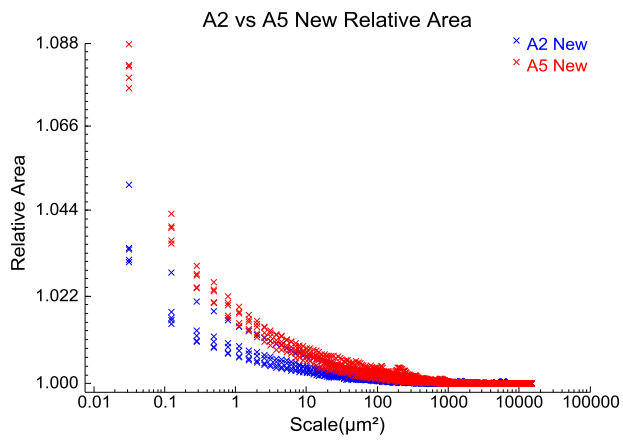
A2 vs. A3



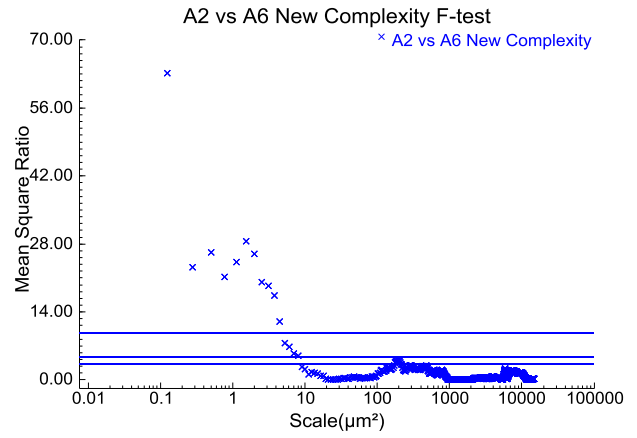
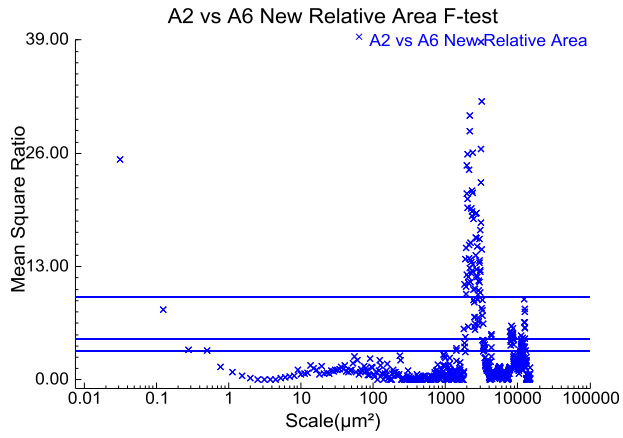
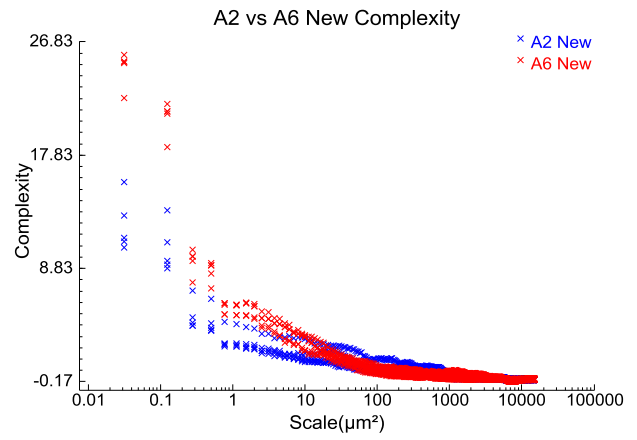
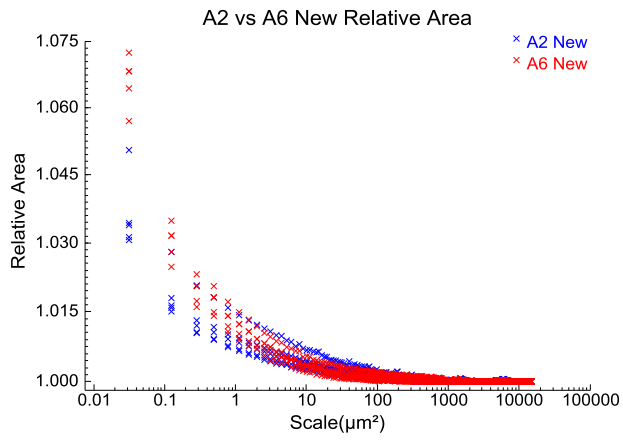
A2 vs. A4



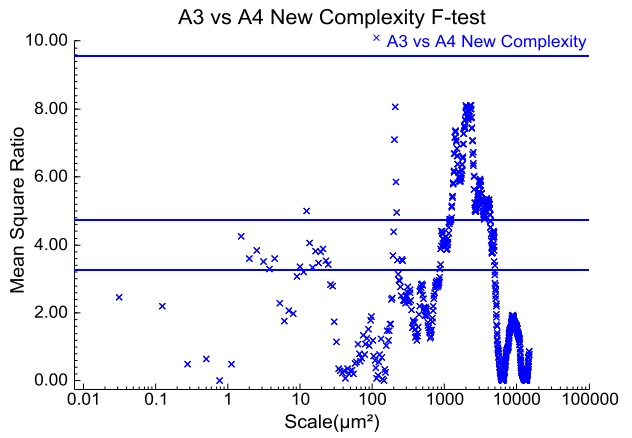
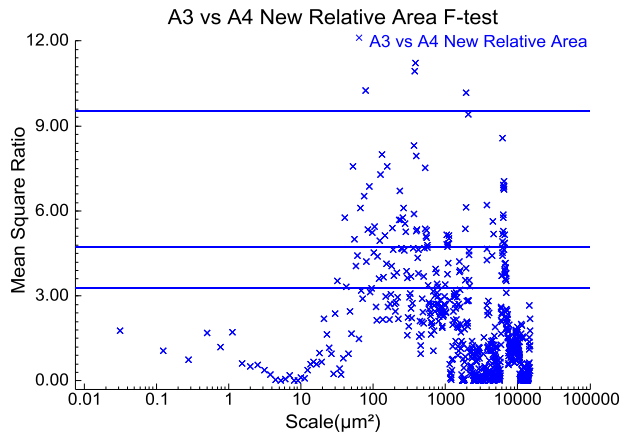
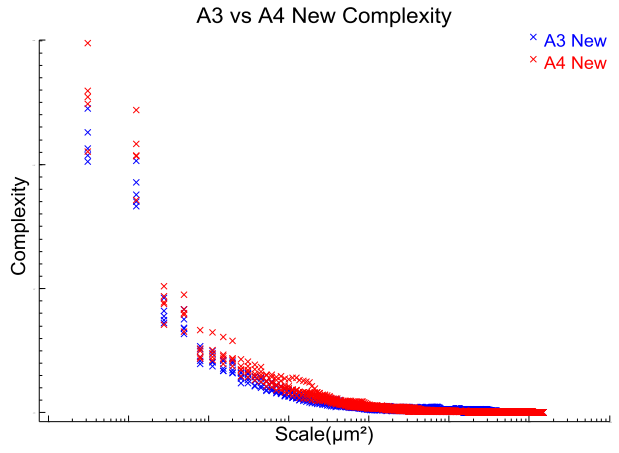
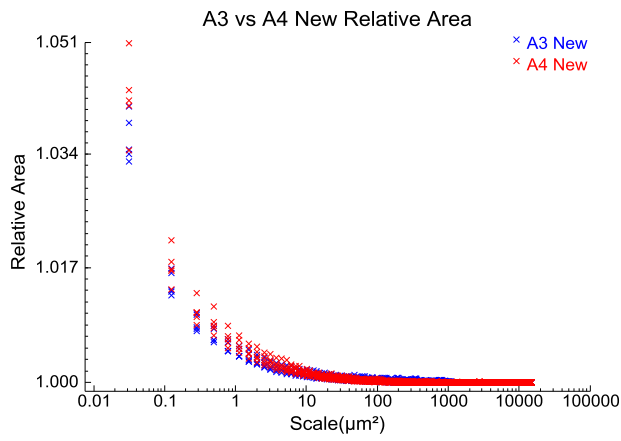
A2 vs. A5



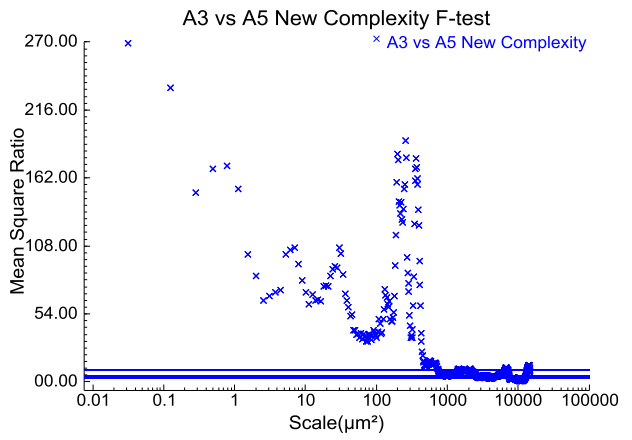
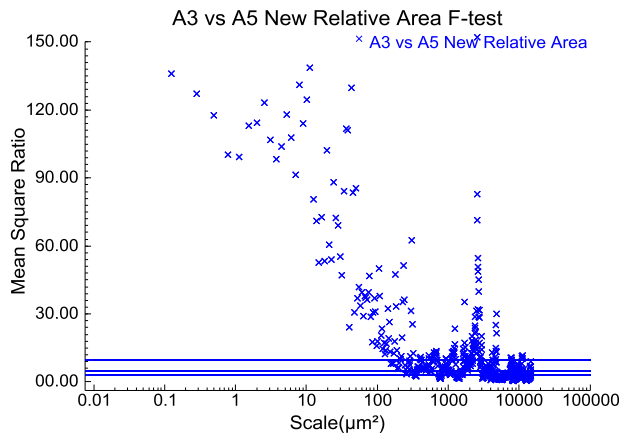
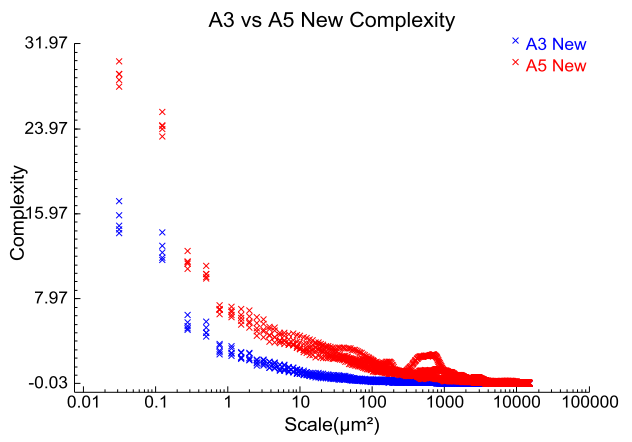
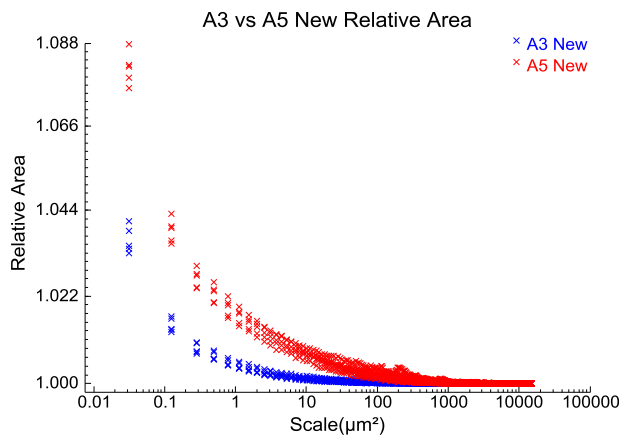
A2 vs. A6



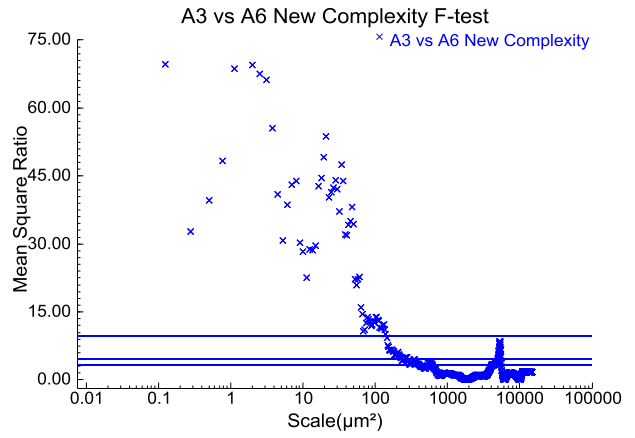
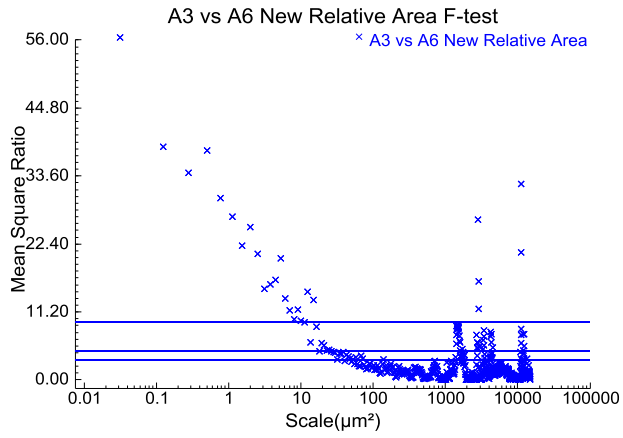
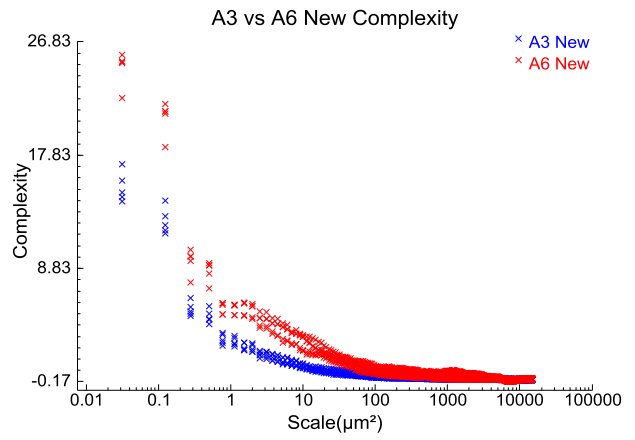
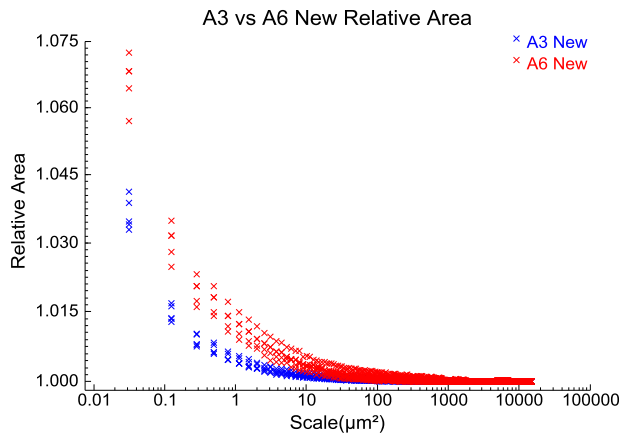
A3 vs. A4



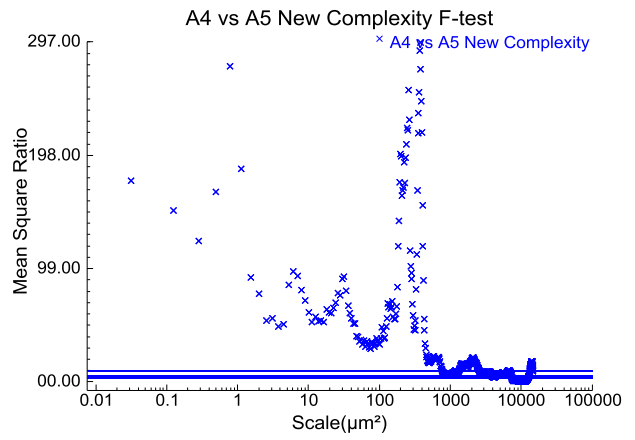
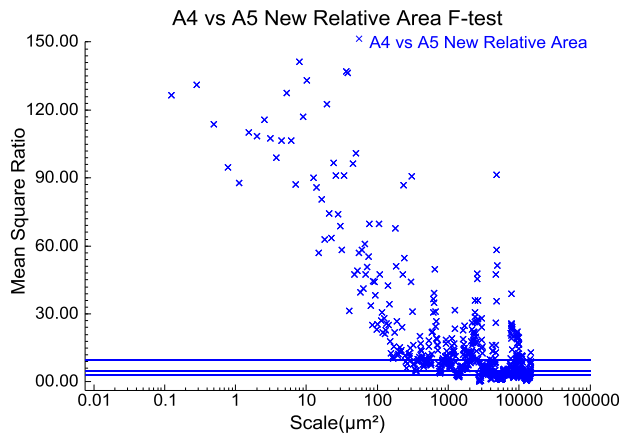
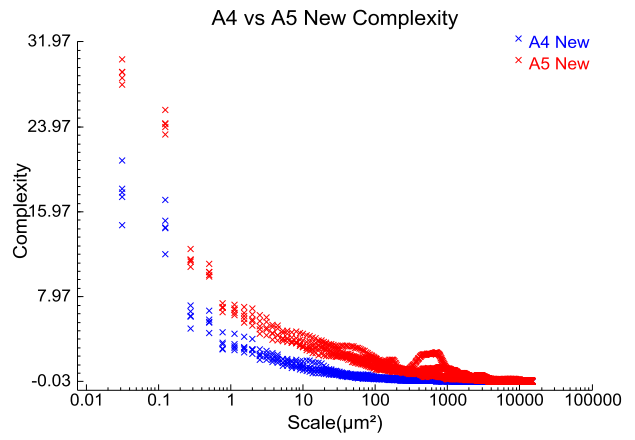
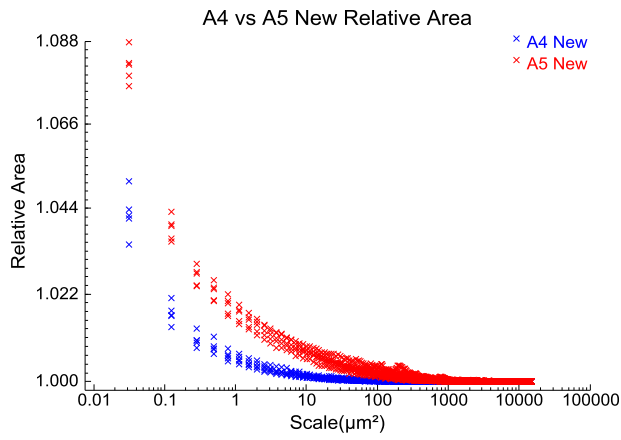
A3 vs. A5



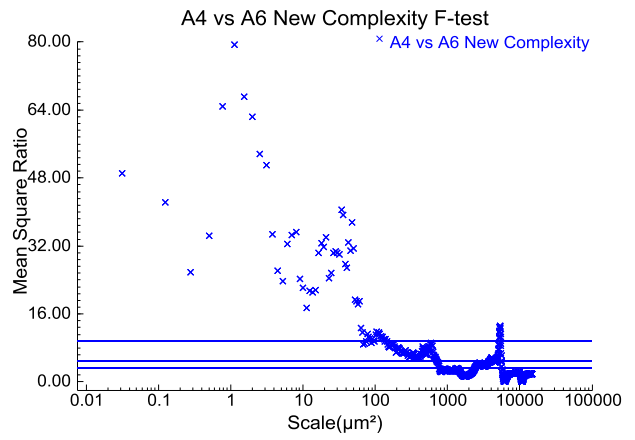
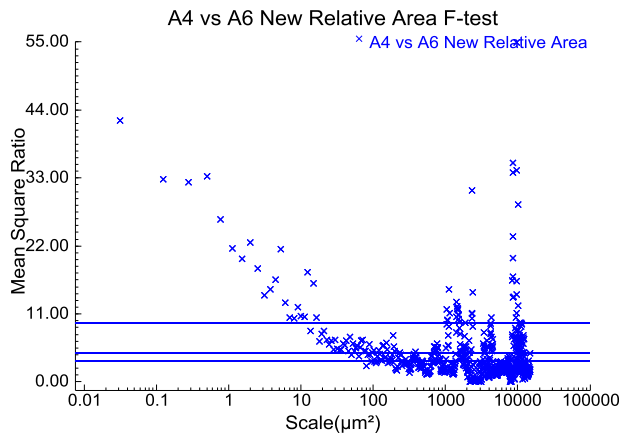
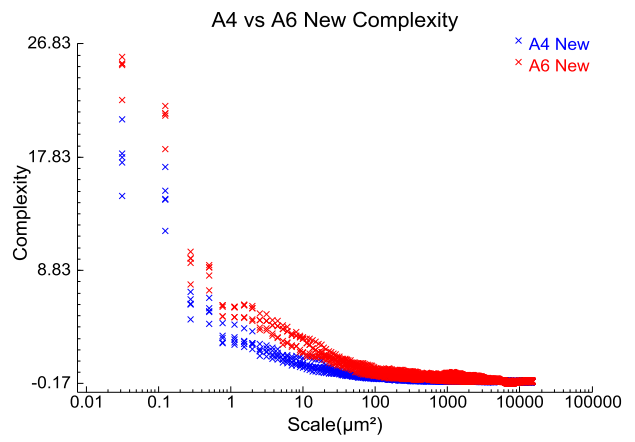
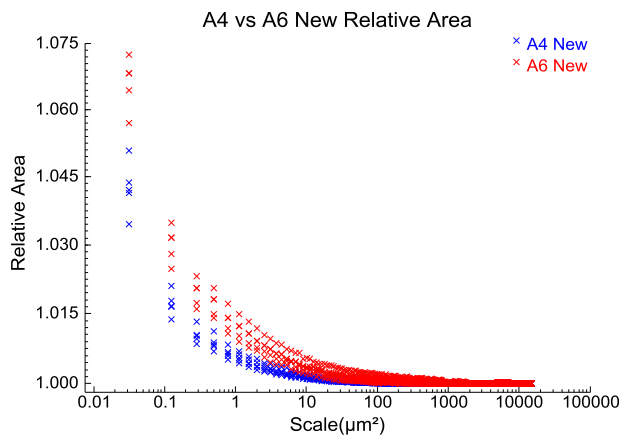
A3 vs. A6



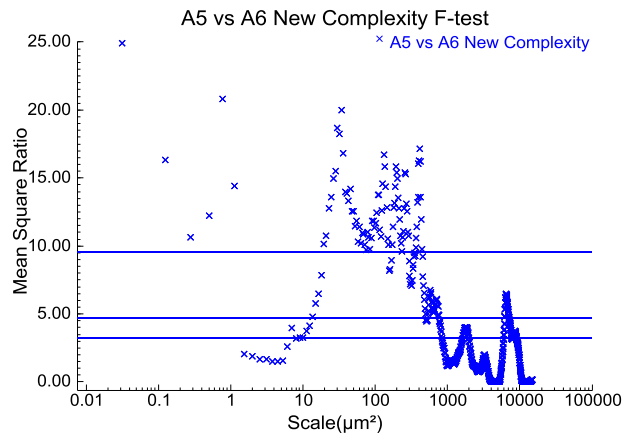
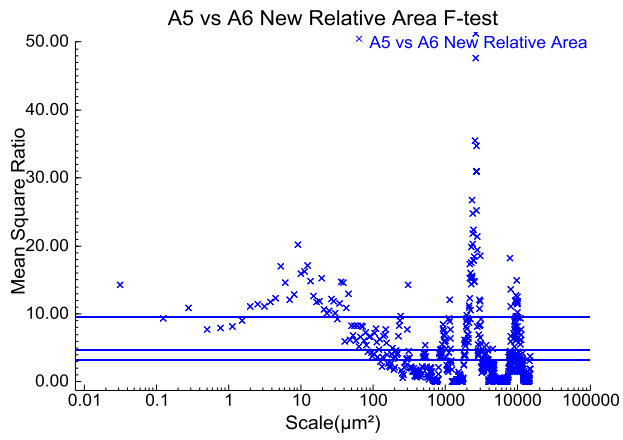
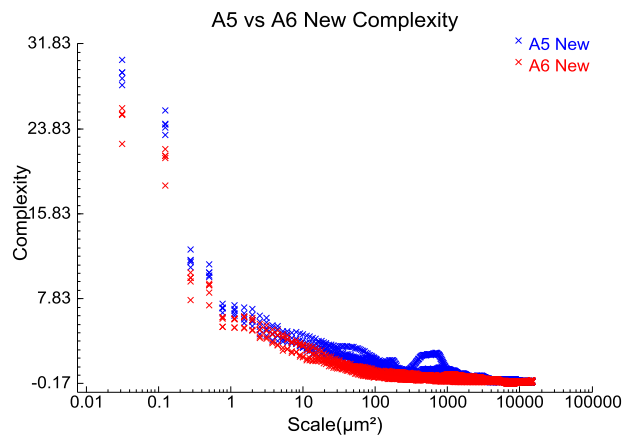
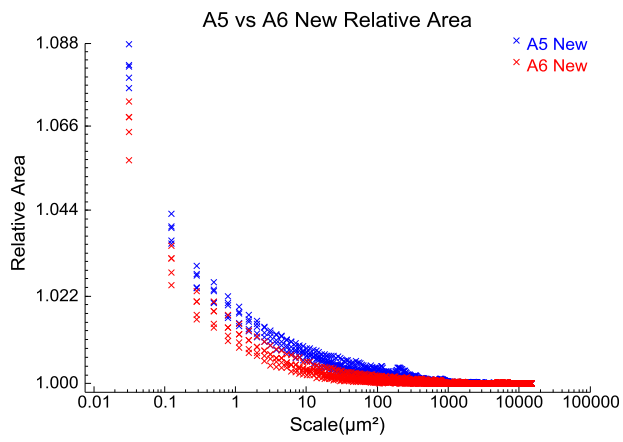
A4 vs. A5



A4 vs. A6

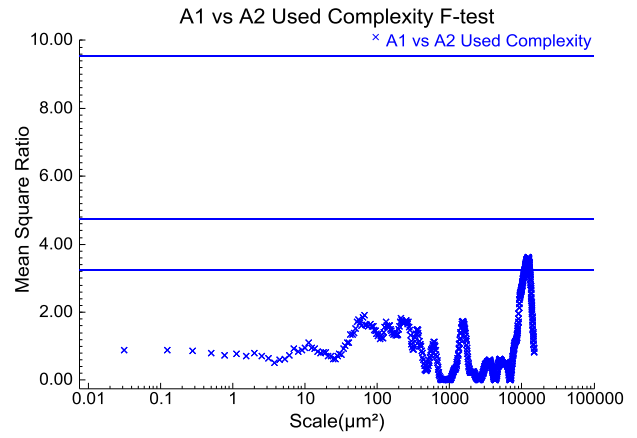
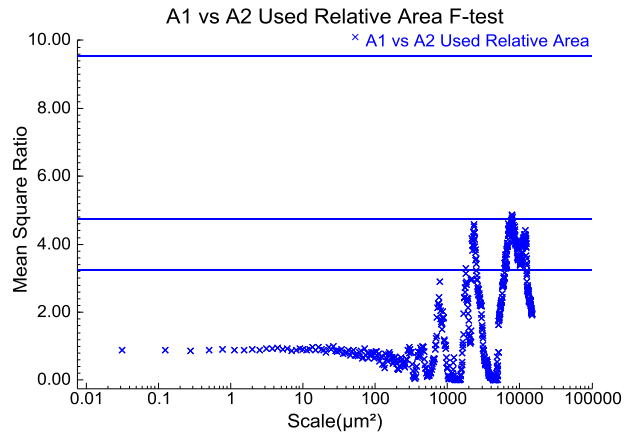
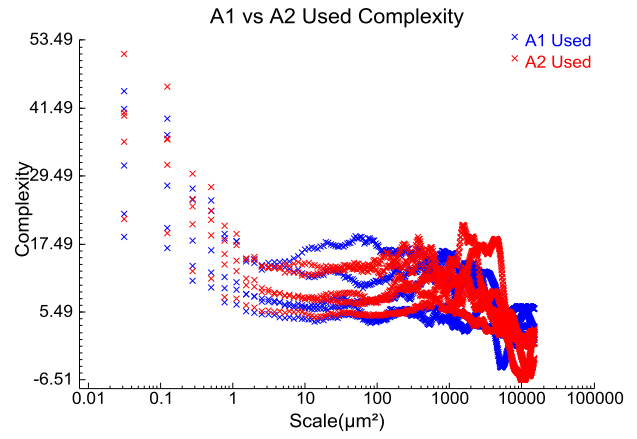
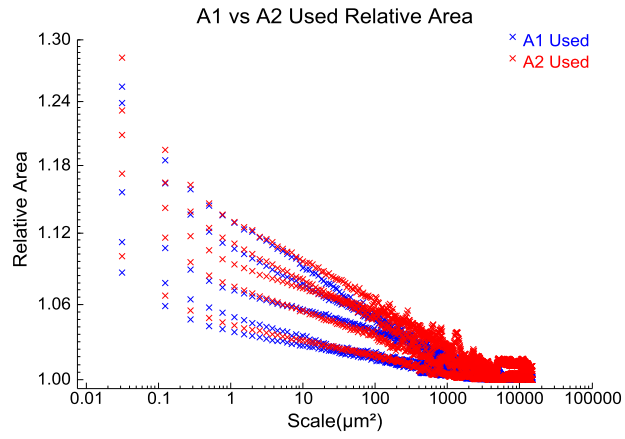


A5 vs. A6

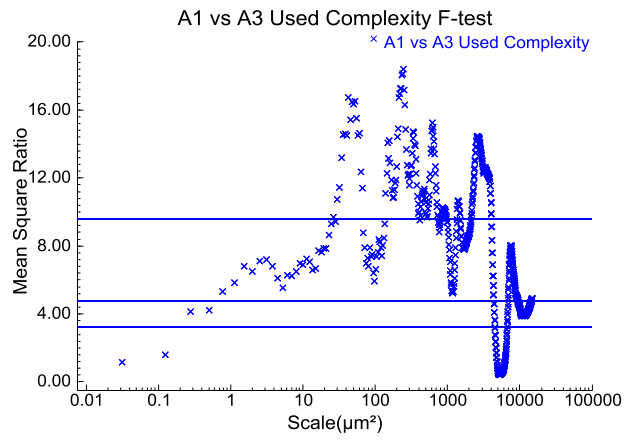
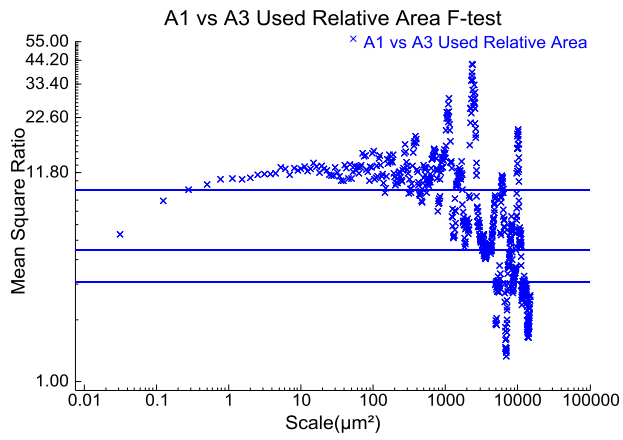
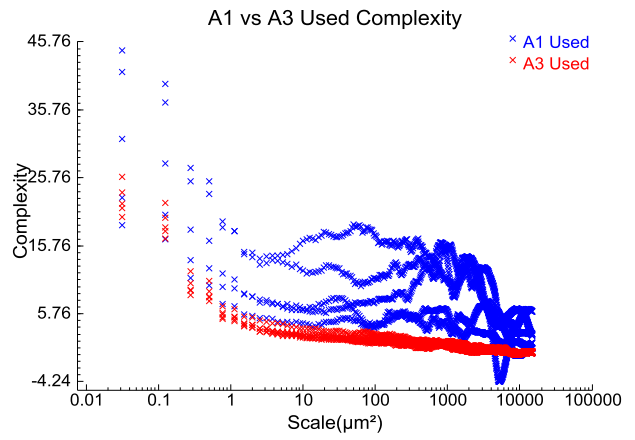
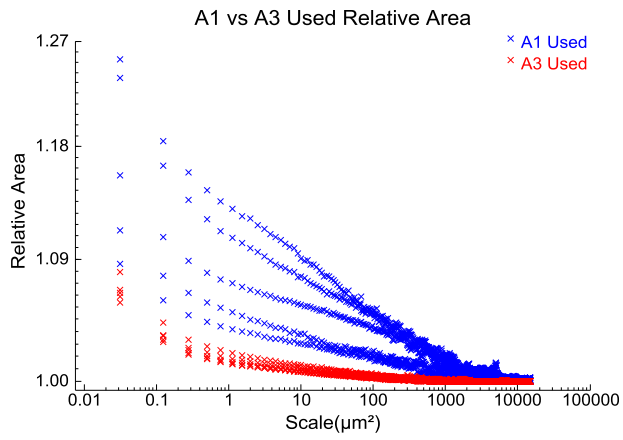


7.6 Appendix F: Used vs. Used - Graphs

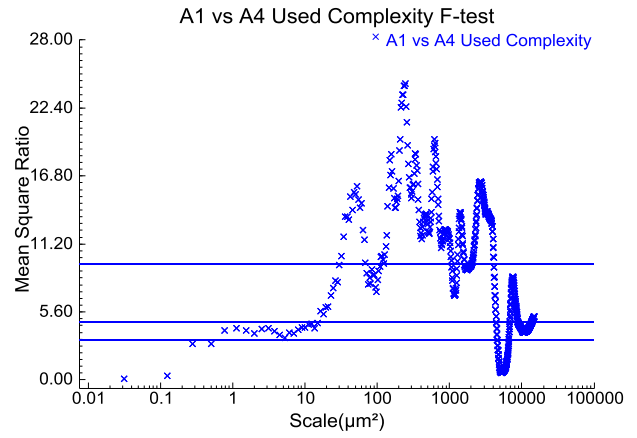
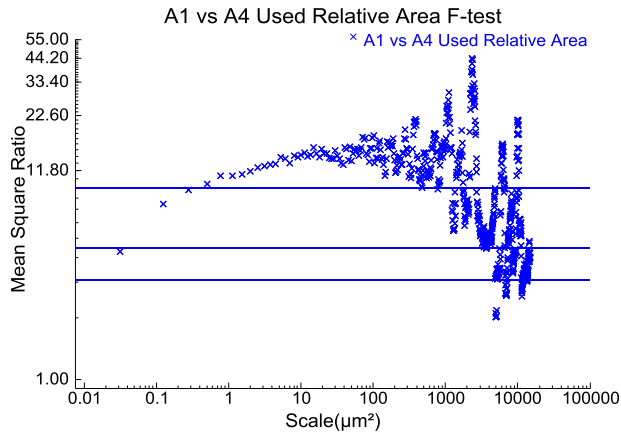
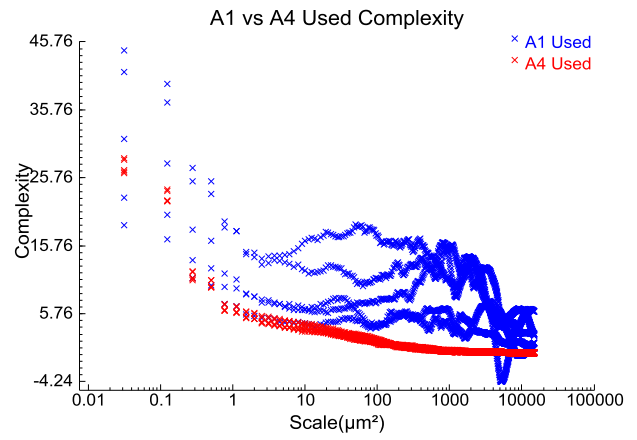
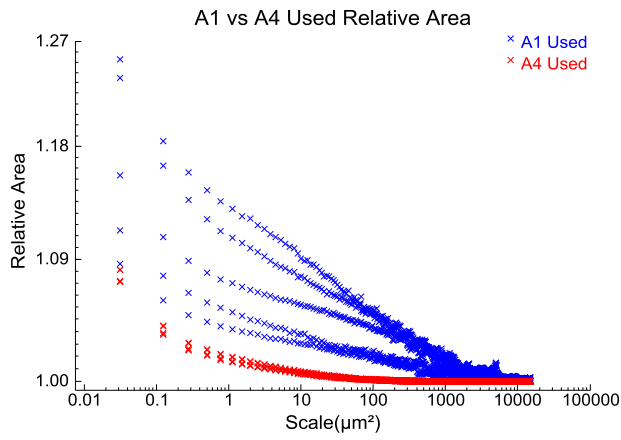
A1 vs. A2



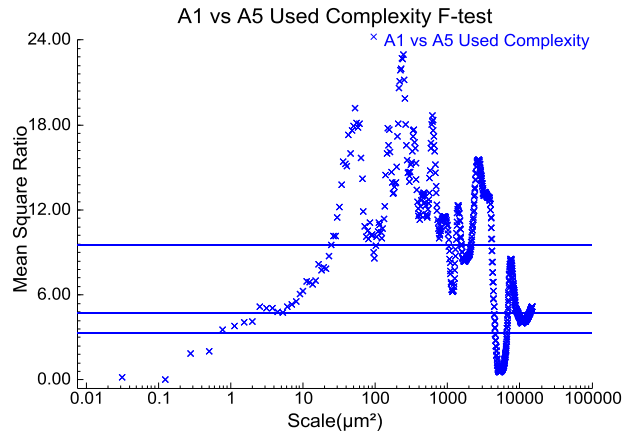
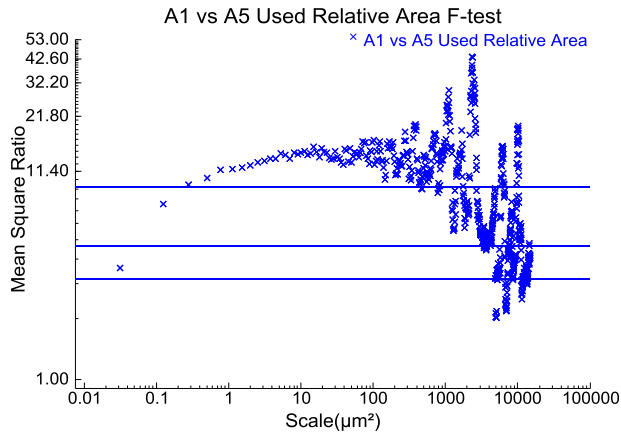
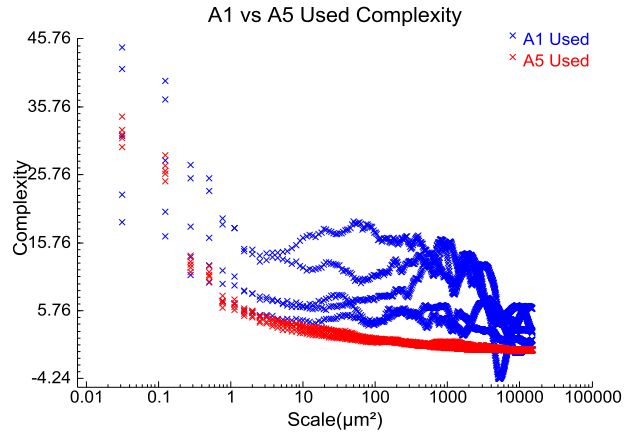
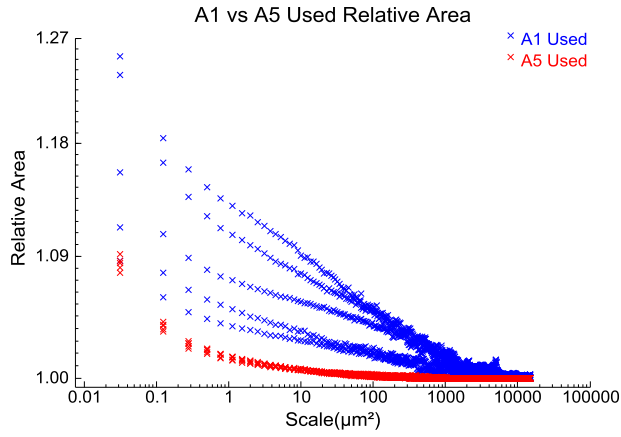
A1 vs. A3



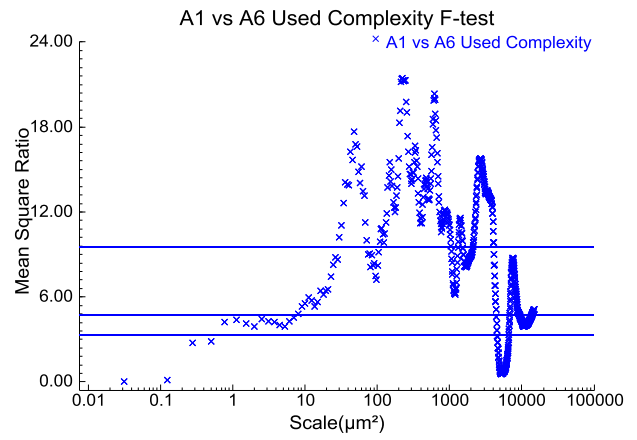
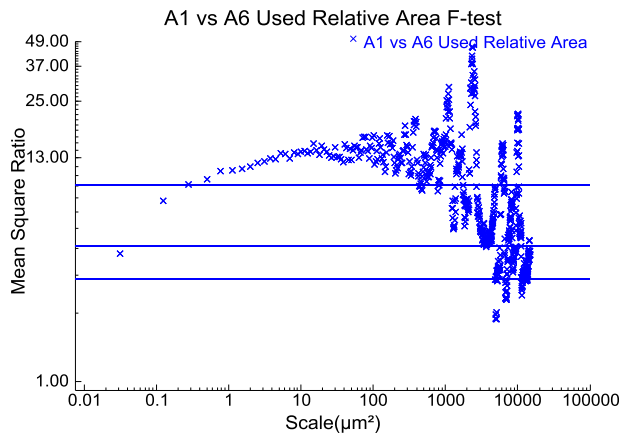
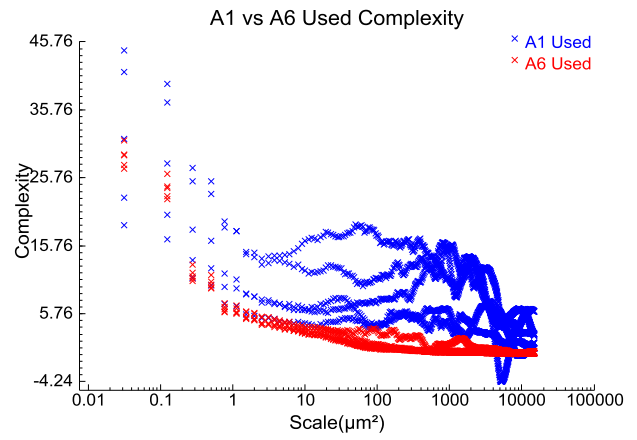
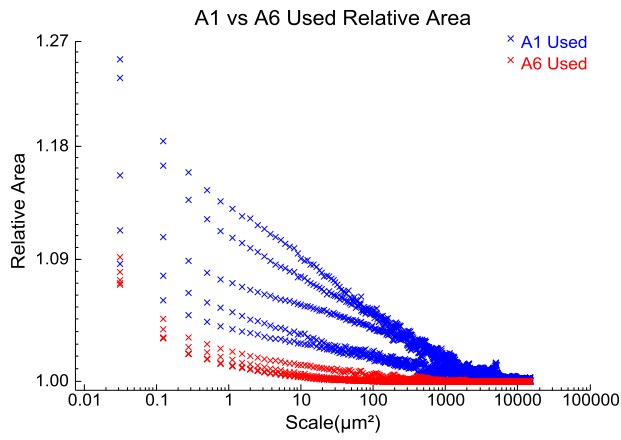
A1 vs. A4



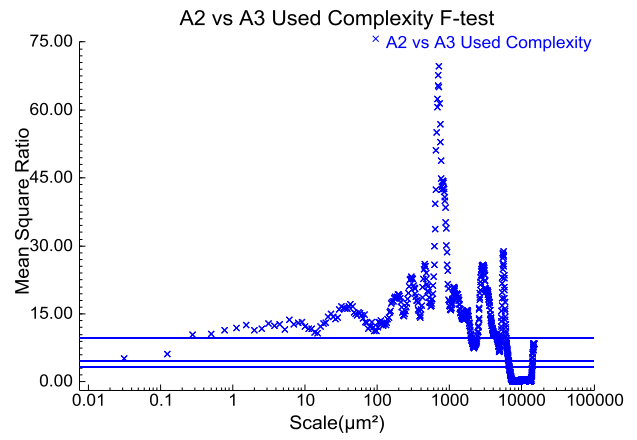
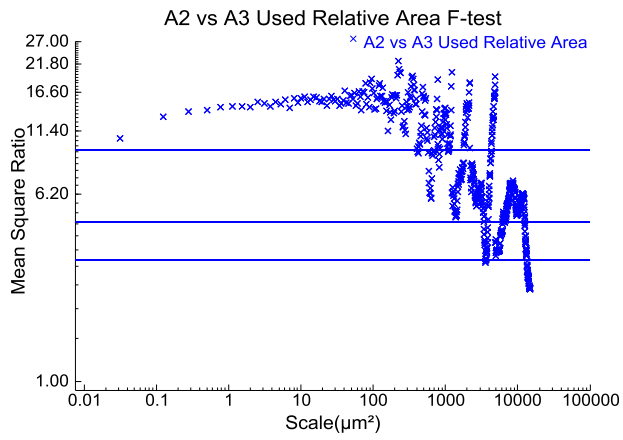
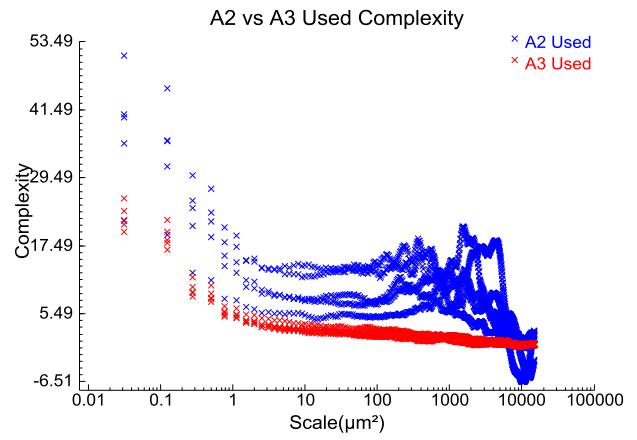
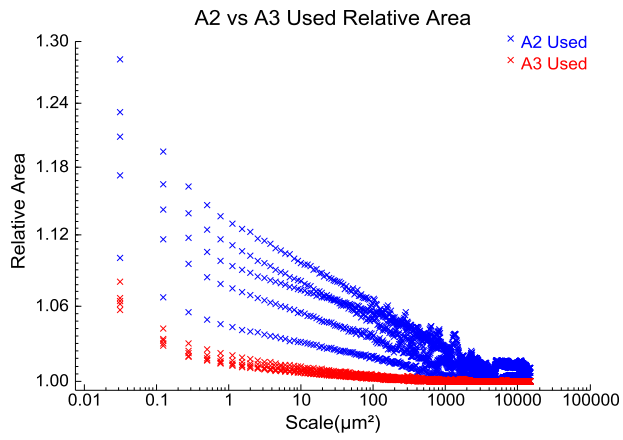
A1 vs. A5



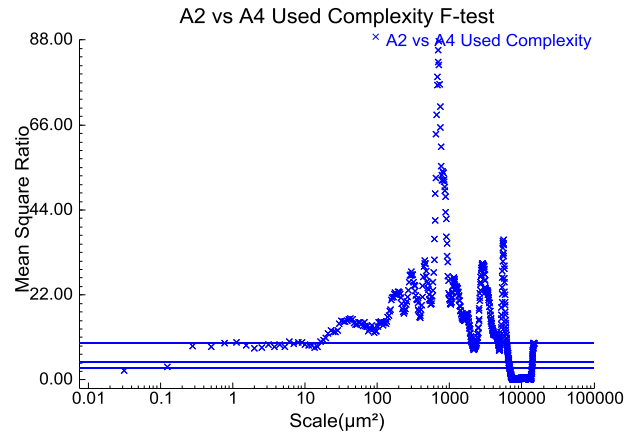
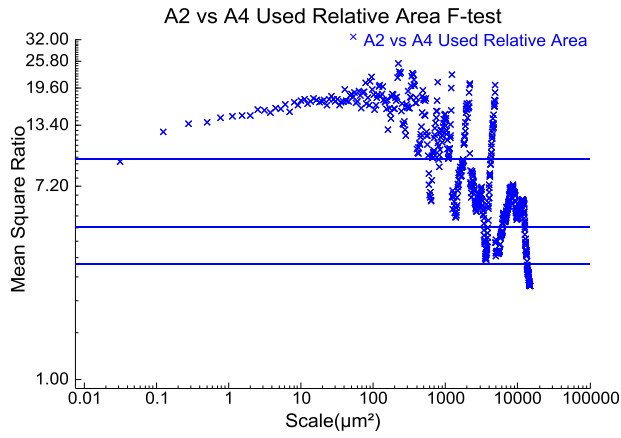
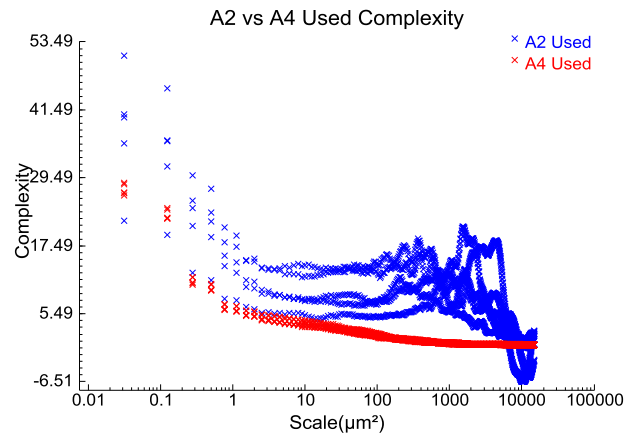
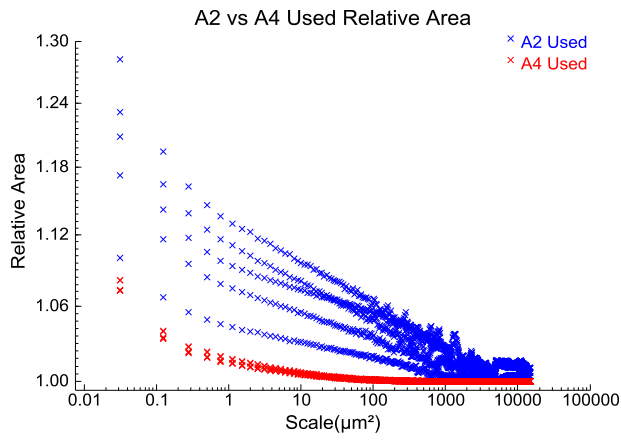
A1 vs. A6



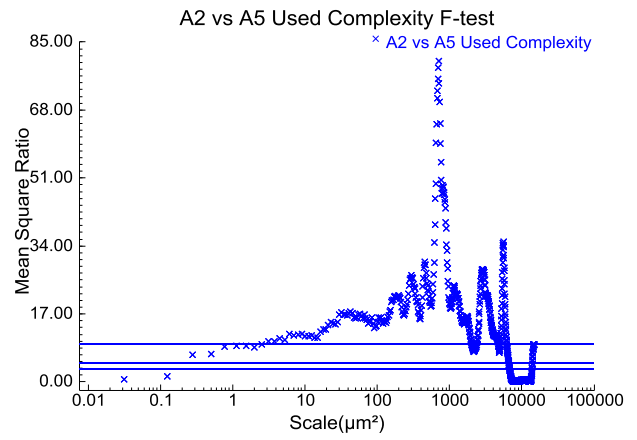
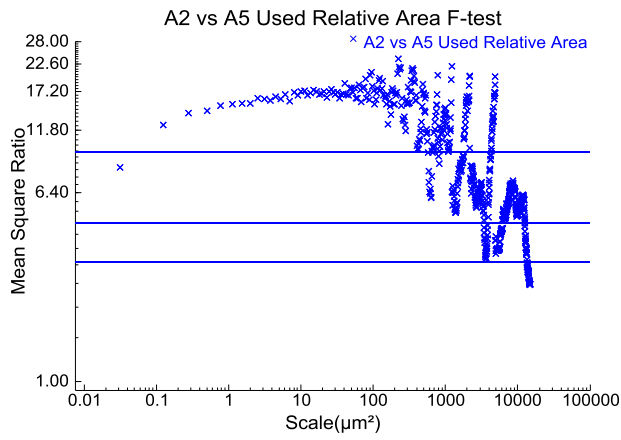
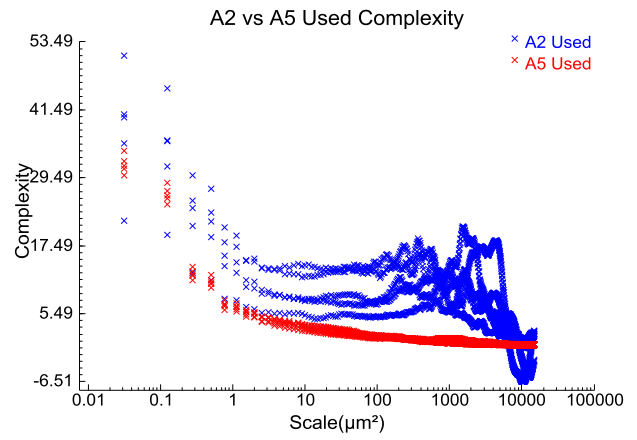
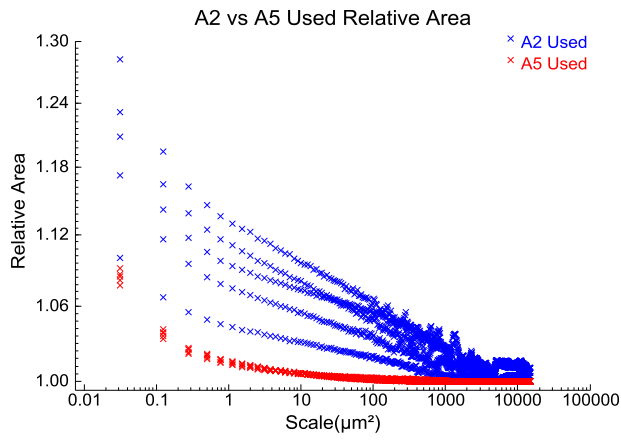
A2 vs. A3



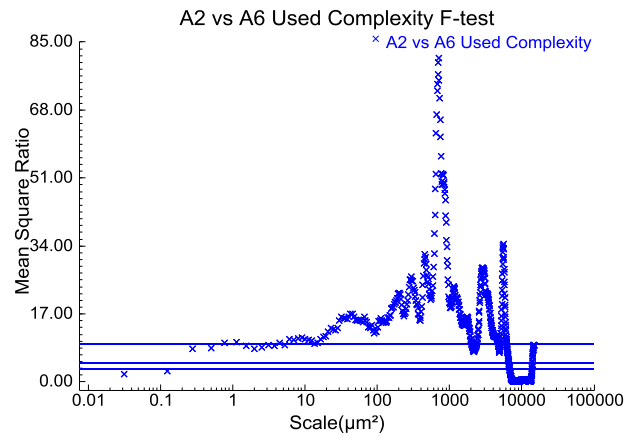
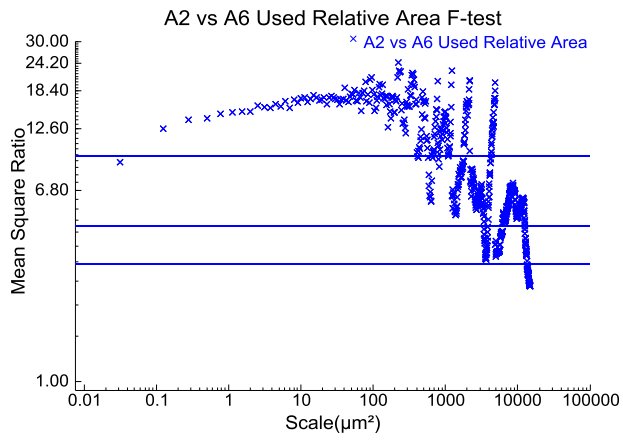
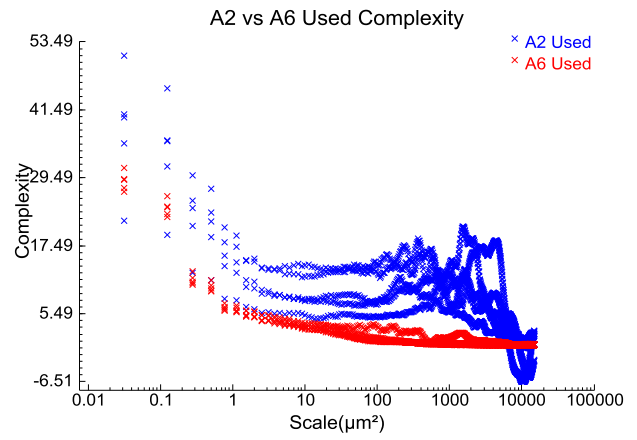
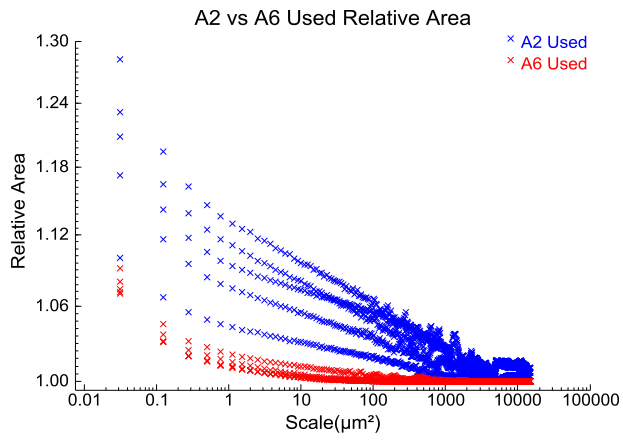
A2 vs. A4



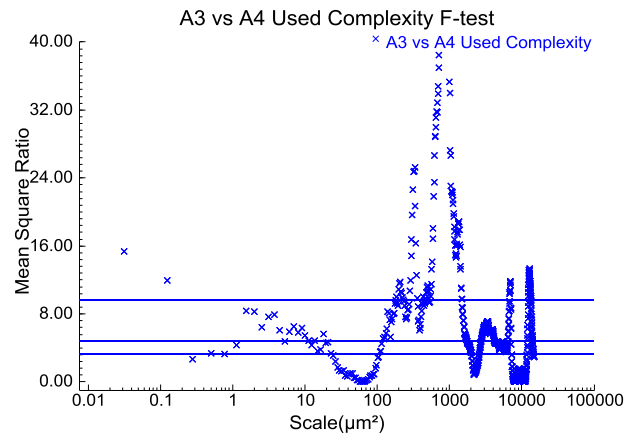
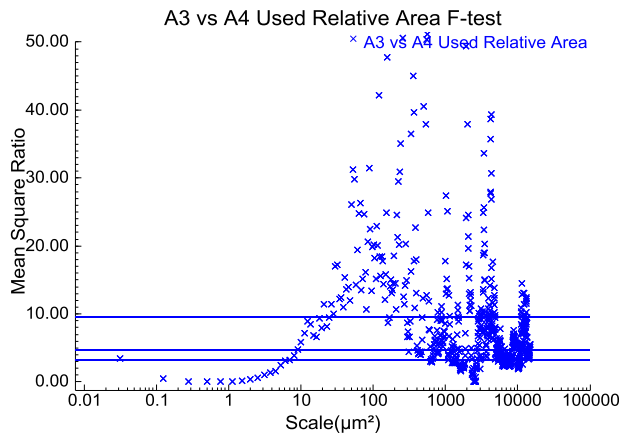
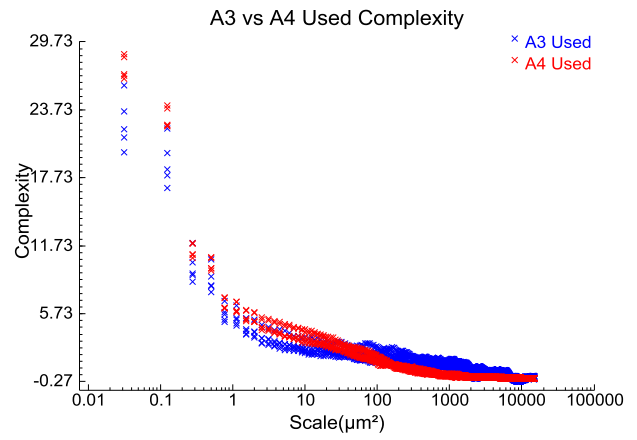
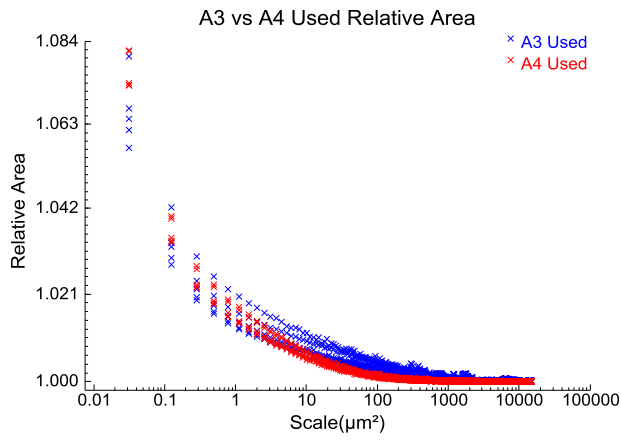
A2 vs. A5



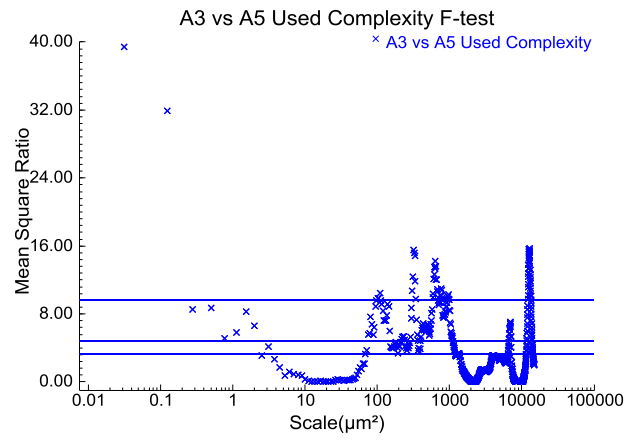
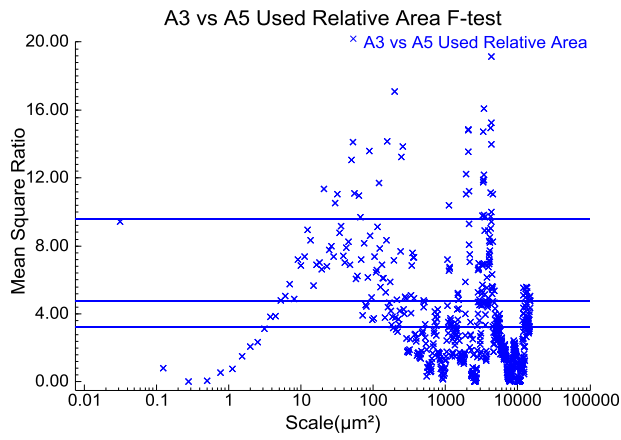
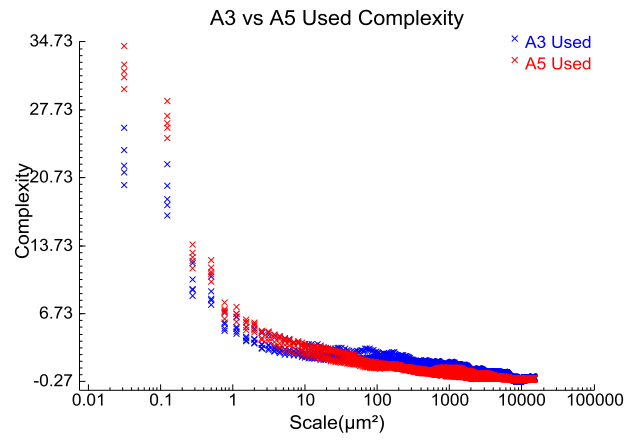
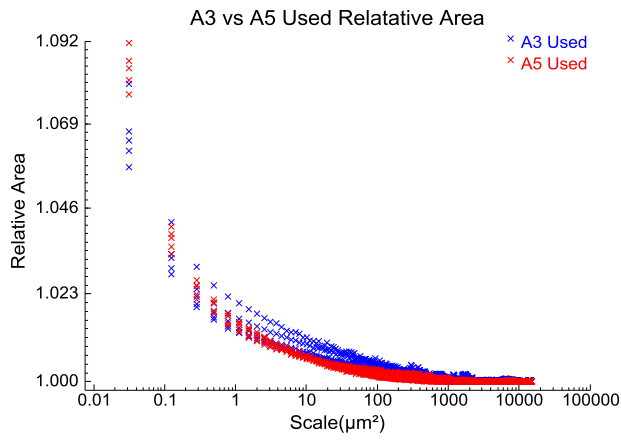
A2 vs. A6



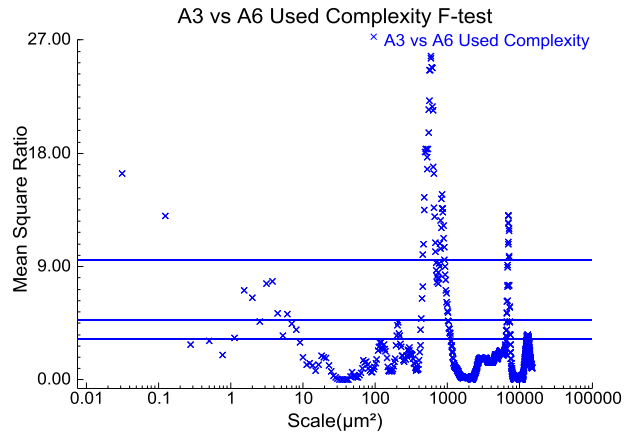
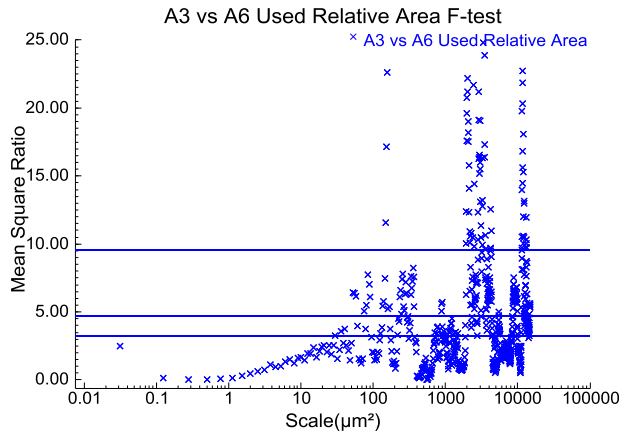
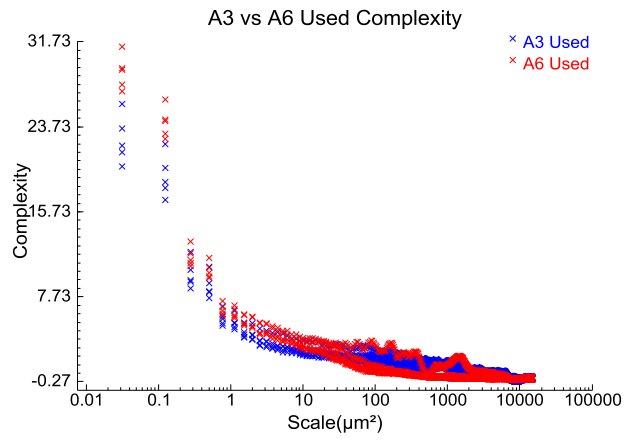
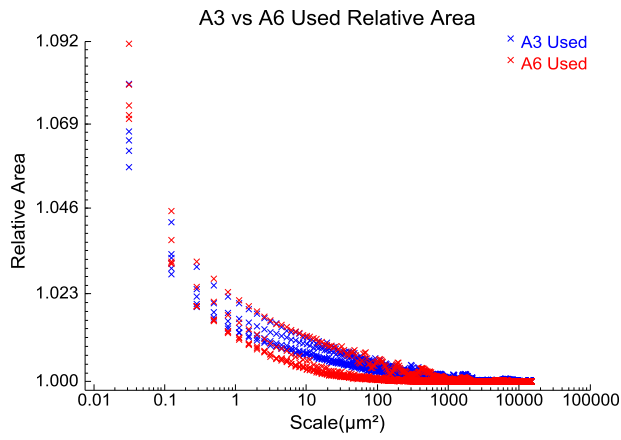
A3 vs. A4



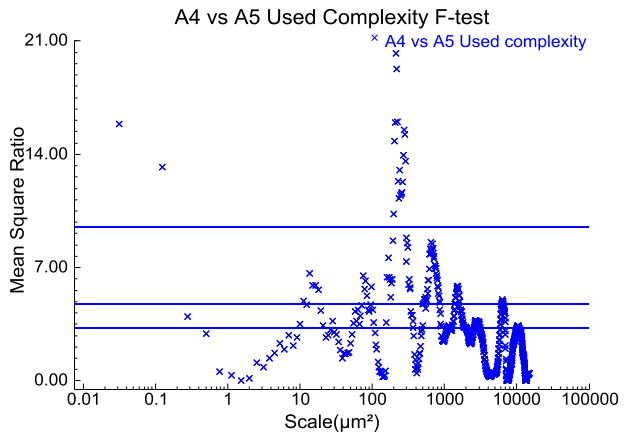
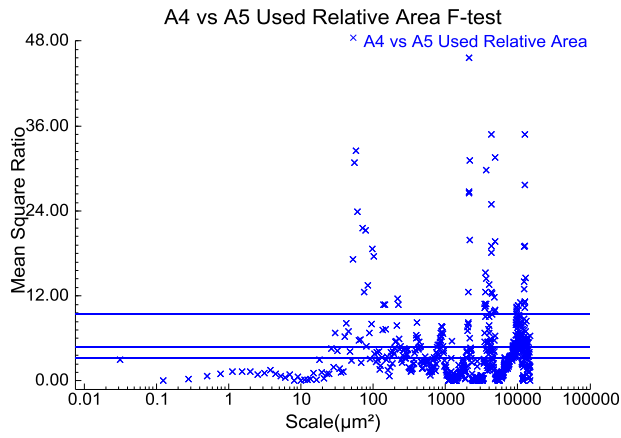
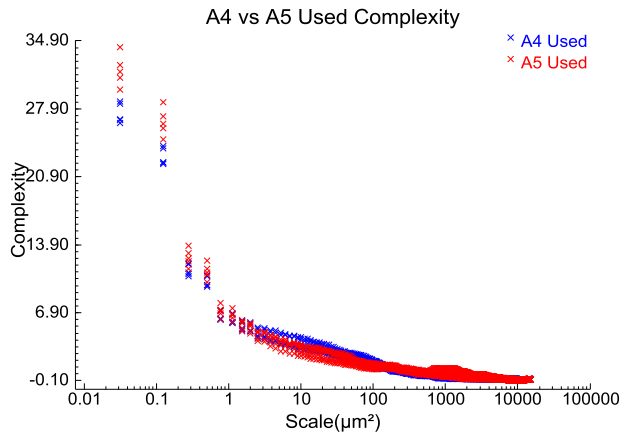
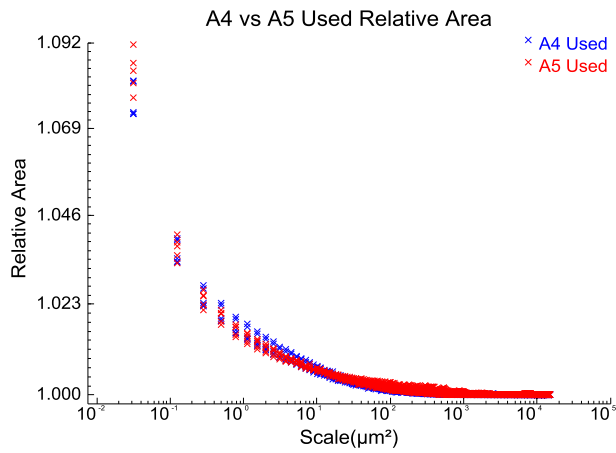
A3 vs. A5



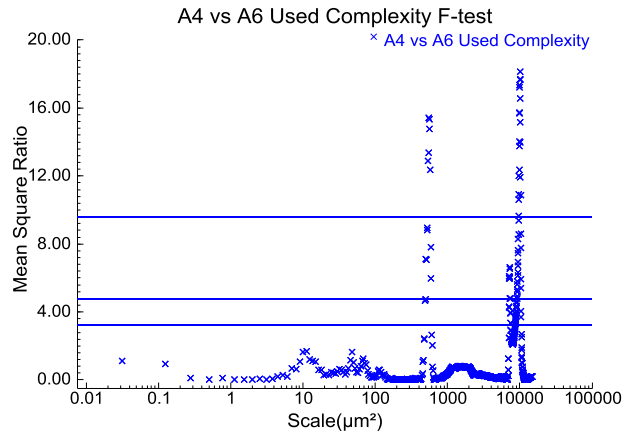
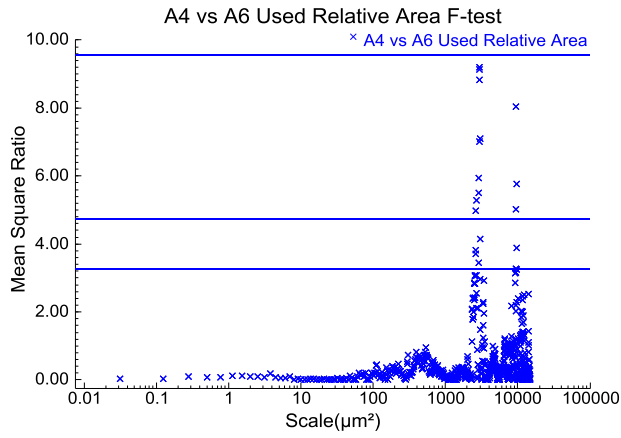
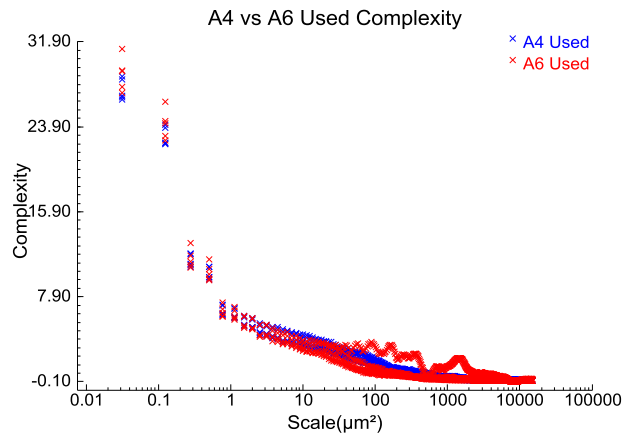
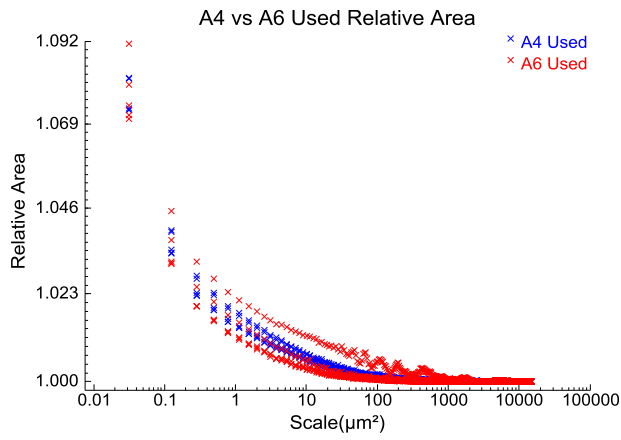
A3 vs. A6



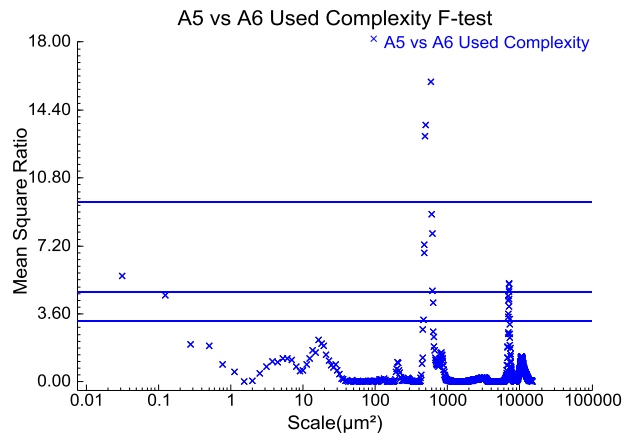
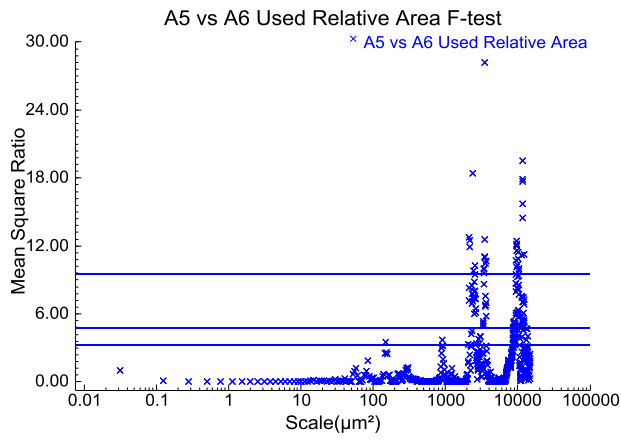
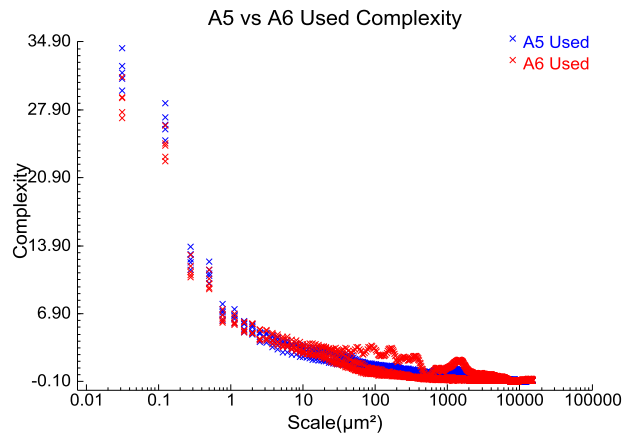
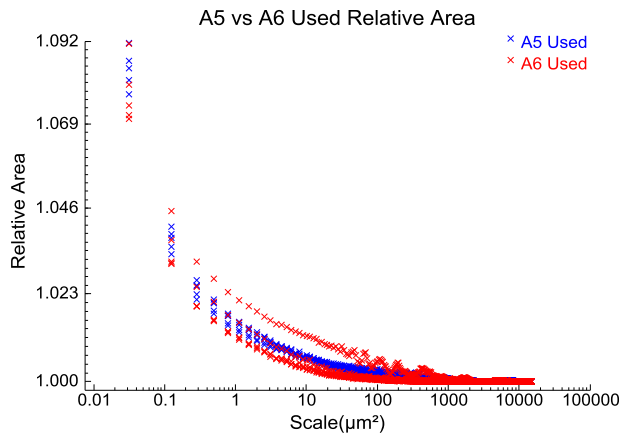
A4 vs. A5



A4 vs. A6



A5 vs. A6



7.7 Appendix G: Conference Materials

Surface Metrology for Quantifying the Difference in Surfaces

Jessica A. Booth, Mackenzie N. Massey, Christopher A. Brown

Worcester Polytechnic Institute

Surface Metrology Lab

Worcester, MA 01609

brown@wpi.edu

Abstract: The objective of this work is to use several characterization methods to determine the extent and nature of the differences in topography between several new and several worn metal forming tools. This is important in providing insights into the possible methods used to manufacture competitor's tools. It can also help to identify the wear mechanisms, which can also provide insights into differences in tool manufacture. Similar problems, of quantifying differences in order to provide similar insights into surface topography modifications made at different times exist in forensics, anthropology, paleontology and archeology. In several domains of application of surface metrology there is value in distinguishing surface features caused by interactions with the surfaces at different times. It is hypothesized that multi-scale analyses can help to sorting out features caused by interactions at different periods in a surface's history. In the current work five measurements are made on three tools from three different manufacturers, each with worn and unworn surfaces. A scanning laser confocal microscope with a 50x objective with a NA of 0.95 was used. The measurement regions were 256x256 μm with heights measured on a grid of 1024x1024 height samples resulting in a height sampling interval of 250nm. Conventional and multi-scale characterizations are used, including area-scale and complexity-scale analyses. A 2nd order polynomial filter is used to remove the form of the tool. Form removal is essential to the ability to discriminate, even with the area-scale and complexity-scale analysis. The ability to discriminate is tested using a modified F-test on relative areas calculated as a function of scale (ASME B46.1 2009). A confidence level of 99% was used down to about 0.03 μm^2 , which is the finest scale in the study and equal to the sampling interval squared divided by two. The largest scale for discrimination is the smooth rough crossover, which depends on the surface and is about 200 μm^2 for the tools. All three unworn tools from different manufacturers can be discriminated and all but two worn surfaces from different manufacturers can be discriminated. The worn and unworn surfaces of one tool and the unworn surfaces of two of the tools can be discriminated at two distinct scale ranges: 0.03 μm^2 to 0.1 μm^2 and 10 μm^2 to 100 μm^2 . The two different ranges could be consistent with two different manufacturing methods and wear mechanisms.

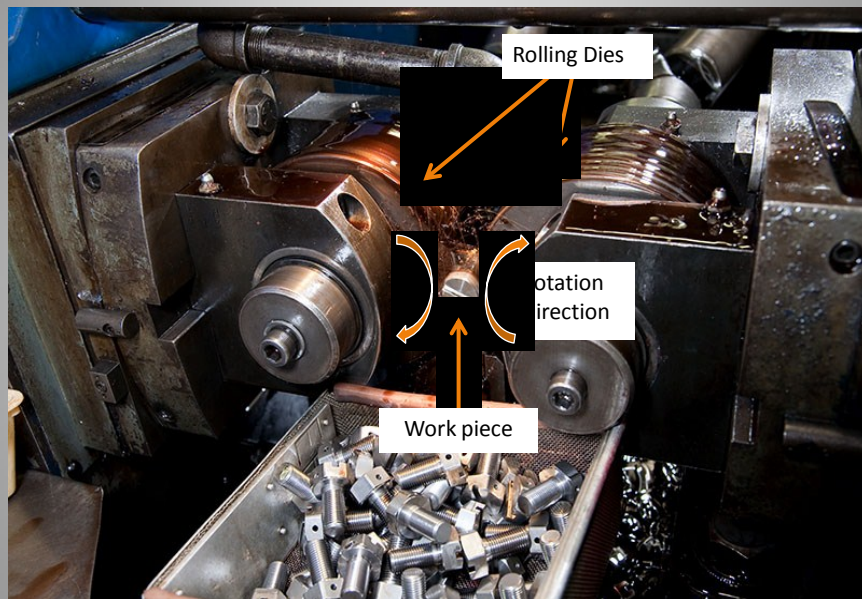
Keywords: multi-scale, relative area, tools, wear, discriminate

Surface Metrology for Quantifying the Difference in Surfaces *on thread rolling dies*

Worcester Polytechnic Institute

Jessica A. Booth
Mackenzie N. Massey
Christopher A. Brown

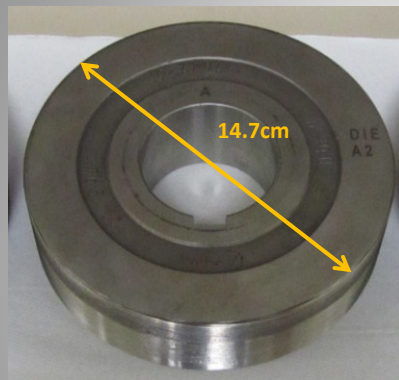
Thread Rolling



Objective & Rationale

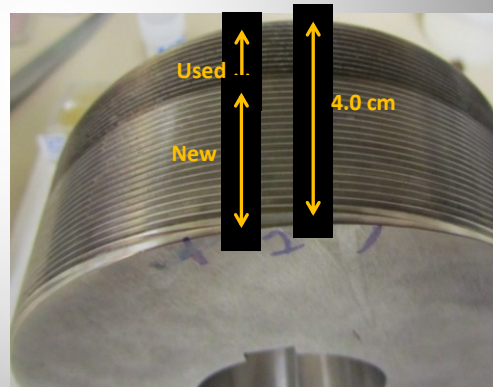
- Objective
 - Discriminate
 - Manufacturer
 - Level of wear
- Rationale
 - Better understand
 - Wear mechanisms
 - Discrimination tools
 - Applications
 - Engineering
 - Anthropology/ Archeology

Tools



Rolled Part

- 3 tools
- 3 manufacturers
- Used to make the same part
- New and Used regions



Method Overview

Measurement

- Confocal laser scanning microscope

Mountains

- Crop 5 μ m border

Sfrac

- Spike Removal

Mountains

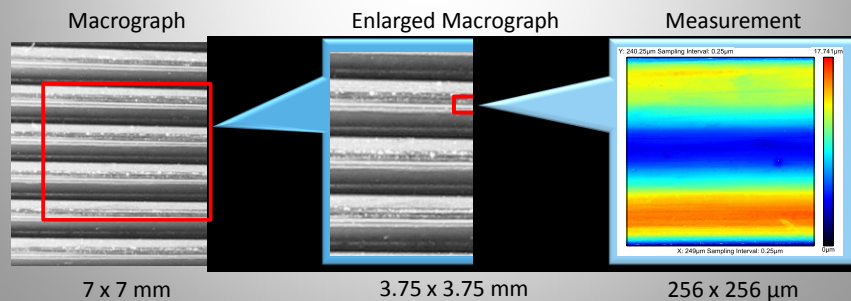
- Form Removal

Analysis

- Multi-scale & Height Parameters

Measurement

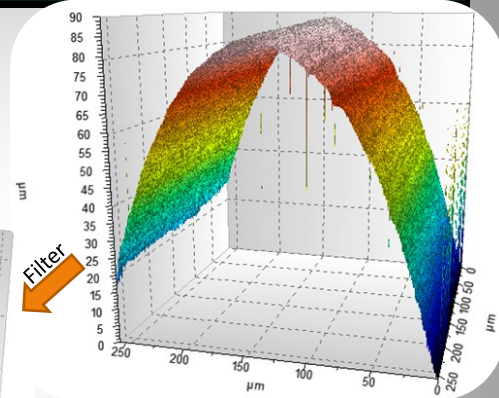
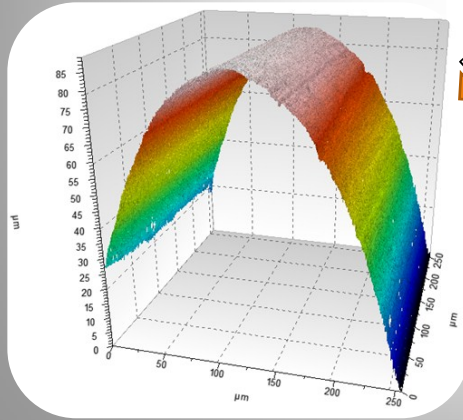
- Olympus LEXT OLS4000 confocal microscope
- 10 regions per die
- 50x objective .95 NA
- 1024x1024 heights
- 250nm sampling interval



Spike Removal

Sfrax

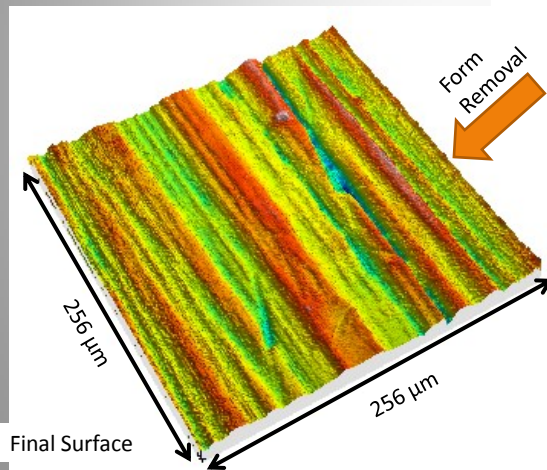
- 85° slope filter for spike removal



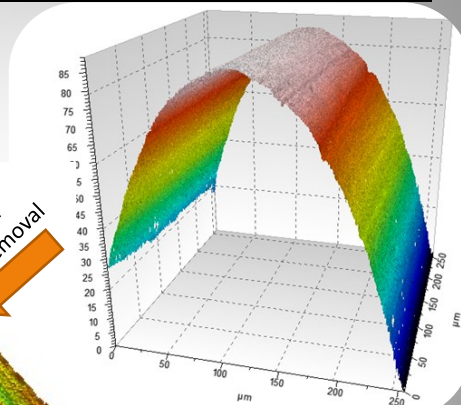
Form Removal

Mountains

- 5th order polynomial Form Removal



Form Removal

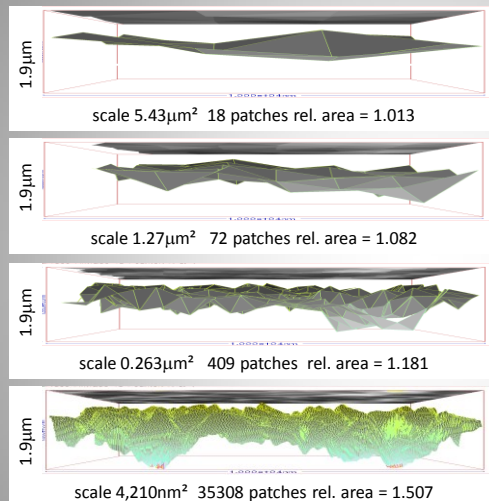


New Die Thread

Analysis

- Multi-scale
 - Area-scale
 - Complexity
 - Modified F-tests in Sfrax
- Conventional
 - ASME B46.1 Height Parameters
 - F-Test in Excel

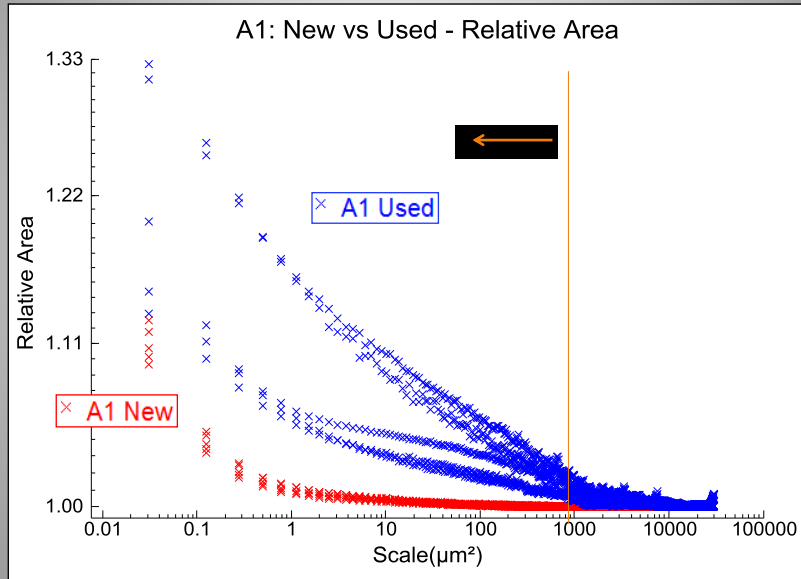
Multi-scale Analysis



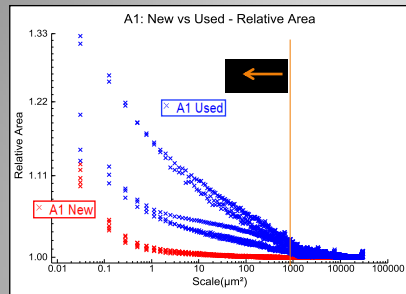
- Relative Area
- Complexity
- Modified F-test
 - 90%
 - 99% confidence

ASME B46.1-2009 Pg 57

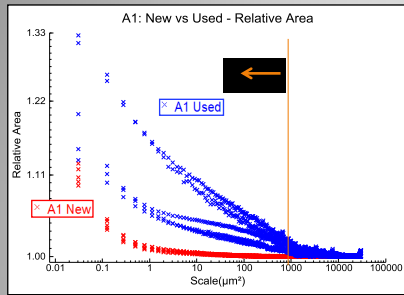
Relative Area & Complexity



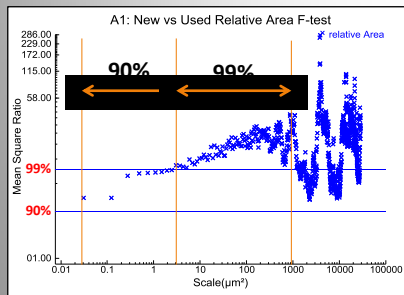
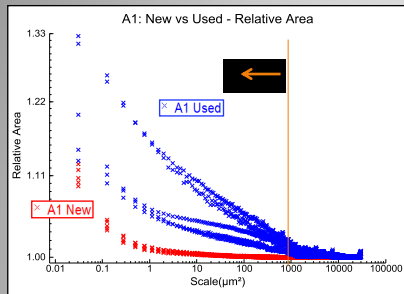
Relative Area & Complexity



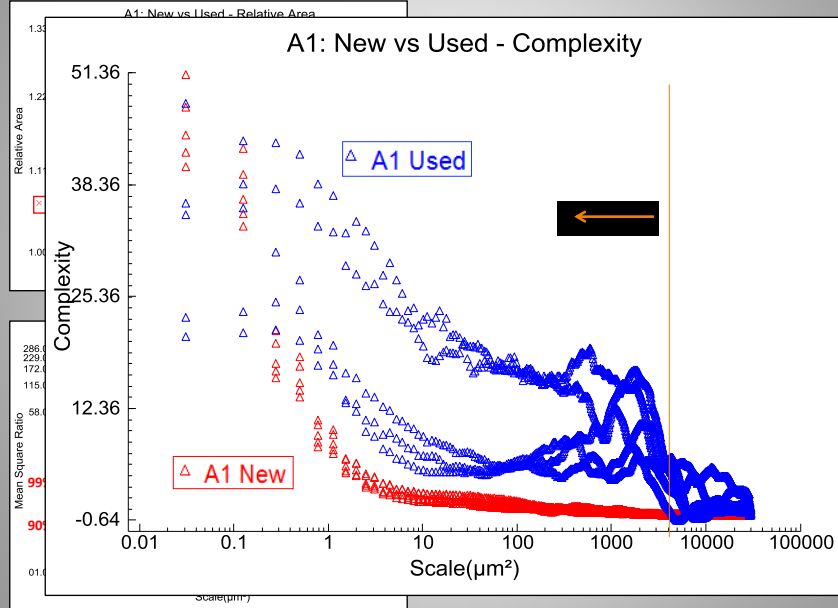
Relative Area & Complexity



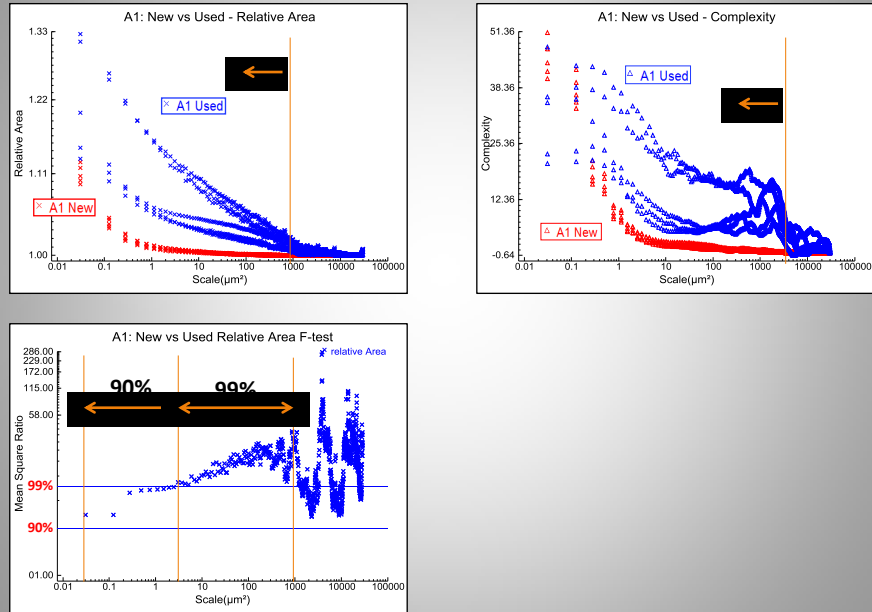
Relative Area & Complexity



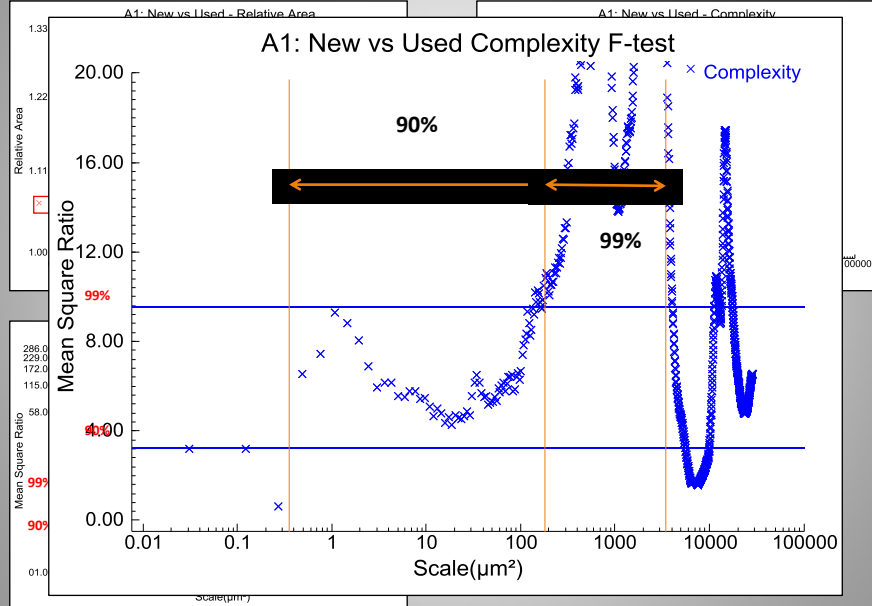
Relative Area & Complexity



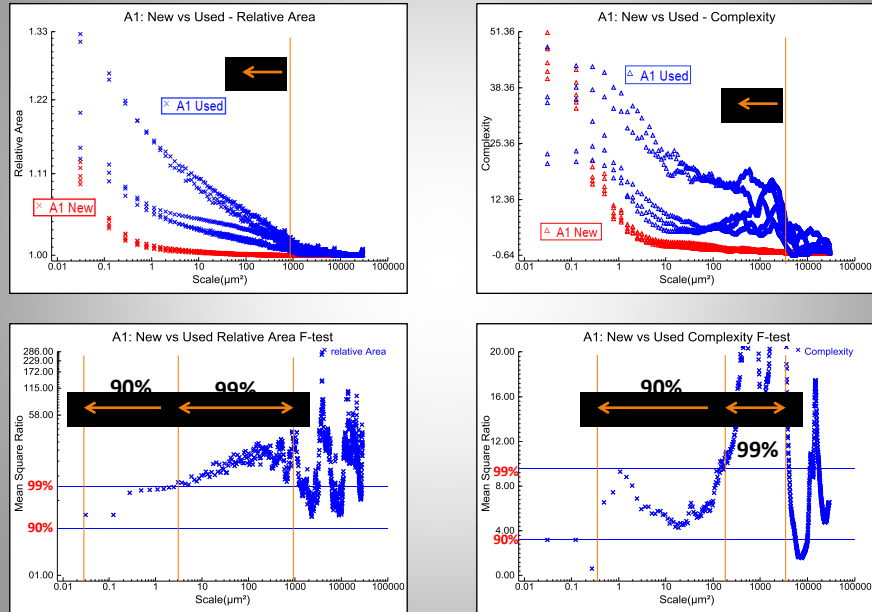
Relative Area & Complexity



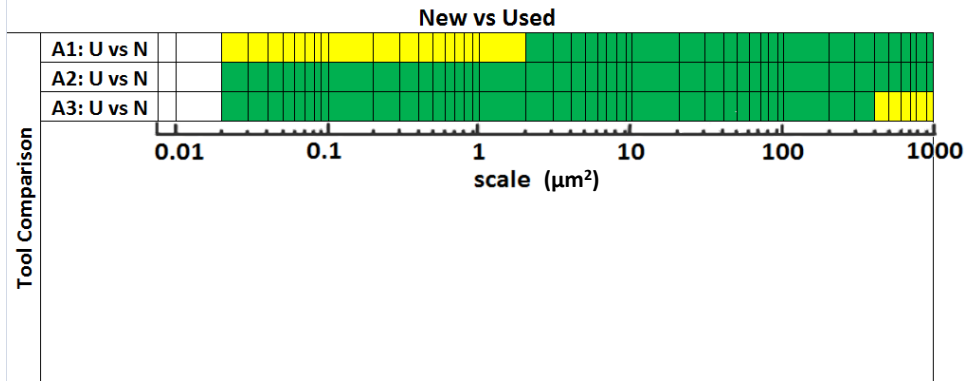
Relative Area & Complexity



Relative Area & Complexity



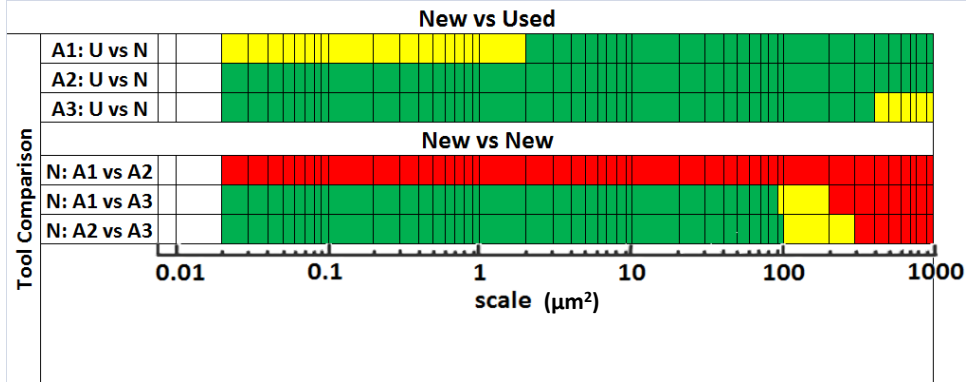
Relative Area F-test Results



Legend



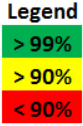
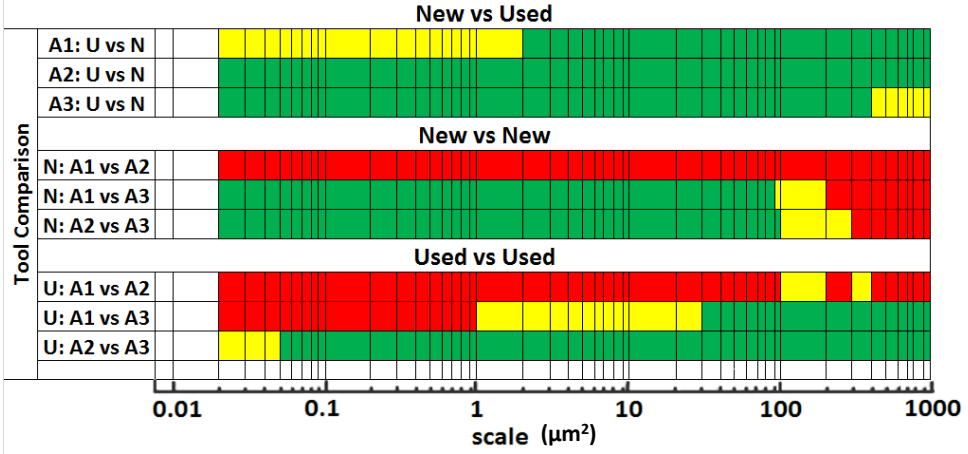
Relative Area F-test Results



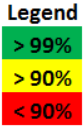
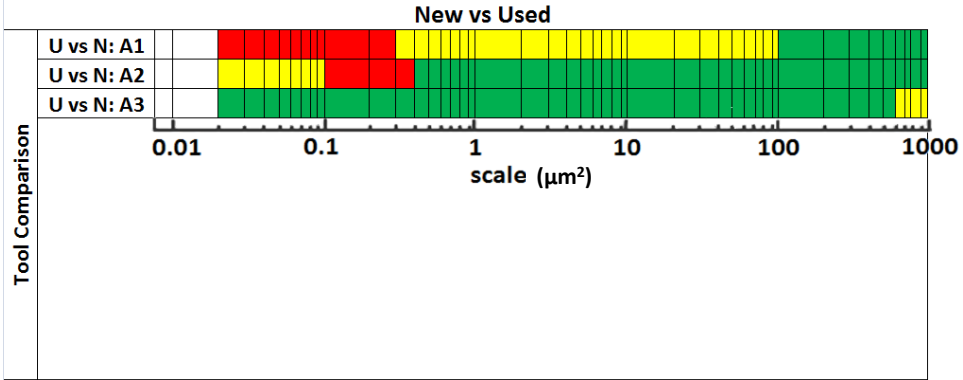
Legend



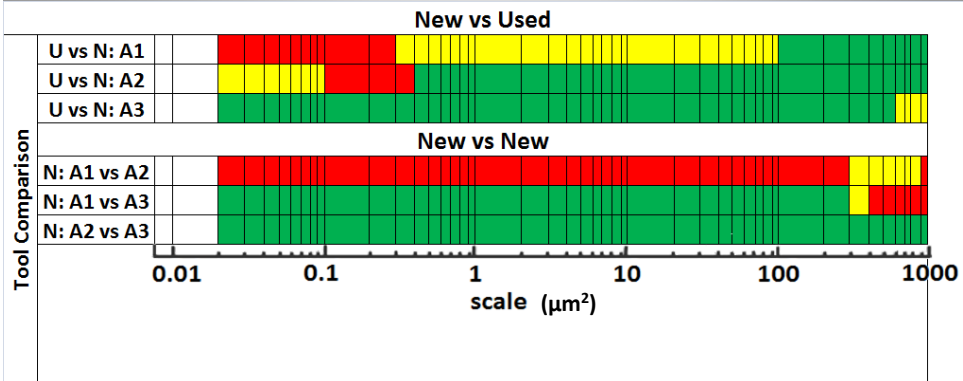
Relative Area F-test Results



Complexity F-test Results



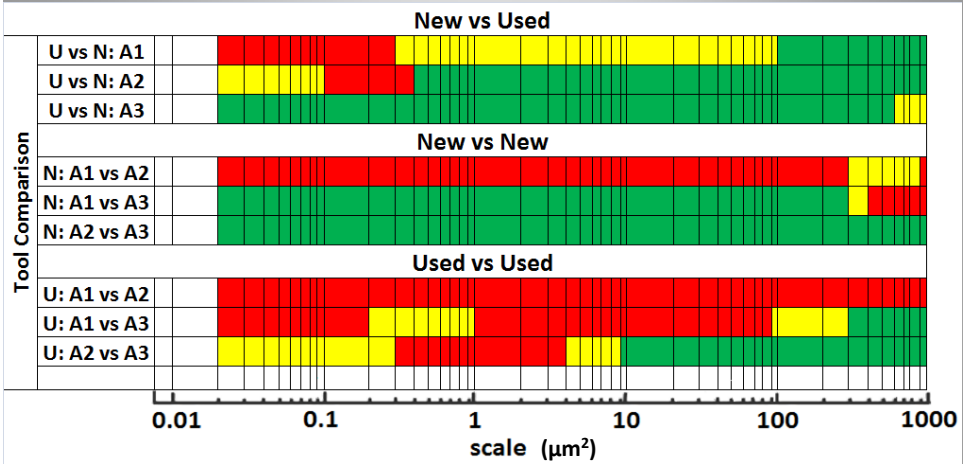
Complexity F-test Results



Legend



Complexity F-test Results



Legend



Conventional Analysis

- Height Parameters
 - **Sa** - Arithmetic mean height
 - **Sp** - Maximum peak height
 - **Sv** - Maximum valley depth
 - **St** - Maximum peak to valley height
 - **Sq** - Root mean square height
 - **Ssk** – Skewness
 - **Sku** – Kurtosis
- F-test
 - Discrimination based on variance
 - Confidence levels:
 - 90%
 - 99%

Conventional Parameters Results

		New vs Used						
Tool Comparison		St	Sp	Sv	Sq	Sa	Ssk	Sku
	A1 New vs A1 Used							
	A2 New vs A2 Used							
	A3 New vs A3 Used							

Legend

- > 99%
- > 90%
- < 90%

Conventional Parameters Results

		New vs Used						
		St	Sp	Sv	Sq	Sa	Ssk	Sku
Tool Comparison	A1 New vs A1 Used	Green	Green	Green	Green	Green	Green	Green
	A2 New vs A2 Used	Yellow	Yellow	Green	Green	Green	Red	Yellow
	A3 New vs A3 Used	Red	Red	Green	Red	Red	Yellow	Yellow
	New vs New							
	A1 New vs A2 New	Yellow	Green	Red	Red	Red	Red	Red
	A1 New vs A3 New	Red	Red	Red	Red	Red	Red	Red
	A2 New vs A3 New	Red	Red	Red	Red	Red	Yellow	Yellow

Legend

> 99%
> 90%
< 90%

Conventional Parameters Results

		New vs Used						
		St	Sp	Sv	Sq	Sa	Ssk	Sku
Tool Comparison	A1 New vs A1 Used	Green	Green	Green	Green	Green	Green	Green
	A2 New vs A2 Used	Yellow	Yellow	Green	Green	Green	Red	Yellow
	A3 New vs A3 Used	Red	Red	Green	Red	Red	Yellow	Yellow
	New vs New							
	A1 New vs A2 New	Yellow	Green	Red	Red	Red	Red	Red
	A1 New vs A3 New	Red	Red	Red	Red	Red	Red	Red
	A2 New vs A3 New	Red	Red	Red	Red	Red	Yellow	Yellow
	Used vs Used							
	A1 Used vs A2 Used	Red	Red	Red	Red	Red	Red	Red
	A1 Used vs A3 Used	Green	Yellow	Yellow	Green	Green	Red	Red
A2 Used vs A3 Used	Green	Yellow	Yellow	Green	Green	Green	Green	

Legend

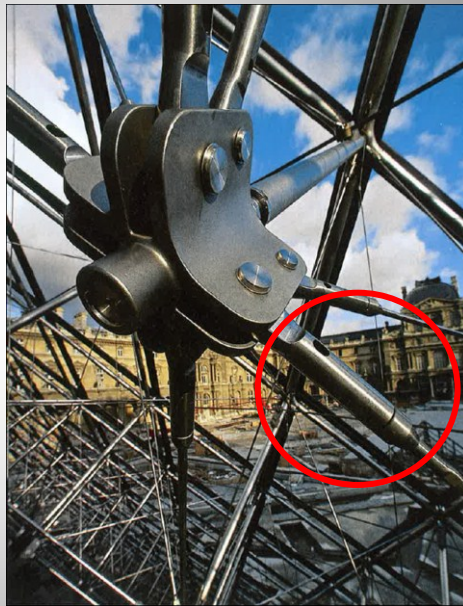
> 99%
> 90%
< 90%

Summary

Tools	St	Sp	Sv	Sq	Sa	Ssk	Sku	Relative Area (μm^2)	Complexity (μm^2)
A1 New vs A1 Used	●	●	●	●	●	●	●	0.03 – 1000	0.3 – 1000
A2 New vs A2 Used	●	●	●	●	●	-	●	0.03 – 1000	0.4 – 1000
A3 New vs A3 Used	-	-	●	-	-	●	●	0.03 - 1000	0.01 – 1000
A1 New vs A2 New	●	●	-	-	-	-	-	-	300 – 1000
A1 New vs A3 New	-	-	-	-	-	-	-	0.03 - 200	0.01 – 300
A2 New vs A3 New	-	-	-	-	-	●	●	0.03 - 300	0.01 – 1000
A1 Used vs A2 Used	-	-	-	-	-	-	-	200, 400	-
A1 Used vs A3 Used	●	●	●	●	●	-	-	1 - 1000	90 – 1000
A2 Used vs A3 Used	●	●	●	●	●	●	●	0.03 - 1000	400 - 1000

Acknowledgements

- Kinefac Corporation
 - Provided tools
- Olympus
 - Donated microscope
- DigitalSurf
 - Donated MountainsMap
- Sfrax
 - Area-scale analysis owned by co-author Brown



Thank You
For Your Attention